

THE LYMPHATIC SYSTEM IN BREAST CANCER METASTASIS

by

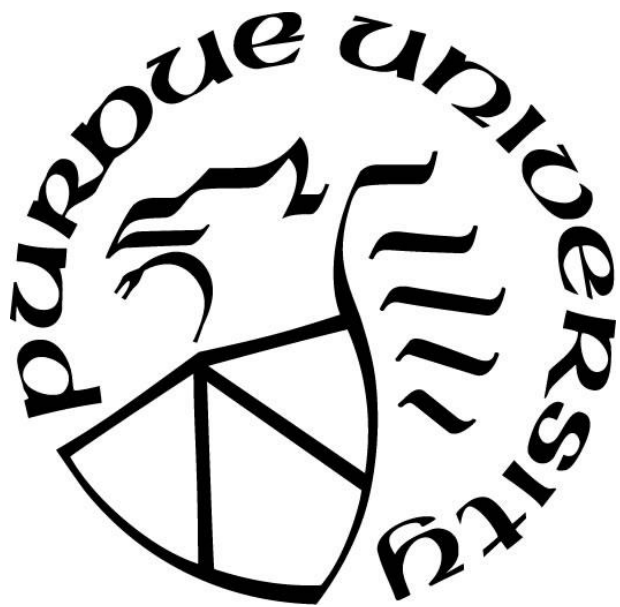
Odalys J. Torres-Luquis

A Dissertation

Submitted to the Faculty of Purdue University

In Partial Fulfillment of the Requirements for the degree of

Doctor of Philosophy



Department of Comparative Pathobiology

West Lafayette, Indiana

August 2021

THE PURDUE UNIVERSITY GRADUATE SCHOOL
STATEMENT OF COMMITTEE APPROVAL

Dr. Sulma I Mohammed, Chair

College of Veterinary Medicine, Department of Comparative Pathobiology

Dr. Suresh K Mittal

College of Veterinary Medicine, Department of Comparative Pathobiology

Dr. GuangJun Zhang

College of Veterinary Medicine, Department of Comparative Pathobiology

Dr. Ignacio Camarillo

College of Science, Department of Biological Sciences

Approved by:

Dr. Sanjeev Narayanan

Dedicated to everyone that lead me and helped me get here

ACKNOWLEDGMENTS

The path to get my Ph.D. was not how I thought it would be. Being the first in my family to go to Graduate School was challenging but fulfilling and empowering. Thus, I would like to thank everyone who made it possible for this ‘boricua’ to be called “Doctor”.

I want to express my sincere gratitude to my advisor Dr. Sulma Mohammed for helping me on this journey, for her continuous support and patience. Besides my advisor, I would like to thank the rest of my thesis committee: Dr. Suresh Mittal, Dr. GuangJun Zhang, and Dr. Ignacio Camarillo, for being such an important part of my academic achievement, for all your guidance and insightful comments. To Dr. Ekramy Sayedahmed, who always kept an eye on how my experiments were doing. Thank you for all your advice and for letting me ask you questions even at your busiest moments. Thank you to my fellow labmate, Xavier Ramos-Cardona for the stimulating research discussion and for having my back.

I want to thank my parents, Noel and Joanny, and my brother, Jesus, for your unconditional love and support and for believing in me even when I wouldn’t. In addition, Irais Luquis-Ramos, for your friendship, always being there for me, and for listening when I needed to talk. I want to thank Gabriel Santiago-Arocho. Your support during this process gave me the motivation to move forward. Thank you for all your love, understanding, and help throughout my doctoral degree. Thank you to Rayla, my dog, for keeping my mental health in check.

I would also like to thank some of my colleagues and co-workers. Dr. Stephanie Santos-Diaz, finding someone at Purdue that was raised a few minutes from my hometown was an amazing motivation and inspiration. I would have loved to meet you earlier in my academic career. Special thanks to Dr. Ashwana Fricker for your friendship, support, advice, and mentorship. Thank you to Dr. Julius Eason and Theresa Bescher from the Office of Graduate Diversity Initiatives at Purdue. Both of you always knew how to create a comfortable environment, thank you for being so kind and supportive.

TABLE OF CONTENTS

LIST OF TABLES	9
LIST OF FIGURES	10
ABSTRACT	12
CHAPTER 1. LYMPHATIC SYSTEM AND BREAST CANCER METASTASIS	13
1.1 Introduction.....	13
1.2 The lymphatic system and lymph formation	13
1.2.1 Initial lymphatic capillaries	14
1.2.2 Pre-Collecting capillaries	14
1.2.3 Collecting lymphatics	14
1.2.4 Lymph node.....	15
1.3 Lymphatic metastasis mechanism in breast cancer.....	16
1.3.1 Lymphangiogenesis	16
1.3.2 Tumor Microenvironment	17
1.3.3 Immunoediting.....	19
1.4 Roles of chemokines in breast cancer.....	20
1.4.1 Chemokines in breast cancer tumor growth	20
1.4.2 Chemokines in breast cancer angiogenesis	21
1.4.3 Chemokines in breast cancer tumor metastasis	22
1.4.4 Chemokine regulation in breast cancer	23
1.5 The clinical implications of the lymphatic system in breast cancer	25
1.6 Conclusion	27
CHAPTER 2. LYMPH-CIRCULATING TUMOR CELLS SHOW DISTINCT PROPERTIES TO BLOOD-CIRCULATING TUMOR CELLS AND ARE EFFICIENT METASTATIC PRECURSORS.	28
2.1 Introduction.....	28
2.2 Materials and Methods	30
2.2.1 Cell lines and culture conditions.....	30
2.2.2 Animal model.	30
2.2.3 Spontaneous metastasis.	31
2.2.4 Lymph fluid and blood collection.....	31
2.2.5 Tumor histology and assessment of metastasis.	32

2.2.6	Lymph- or blood-circulating tumor cells' isolation and propagation.	32
2.2.7	Activsignal IPAD assay.	32
2.2.8	NanoString nCounter analysis.	33
2.2.9	RNA expression analysis	33
2.2.10	Lymph chemokine/cytokine determination.	33
2.2.11	Western blot analysis.	34
2.2.12	Statistical analysis.	35
2.3	Results.....	35
2.3.1	Visualization and mapping of lymphatic vessels allow the isolation of LCTCs before they reach the regional lymph nodes.	35
2.3.2	Lymph node metastasis was confirmed in MTLn3 tumor-bearing animals.....	35
2.3.3	LCTCs existed in clusters and could be reliably harvested in the MTLn3 tumor-draining lymph prior to their entry into the SLN.	36
2.3.4	LCTCs and BCTCs share similar gene profiles that are distinct from those of the primary tumor and LNMs.	36
2.3.5	LCTC and BCTC protein expression and phosphorylation status.....	38
2.3.6	LCTCs display a hybrid E/M phenotype.....	39
2.3.7	LCTCs display cancer stem cell properties and have a higher propensity than BCTCs to form mammospheres in culture and to form tumors in vivo.	39
2.3.8	LCTCs and BCTCs downregulate antigen presentation pathways to escape the immune response.....	40
2.3.9	The lymph immune microenvironment.....	41
2.3.10	Primary tumor-derived factors in the lymph are also produced by LCTCs and act in a paracrine manner.	42
2.4	Discussion.....	42
2.5	Conclusion	46
2.6	Acknowledgements	47
CHAPTER 3. TUMOR-DRAINING LYMPH SECRETOME EN ROUTE TO THE REGIONAL LYMPH NODE IN BREAST CANCER METASTASIS.....		55
3.1	Introduction.....	56
3.2	Materials and methods.....	57
3.2.1	Cell Lines and Culture Condition	57
3.2.2	Collection of Lymph and Blood from Tumor-Bearing and Non-Tumor-Bearing Rats	57
3.2.3	Mass Spectrometry (MS) Data Acquisition and Analysis	58

3.2.4	Bioinformatic Analysis	59
3.3	Results.....	60
3.3.1	Afferent Lymph Collection from Metastatic Mammary Tumor Syngeneic Model	60
3.3.2	Tumor-Derived Secretome Profiled in Lymph Before Reaching the Draining Lymph Node.	60
3.3.3	Molecular Pathway Analysis of Lymph Proteins Demonstrate Up Regulation of Key Metastatic Pathways and Immunomodulation Network.	61
3.3.4	Lymph Protein Profile Revealed Exosomal Proteins That Associate with Patients Survival.	62
3.4	Discussion.....	63
3.5	Acknowledgements	65
CHAPTER 4. ACTIVATION OF TLR3 CONTRIBUTES TO TUMOR CELL MIGRATION AND METASTASIS THROUGH THE LYMPHATIC SYSTEM.....		72
4.1	Introduction.....	72
4.2	Materials and methods.....	74
4.2.1	Cell lines and cell culture conditions	74
4.2.2	Animal model and tumor assay	74
4.2.3	Real-Time Quantitative PCR.....	75
4.2.4	Cell viability assay.....	75
4.2.5	Western Blot.....	75
4.2.6	Immunofluorescence and confocal imaging.....	76
4.2.7	Flow Cytometry	76
4.2.8	RNA interference.....	77
4.2.9	Migration Assay.....	77
4.2.10	NF- κ B Transcription Factor Assay.....	77
4.2.11	Immunohistochemistry.....	78
4.2.12	Statistical analysis.....	78
4.3	Results.....	78
4.3.1	Mapping of lymphatic vessels and the collection of lymph and LCTCs before reaching the regional lymph nodes in a breast cancer model.	78
4.3.2	Lymph circulating tumor cells (LCTCs) express TLR3.	79
4.3.3	TLR3 activation increases LCTCs, not BCTCs, migration and invasion in vitro and in vivo.	79
4.3.4	Upregulation of TLR3 in LCTCs leads to NF- κ B and IRF3 nuclear translocation.	80

4.3.5	Activation of NF- κ B and IRF3 result in the induction of CXCL10 in LCTCs.	81
4.4	Discussion	81
CHAPTER 5. LXR/RXR PATHWAY SIGNALING ASSOCIATED WITH TRIPLE-NEGATIVE BREAST CANCER IN AFRICAN AMERICAN WOMEN.....		89
5.1	Introduction.....	90
5.2	Materials and Methods	91
5.2.1	Chemicals and reagents.....	91
5.2.2	Breast cancer tissue preparation.	91
5.2.3	Breast cancer tissues' protein extraction.....	92
5.2.4	2-Dimensional gel electrophoresis.....	92
5.2.5	Mass spectrophotometry analyses.	93
5.2.6	IHC.....	93
5.2.7	Western blot analysis.	93
5.2.8	Ingenuity pathway analysis (IPA).....	94
5.2.9	Statistical analysis.....	94
5.3	Results.....	94
5.3.1	The proteome landscape of LA tumors and TNBC in AA and EA women shows some similarity.....	94
5.3.2	Differentially expressed proteins in LA vs TNBC in AA and EA women are different.	95
5.3.3	Molecular pathway analysis of LA and TNBC proteins of AA women demonstrates upregulation of key nuclear receptors' signaling and immunomodulation networks.	95
5.3.4	Validation of selected differentially expressed proteins.	96
5.4	Discussion.....	97
5.5	Acknowledgements	99
REFERENCES		108
PUBLICATIONS.....		131

LIST OF TABLES

Table 3.1: Proteins Differentially (>175 Fold) Expressed in Lymph from Metastatic Tumor-Bearing Compared to Lymph from Non-Metastatic Tumor-Bearing Animals	71
Table 5.1: Patient's characteristics	105
Table 5.2: Proteins altered in expression between TNBC and LA in African American and European American women	106
Table 5.2: Continued.....	107

LIST OF FIGURES

Figure 2.1: Lymph vessel visualization, lymph and LCTC collection, identification, and growth.	48
Figure 2.2: Volcano plot displaying differentially expressed genes between LCTC, BCTC, and LNMs (using the primary tumor as reference).	49
Figure 2.3: Pathway activation scores for LCTC, BCTC, LNMs, and primary tumor were compared to identify the pattern of pathway activation in each.	50
Figure 2.4: Signaling pathways alerted in LCTCs, BCTCs, and LNMs relative to primary tumor. Heat maps demonstrating changes.	51
Figure 2.5: Epithelial–mesenchymal transition phenotype and markers expressed by LCTCs, BCTCs, and MTLn3.	52
Figure 2.6: Cancer stem cell signatures of LCTCs and BCTCs.	53
Figure 2.7: Heat map plot of directed global significance score and multiplex quantification of cytokines and chemokines using the multiplex map rat cytokine/chemokine magnetic bead 27-plex immunoassays.	54
Figure 3.1: Experimental plan and concept of lymph collection.	66
Figure 3.2: Protein expression statistics from metastatic and non-metastatic tumor-bearing animals.	67
Figure 3.3: Pathways enriched in differentially expressed proteins in lymph.	68
Figures 3.4: Protein expressions in tumor-draining lymph from animals with metastatic tumor and the involvement of signaling pathways.	69
Figure 3.5: Kaplan-Meier survival analysis of human patients (n=3951) with invasive breast cancer divided into two groups based on the expression level of HSPA8.	70
Figure 4.1: TLRs expression and effect of Poly(I:C) on cell viability.	84
Figure 4.2: LCTCs highly express TLR3 when stimulated with Poly (I:C).	85
Figure 4.3: Knockdown of TLR3 in LCTCs decreased their migration and invasion in vitro and in vivo.	86
Figure 4.4: Stimulation of Poly (I:C) in LCTCs leads to NF-kB and IRF3 nuclear translocation.	87
Figure 4.5: CXCL10 and its receptor, CXCR3, are highly expressed in LCTCs.	88
Figure 5.1: Representative 2-DE gel images of protein profiles of invasive breast carcinoma. .	100
Figure 5.2: Differentially expressed proteins in breast cancer tissues from AA compared to European women regardless of hormonal status.	101

Figure 5.3: Differentially expressed proteins102

Figure 5.4: IPA of canonical pathways of differentially altered protein expressed in breast carcinoma.103

Figure 5.5: Western Blot, Immunohistochemistry and bar graphs of selected proteins.104

ABSTRACT

The leading cause of breast cancer-associated death is metastasis. During metastasis, tumor cells metastasize from primary tumors to distant organs via the circulatory and lymphatic systems. However, in 80% of solid tumors, metastasis via the lymphatic system precedes metastasis via the vascular system. There is a lot of information about metastasis through the circulatory system. However, not much information is available about the tumor cell dissemination through the lymphatic system or the lymphatic microenvironment that aids in this process in breast cancer metastasis. In addition, the molecular properties of tumor cells as they exit the primary tumor into the afferent lymphatics en route to the sentinel lymph nodes (SLNs) are not yet known.

This project aims to determine why and how tumor cells metastasize to the lymphatic system. The proposal is based on the hypothesis that active migration is needed for tumor cells to spread via the lymphatic vessels. Thus, finding and understanding the molecules that contribute to this can be a breakthrough for breast cancer metastasis therapy.

The goals of this thesis are to 1) Examine the molecular, genetic, and proteomic characteristics of circulatory tumor cells and compare these to the primary tumor and lung metastasis, 2) Examine the role of Toll-like receptors in tumor cell migration to the lymph node, and 3) Identify the difference in protein expression among two different types of breast cancer (Triple-Negative and Luminal A) and understand their aggressive biology.

CHAPTER 1. LYMPHATIC SYSTEM AND BREAST CANCER METASTASIS

1.1 Introduction

Breast cancer death declined in the last decade due to advances in early detection and treatment. However, it still claims the lives of more than half a million women each year. In 2020 alone, there were 2.3 million women diagnosed with the disease and 685,000 deaths in the world¹. Thus, making it the second leading cause of cancer death in women². The cause of death in 90% of breast cancer patients is metastasis³. Metastasis is the dissemination of tumor cells from the initial tumor and their establishment and development in distant organs such as the lung, liver, and brain. The metastatic lesions in these organs are difficult to remove surgically and are resistant to current treatments⁴. During metastasis, tumor cells detach from the primary tumor and spread to distant organs using either the vascular or the lymphatic system⁵⁻⁷. It is critical to assess the relative contributions of both pathways equally; However, most research studies have focused on hematogenous tumor spread with little attention paid to lymphatic dispersion and its cell cargo. In 80% of solid tumors, like breast cancer, metastasis via the lymphatics proceeds metastasis through the blood circulation, leading to the patient's poor prognosis and worst outcome^{5,8-10}.

This review focuses on breast cancer metastasis through the lymphatic system, the lymphatic structure, composition, and what enables a cancer cell to gain access to the lymphatics and the current therapeutic targets.

1.2 The lymphatic system and lymph formation

The lymphatic system works alongside the blood vascular system. In the blood circulatory system, the blood leaves the heart, runs through a series of vessels, and returns to the heart¹¹. In contrast, the lymphatic system is a linear network of vessels designed to accomplish homeostasis functions, lipid absorption, and immune cell trafficking^{12,13}. The lymphatic vessels transport the lymph, composed of water, macromolecules, and lymphocytes that return to the blood. These lymphocytes help the lymphatic system fight infections by filtering out waste products and destroying cancer cells^{14,15}. The lymphatic system consists of initial lymphatic capillaries, pre-collecting vessels, collecting capillaries (lymphangion), lymph node, lymphatic trunks, and ducts.

1.2.1 Initial lymphatic capillaries

The initial lymphatic capillaries emerge from the dermis, galea, and mucosal membrane¹⁶; they are a system of (10-60 μ m in diameter) bulbous blind-ended sacs¹⁷ with a single thin layer of over-lapping lymphatic endothelial cells (LEC)^{15,18}. The LEC is joined with one another by oak leaf-shaped junctions that are attached to the surrounding extracellular matrix (ECM) by anchoring filaments (6-10nm in diameter) of fibrillin and emilin^{12,14,18}. This structure form valves allowing for a one-directional flow of fluids, solutes, and cells into the lumen¹⁷. When the tissue fluid pressure is higher than the pressure in the initial lymphatic, due to an increase in fluid leakage from hyper-permeable blood vessels, the anchoring filaments can stretch, leading to the opening of the valves¹². However, if the pressure is higher inside the initial lymphatic capillaries, the valves close¹⁵

1.2.2 Pre-Collecting capillaries

After lymph enters the initial lymphatic capillaries, it drains into pre-collecting lymphatic capillaries located in the deep dermis^{13,19,20}. The pre-collecting capillaries are uni-directional valves whose primary function is to absorb and propel the lymph away from the capillaries towards the collecting vessels. These pre-collecting capillaries can achieve spontaneous contractions due to one or more layers of smooth muscle cells (SMCs) within their walls that enable the flow promotion of the lymph^{13,19}. These pre-collecting capillaries turn into the collecting lymphatics vessels.

1.2.3 Collecting lymphatics

The collecting lymphatics vessels (>200 μ m in diameter) have a complete continual basal. The vessel walls have a three-layer composition which makes them very similar to the structure of the blood vessels^{13,21}. The outer layer is called adventitia which is composed of fibroblasts, connective tissue, and nerves. The middle layer is known as media and is composed of smooth muscles mixed with collagen and elastic fibers; together, they support the circumference structure. Lastly, the inner layer consisting of endothelial cells is called intima²¹. The collecting lymphatics vessels contain a secondary valve. The region of the vessel between the two intraluminal valves is called lymphangion. The lymphangions are the main pumping structure¹⁵ and are responsible for

the rhythmic contractions¹³. The propulsion of lymph against a pressure gradient towards the next lymphangion compartment occurs at $\sim 10\mu\text{m}/\text{sec}$. The valves open and close periodically 1-15 times/minute, preventing reverse flow due to the intrinsic wall motion caused by skeletal/smooth muscle contraction and compression created by arterial pulsations. Prostaglandins and thromboxane can also regulate lymphangions^{15,21}. The average measure of the lymphangions in the head and neck of humans is about 0.2mm in diameter and 2mm in length¹³. However, there are differences in sizes among lymphatic valves of the pre-collecting and collecting lymph vessels, and also different lengths of lymphangions¹⁶.

1.2.4 Lymph node

The lymphatic system consists of primary and secondary organs. The primary organs consist of the thymus and bone marrow, where the production and maturation of lymphocytes occur. Secondary organs are those responsible for further maturation and immune response commencement, and these are the spleen, Peyer's patches, appendix, tonsils, and lymph nodes¹³. Lymph nodes consist of multi-lobules in lymph-filled sinuses enclosed by a thick capsule²². The sinuses are endothelium and reticulum cells²³. Three compartments comprise the lymph node structure that includes the cortex, paracortex, and medulla. The cortex contains primary follicles and germinal centers with B cells and is also the site for high endothelial venules (HEVs). HEVs are high cuboidal endothelial cells that use ligands to direct the flow direction of the lymphocytes from the blood circulation into the lymph node^{21,22}. The paracortex or deep cortex region is where T cells and dendritic cells (DCs) exist. The medulla and inner area of the lymph node are where the macrophages reside^{21,24,25}. The compartments in each lymph node lobule enable interaction between T cells and B cells with antigen-presenting cells (APCs)²². These primary and secondary organs are vital for transporting these immune cells²⁶ and inducing an immune response²³.

Finally, the lymph flows through the sinuses of the lymph node from different afferent vessels into a single efferent lymph vessel¹⁴. It flows towards the thoracic duct and later returns to the blood circulation^{12,22}.

1.3 Lymphatic metastasis mechanism in breast cancer

The lymphatic system has an advantage over the circulatory system because of the discontinuous structure of the lymph capillary components, low lymph flow, minimum shear stress, and high hyaluronic acid content, providing a suitable environment for cell preservation and survival²⁷. Lymphatic vessels are leakier than blood vessels, thus essential for tumor cell spread. Under normal circumstances, the shape of blood vessels would compel tumor cells to spend more energy during intra- and extravasation. In addition to the composition of the lymphatic vessels compared to blood vessels, new vessels and the favorable environment can serve as effective mechanisms for lymphatic metastasis.

1.3.1 Lymphangiogenesis

Lymphatic metastasis can occur through preexisting vessels incorporated into the tumors; however, evidence suggests that lymphangiogenesis plays an active role and contributes to tumor cell metastasis¹⁹. Lymphangiogenesis is the formation of new lymphatic vessels, and the identification of critical lymphatic-specific molecular markers has led to a better understanding of physiological and pathological situations. Lymphangiogenic factors can create a favorable environment for new lymphatic vessels²⁸, and the use of these factors as markers has made it easier to examine tumors for the presence of an intratumoral lymphatic network. Clinical breast cancer studies suggested an association between increased densities of intratumoral and peritumoral lymphatic vessels, metastasis, and reduced survival^{29,30}. In addition, increased lymph node lymphangiogenesis and lymph flow in tumor-draining lymphatic arteries lead to metastatic dissemination.

Vascular endothelial growth factor-C (VEGF-C) overexpression in breast cancer cells facilitates the spread of tumor cells from the primary tumor by increasing the number of lymphatic vessels in the tumor surroundings. Meanwhile, VEGF-D promotes tumor growth rate, angiogenesis, and metastasis³¹. VEGF-C and VEGF-D are binding ligands and activators of the vascular endothelial growth factor receptor-3 (VEGFR-3) pathway³². VEGFR-3 is a tyrosine kinase receptor commonly expressed in lymphatic endothelial cells (LEC) and the primary regulator of lymphangiogenesis³³. Overexpression of this receptor contributes to lymph node metastasis and an unfavorable prognosis³⁴. Agents that disrupt VEGFR-3 signaling or neutralize

VEGF-C and VEGF-D decrease new lymphatic vessels' development, and tumor spread in experimental cancer models ³⁵. Significantly, decreased VEGFR-3 expression is associated with fewer positive lymph nodes and more prolonged patient survival. In summary, these findings imply that controlling tumor-induced lymphangiogenesis might prevent or minimize cancer-related mortality by preventing metastasis to the lymph nodes, which are potential repositories for future dissemination to distant organs.

However, VEGF-C and VEGF-D's association in metastasis has been contradictory in many studies ³⁶. These contradictory findings are attributable to differences in the tumor microenvironment, tumor tissue dissimilarities, and interactions with other lymphangiogenic factors.

1.3.2 Tumor Microenvironment

A tumor microenvironment is a specialized environment that forms during tumor growth due to the tumor's interactions with the host. The tumor microenvironment is created, shaped, and dominated by the tumor, orchestrating molecular and cellular events in surrounding tissues. Tumor cells transform the resident normal stroma cells or recruit other metastasis-promoting stroma cells to facilitate their growth/invasion and remodel the microenvironment.

The tumor microenvironment consists of ECM as well as myofibroblasts and cellular players, such as cancer-associated fibroblasts (CAFs), neuroendocrine (NE) cells, adipose cells, immune-inflammatory cells (including DCs), tumor-associated macrophages and tumor-infiltrating lymphocytes), and the blood and lymphatic vascular networks³⁷.

One of the tumor microenvironments cellular events in breast cancer stroma are fibroblasts, also known as CAFs ³⁸. CAF secrete many soluble factors, like chemokines or growth factors, which modulate the tumor stroma and enhance tumor growth and invasion. It also influences the transcriptional profile of breast cancer cells. Many xenograft model studies have shown that CAF from primary human breast cancer significantly enhanced tumor growth and angiogenesis ³⁸.

The ECM is a complex network of proteins that surrounds and stabilizes cells. It consists of structural proteins, glycoproteins, and proteoglycans ³⁹. In pathological conditions, the ECM is disorganized and deregulated, resulting in aberrant cell activity via feedback regulatory mechanisms ⁴⁰. An abnormal ECM promotes tumor cell transformation, tissue invasion and creates a tumorigenic microenvironment to facilitate cancer progression. The ECM can differ in physical

and biochemical properties when compared to normal conditions. In breast cancer, the stroma is typically stiffer, which is why breast cancer stroma becomes palpable. Lysyl oxidase (LOX), which cross-links collagen fibers, is responsible for the enhanced tissue stiffness⁴⁰. Overexpression of LOX enhances breast cancer growth and invasiveness in mice models, whereas inhibition of LOX lowers breast cancer incidence⁴¹.

Another microenvironment component is DCs. DCs can cross-present antigens to CD4+ and CD8+ T cells and activate them to attack neoplastic cells, thus playing an essential role in inducing anti-tumor responses⁴². The maturation of DCs influenced by the local microenvironment, which includes various factors that influence the formation of either tolerogenic or immunosuppressive DC⁴². An abundance of immature DC has impaired capacity to stimulate anti-tumor immunity in the tumor-associated stroma⁴³. Tumor-associated cytokines and growth factors, like VEGF, IL-10, and prostaglandin E2, may steer DC maturation toward a regulatory phenotype, inhibiting T-cell proliferation⁴⁴.

Tumor-associated macrophages (TAM) are another component of the tumor microenvironment. These form a significant cell population in breast cancer and display a characteristic phenotype oriented towards promoting tumor growth, angiogenesis, and adaptive immunity suppression⁴⁵. TAM secretes many tumor-promoting factors, including VEGF, cytokines, and enzymes that aid in invasion, angiogenesis, and metastasis⁴⁵. Many studies have linked increased levels of TAM to a worse prognosis in breast cancer; this suggests that TAM depletion or reprogramming could represent a viable therapeutic strategy.

Finally, one of the critical components of the tumor microenvironment is the tumor-infiltrating lymphocytes. The majority of these tumor-infiltrating lymphocytes are T cells⁴⁶. T reg, a type of T cells, typically protects against autoimmune illnesses by inhibiting self-reactive T cells, but in the tumor microenvironment, anti-tumor responses are blocked⁴⁵. They can inhibit various immune cells, including CD8+ T cells, natural killer cells, B cells, and antigen-presenting cells⁴⁷. In addition, T reg cells produce large amounts of RANKL, activating RANK-expressing breast cancer cells and enhancing metastasis⁴⁸. As a result, having large numbers of T reg is related to a poor prognosis in breast cancer^{49,50}.

1.3.3 Immunoediting

Once created, the tumor microenvironment serves as a reliable impediment to immune cell activity. Because tumors are not passive targets for host immunity; instead, they actively downregulate all phases of anti-tumor immune responses employing various methods and mechanisms. Many pathways responsible for immune cell dysfunction in the tumor microenvironment have been discovered to date. Some are directly mediated by tumor-produced substances, whereas others are caused by changes in normal tissue homeostasis that occur in the presence of cancer. Some mechanisms orchestrated by the tumor that contribute to its escape from the host immune system are the interference with the induction of anti-tumor immune responses, impaired effector cell function in the tumor microenvironment, insufficient recognition signals, and development of immunoresistance by the tumor ⁵¹.

In breast cancer, studies suggest that the tumor creates an immunosuppressive microenvironment by using prostaglandin E2 secretion and TGF- β signaling to recruit T regs and secretes IL-10 and TGF- β to suppress the functions of effector cells ⁵². In contrast, CD8+ effector T cell infiltration is related to prolonged breast cancer-specific survival, regardless of other prognostic variables such as tumor grade, lymph node stage, tumor size, vascular invasion, or HER2 status ⁴⁶. The effect of CD8+ cytotoxic T cells, on the other hand, is controlled by the balance of co-stimulatory and co-inhibitory signals at immune checkpoints ^{53,54}. Immune checkpoint molecules like programmed death-1 (PD-1) can inhibit T-cell function and prevent inappropriate immune reactions by limiting the duration of immune responses. The most thoroughly researched immune checkpoint receptor, PD-1, is becoming recognized as playing a critical role in immunoediting ⁵⁵. PD-1 is a co-inhibitory receptor that suppresses T-cell activity by binding to its ligands PD ligand (PD-L) 1 and PD-L2 ⁵⁴.

However, tumor cells can exploit this route to reduce or avoid anti-tumor T-cell immunity and establish an immunosuppressive microenvironment, a phenomenon known as a "molecular shield" that promotes tumor development. Multiple human malignancies, including breast cancer, have been shown to express PD-1 on tumor-infiltrating lymphocytes and PD-L1 on tumor cells ^{56,57}, where it is associated with a worse prognosis. The use of this mechanism by cancer cells may also explain why, despite the activation of cancer-specific T cells in numerous studies of adoptive cell therapy, tumor growth is seldom controlled ⁵⁸. Thus, targeting PD-1 or PD-L1 with antibodies capable of inhibiting this pathway could be a potential therapeutic option in breast cancer ⁵⁴.

1.4 Roles of chemokines in breast cancer

The attraction and entry of cancer cells into lymphatic vessels and the penetration into draining lymph nodes were thought to be passive and regulated at multiple steps. Functional lymphatic vessels are limited to the tumor margin and peritumor regions surrounding tumors⁵⁹. Since tumors lack intratumor functional lymphatic vessels, the elevated interstitial fluid pressure can alter lymph flow to tumor-draining lymph nodes⁶⁰. Tumor cells that arrive at the lymphatic vessels may enter passively or use active signaling mechanisms. Recent evidence suggests that chemokine ligands and receptors expressed by tumor and stromal cells can facilitate the process of tumor cell intravasation into the lymphatic vessels.

Chemokines are a superfamily of cytokine-like molecules categorized into several subfamilies based on variations in the quaternary structure, cysteine residues, CXC, CC, and XC and CX3C⁶¹. They are associated with G-protein coupled receptors with seven transmembrane domains that can induce directional migration of cells. Chemokines function by generating gradients that direct random or controlled cell migration with cognate receptors from lower to higher ligand concentrations. Interactions with proteoglycans on the cell surface or in the ECM can produce these gradients. Chemokines and chemokine receptors are involved in various physiological and pathological processes and the detection and progression of breast cancer⁶².

The paradigm of chemokine action involving lymphatics is potentially complex. The lymphatics can be the source of chemokine production, express the receptors, or do both. As a route for the passage of numerous circulating cells, lymphatics also serves as a conduit for the flow of chemokines or cells to other destinations, such as lymph nodes.

1.4.1 Chemokines in breast cancer tumor growth

The vicious cycle of inflammatory regulation is well observed in breast cancer. Breast cancer cells secrete inflammatory regulatory factors that promote the progression of inflammation that further accelerate cancer progression⁶³. Proinflammatory cytokines that induce chemokine expression are due to the inflammatory mediators released by the inflammatory response⁶⁴. Thus, chemokines and their receptors can help maintain tumor growth in inflammatory microenvironments.

Chemokines and chemokines receptors are critical molecules in tumor growth. For example, CXCR4/CXCL12 axis promotes cancer cell growth, invasion, and metastasis in most tumors, including breast cancer⁶⁵. Furthermore, CXCR4 derived from fibroblasts promotes breast tumor growth and is associated with a poor prognosis⁶⁶.

Chemokines and their receptors can promote breast cancer growth, but this role is not understood yet. Recent studies suggest that overexpression of CCL28 increases the proliferation of breast cancer cells and effectively inhibits apoptosis⁶⁷. In addition, CCL5 derived from bone marrow regulates the production of myeloid-derived suppressor cells (MDSCs) and promotes the growth of triple-negative breast cancer (TNBC)⁶⁸. These studies suggest that chemokines influence the recruitment of tumor-related immune cells, thereby indirectly promoting breast cancer development.

Upon entering the lymphatics, tumor cells need to survive in a low-oxygen environment. Hypoxia is a significant factor in tumor development and linked to cancer progression⁶⁹. Studies found that CCR5 overexpression increases cell migration; however, CCR5 knockout reduces cell migration triggered by hypoxia. In addition, CCR5 mRNA and CCL5 mRNA levels in clinical samples were associated with the high expression of hypoxia-inducible factor 1 (HIF1) mRNA⁷⁰. Thus, results showed that under hypoxia, HIF-1 regulates CCR5/CCL5 axis. CCL5 and tumor-derived colony-stimulating factors collaborate to promote the development of MDSCs in bone marrow, which aids breast cancer growth⁷¹. In summary, these results suggest that chemokines ligands and their receptors interact with other tumor microenvironment factors to maintain breast cancer cells' growth.

1.4.2 Chemokines in breast cancer angiogenesis

Tumor neovascularization is essential for tumor progression, including cell malignancy, clonal proliferation of transformed cells, local invasion, and distant metastasis⁷⁰. Angiogenesis provides oxygen and nutrients for tumors. In breast cancer patients, the copious blood vessels around the cancerous tissue provide favorable tumor growth and metastasis⁷². Chemokines and their receptors play an essential role in regulating tumor angiogenesis by increasing angiogenic factors or inhibitors.

In theory, CXC family ELR+ chemokines (CXCL1-3,5,6,8) can effectively promote tumor angiogenesis, and ELR- chemokines (CXCL4, 9-10) inhibit angiogenesis. In contrast, some

evidence indicates that chemokine ELR- CXCL12 promotes tumor angiogenesis ⁷³. The secretion and aggregation of CXCL12 in tumor tissues increases under the stimulation of hypoxia and angiogenic factor ⁷⁴. CXCL12 significantly promotes the secretion of vascular endothelial growth factors (VEGFs), which can enhance the proliferation and migration of endothelial cells; but can also enhance the activation of endothelial cells by increasing the expression of intercellular adhesion molecule-1 (ICAM-1) ⁷⁵. The transcription of hypoxia-inducible factors regulates the expression of many angiogenesis molecules, including vascular endothelial growth factor and the chemokine CXCL8 ⁷⁶. Tumor-associated macrophages (TAMs) promote angiogenesis and tumor progression in breast cancer by releasing CCL18. In addition, there is a relationship between chemokines and matrix metalloproteinases in angiogenesis since CCL5 can promote the production of MMP-9 in breast cancer tumor cells ⁷⁷. Another way chemokines can enhance angiogenesis and promote tumor growth is by recruiting immune cells and tumor-related macrophages ⁷⁸. CXCL6 also promotes angiogenesis through the recruitment of centralized granulocytes ⁷⁹. Overall, these results suggest that chemokines directly promote tumor angiogenesis in a variety of ways.

Chemokines promote the development of breast cancer and can inhibit it. CXCL14 can inhibit tumor angiogenesis and reduce cell migration ⁸⁰. In addition, CXCL14 overexpression suppressed breast cancer cell proliferation and invasion, as well as xenograft tumor development and lung metastasis ⁸¹. In summary, CXCL14 inhibits breast cancer cell growth and metastasis, implying that CXCL14 is an anticancer chemokine in breast cancer.

1.4.3 Chemokines in breast cancer tumor metastasis

Tumor angiogenesis is the foundation for tumor metastasis, a key characteristic of malignant tumors and the leading cause of death in advanced breast cancer patients ⁸².

Under physiological conditions, leukocyte migration requires passage through vascular barriers, entry into the circulation, and extravasation at distant organ-specific locations. Chemokines and their ligands regulate these leukocyte trafficking steps. For example, the chemokine ligand CCL27 causes leukocyte antigen CLA+ T cells, which express the chemokine receptor CCR10, migrate to the skin ⁸³, and the bone marrow ligand CXCL12 attracts hematopoietic stem cells that express the receptor CXCR4 ⁸⁴. However, tumor cells also require the regulation of chemokines and their

ligands to spread to distant organs. Thus, chemokines and their receptors play a crucial role in initiating tumor cell migration and metastasis.

Tumor cells can take advantage of these chemokines by expressing the appropriate receptors. For example, in physiological conditions, the chemokine Fractalkine (CX3CL1) solely binds to CX3CR1 and plays a crucial role in the multistep process of leukocyte trafficking using adhesion and chemoattractant properties ⁸⁵. However, in pathological conditions, CX3CL1/CX3CR1 has a histotype-dependent effect on biological disease activity. For example, in breast cancer, abundant expression of CX3CR1 is associated with a risk increase for the development of brain metastasis ⁸⁶. A similar case occurs with the chemokine CXCR3 and its receptor CXCL10. Under physiological conditions, CXCR3/CXCL10 axis regulates immune cell migration, differentiation, and activation, leading to tumor suppression. However, overexpression of CXCR3 is associated with tumor differentiation and lymph node metastasis. In addition, patients with high CXCR3 expression showed poorer overall survival than those with low CXCR3 expression ⁸⁷. Furthermore, our studies show that lymph circulating tumor cells express CXCR3 and CX3CR1 chemokine receptors ⁸⁸. These data suggest that tumor cells do take advantage of chemokines mediating migration through the lymphatic system.

Many other studies have shown that chemokines and their receptors are involved in the process of metastasis. CCR7 ligands (CCL19 and CCL21) are significantly increased in lymph nodes of breast cancer patients. Interestingly, CCL21 expression is higher than CCL19, indicating a higher interaction between CCL21/CCR7 axis ⁸⁹. CCR7 is highly expressed in TNBC cell lines and tissues; however, when absent, it reduces proliferation, migration, and invasion ⁹⁰. In an in vivo murine model of TNBC, knockout of CCR7 reduced the metastasis of 4T1 cells. These results indicate that CCR7 expression in TNBC is related to tumor metastasis.

1.4.4 Chemokine regulation in breast cancer

As mentioned before, functional lymphatic vessels occur at the tumor edge and peritumor regions surrounding the primary tumor ⁵⁹. Thus tumor cells can only enter the lymphatic vessels at the interface between the edge of the tumor and the adjacent host stroma that contains the lymphatic circulation. Active migration by chemotactic factors is likely to occur in tumor cells to facilitate their entry into the lymphatic drainage ⁹¹. During the early stages of infection, the toll-

like receptor (TLR) pathway controls the production of cytokines and chemokines as part of lymph node activation.

TLRs play an essential role in the innate immune response and the subsequent induction of adaptive immunological responses ⁹². TLRs are expressed by several types of immune cells at physiological conditions and found on the cell surface (e.g., TLR1, TLR5, TLR6, and TLR10) or intracellular (e.g., TLR3, TLR7–9, TLR11) in tumor cells ⁹³. TLR signals activated on tumor cells promote cancer development, anti-apoptotic activity, and resistance to host immune responses ^{94–96}. In addition, according to recent research, activated TLRs expressed on tumor cells can decrease the anti-tumor capabilities of invading immune cells, modifying the inflammatory response in a way that favors tumor growth ⁹⁷.

TLRs bind various damage-associated molecular products (DAMPs) that result from endogenous chemicals released by injured or dying cells. Also bind pathogen-associated molecular products (PAMPs), conserved molecular products formed from Gram-positive and Gram-negative bacteria, fungi, and viruses. TLRs trigger immune responses in these two products ⁹⁸. TLRs expressed on tumor cells can activate the NF- κ B cascade releasing anti-apoptotic proteins aiding carcinogenesis and cancer cell proliferation. They can also trigger the release of cytokines and chemokines by tumor cells, which can recruit immune cells and boost immunity in the tumor microenvironment ⁹². These enhanced immune cells secrete more pro-inflammatory cytokines, proangiogenic factors, and growth factors, which degrade the anti-tumor performance of antigen-presenting cells (APCs) and effector T-cells ⁹⁹.

Many breast cancer studies documented the presence of these TLRs-expressing malignant cells. MDA-MB-231 breast cancer cells are highly invasive, but the processes by which they do so remain unknown. One study suggested that their invasiveness is due to the high expression of TLR2 and its activation increases NF- κ B activity in MDA-MB-231 cells but not in MCF-7 cells, a less invasive breast cancer cell line ^{100,101}. TLR3 was also suggested to play a role in breast cancer development and metastasis. Amarante et al. ¹⁰² examined the expression of TLR3, CXCR4, and IFN γ in invasive breast cancer patients; although no statistically significant association was found, TLR3 mRNA levels were positively associated with CXCR4 and IFN γ mRNA levels. Breast cancer patients' tissue study showed that tumors with high TLR3 expression strongly linked with a greater risk of metastasis ¹⁰². These studies show that TLR3 plays a role in breast cancer invasiveness and metastasis ⁹⁹.

1.5 The clinical implications of the lymphatic system in breast cancer

As mentioned above, breast cancer metastasis occurs mainly via the lymphatic system. Sentinel lymph nodes (sLN) are usually the first sites to get involved in metastasis, followed by the lungs, liver, and bones. Although several prognostic markers are known, lymph node status is one of the most important predictive markers for survival in patients with breast cancers, independent of tumor size, histological grade, and other clinicopathological markers ¹⁰³. Patients with axillary metastasis at the time of diagnosis have a much poorer prognosis than those who do not have metastasis. Until recently, complete axillary lymph node dissections (ALND) were performed regularly and were positive in 30% of patients. However, this procedure is associated with long-term morbidity and poor quality of life, manifesting decreased shoulder movement, sensory disturbance, and lymphedema ¹⁰⁴.

The sentinel lymph node (SLN) biopsy, a significantly less invasive method, predicts tumor cell dissemination to regional nodes. The SLN is the first lymph node to receive lymphatic drainage from a tumor containing metastatic cells ¹⁰⁵. In sentinel lymph node dissection (SLND), one or two tracer dyes are injected into the breast during SLND, and the first group of lymph nodes to absorb the dyes is removed for assessment ¹⁰⁶. A sentinel lymph node can be identified in up to 96% of patients using modern techniques and predicts axillary nodal status in at least 95% of patients. Furthermore, SLND has a reduced risk of postoperative morbidity than axillary lymph node dissection ¹⁰⁷. SLND initial therapy of the clinically negative axilla as the standard of treatment is supported by compelling data from several clinical trials ^{108,109}. These findings support the rationale for restricting axillary surgery in patients with minor axillary illness without jeopardizing clinical results.

Although lymph node status is essential in breast cancer management, new research suggests that axillary lymph node metastases may play only a minor role in seeding distant organ metastases ¹¹⁰. The unexpected findings of these studies appear to contradict the long-held belief that there is a clinical relationship between axillary lymph node metastases and patient outcomes. These contradictory findings might be attributed to the increased heterogeneity of tumor cells in lymph nodes. A recent study found that lymph node metastasis had more intratumor heterogeneity than distant metastasis ¹¹¹. This study suggests that lymph node metastasis may be more polyclonal than distant organ metastasis due to a high seeding frequency caused by its physical proximity to the primary tumor. Moreover, to metastasize and colonize other sites, distant metastases may be

subjected to increasing selective pressure. As a result, even if they do not have identical genetic profiles, distant metastasis may seed from lymph node metastasis. Furthermore, emerging technology, such as single-cell analysis, may aid in capturing the heterogeneity of metastatic cells. Deep sequencing coverage may also enable the discovery of less common genomic alterations. As indicated in a previous study, this is especially essential in determining if a dormant subclone seeded distant metastasis within the lymph node ¹¹¹.

As mentioned before, the presence of lymph node disease in cancer patients corresponds with a worse prognosis and, in part, determines the course of therapy ¹¹². However, there is an ongoing debate over the significance of lymph node metastasis in disease development. According to some specialists, isolated lymph node metastases are clinically insignificant ¹¹³. Others argue that lymph node metastases have the potential to seed other organs and should thus be treated to avoid distant metastasis ^{114,115}. With the recent conclusion of clinical studies indicating that nodal dissection beyond the sentinel (first) lymph node does not provide a therapeutic advantage to patients who have undergone adjuvant radiation treatment and systemic therapies ¹¹⁶, this topic has taken on new importance. Other studies have found that radiation therapy to the regional lymph nodes improves the prognosis of patients with early-stage breast cancer ^{115,117}, indicating that treatment of metastatic lymph nodes benefited a subset of individuals ¹¹⁸.

Large lymph node metastases have been associated with distant metastases in animal studies ¹¹⁹. Furthermore, research utilizing patient lymph node samples, human mammary carcinoma cells, and xenograft tumors in immune-deficient mice has revealed that cancer cells can infiltrate lymphatic arteries in the sentinel lymph node and disseminate to other nodes ¹²⁰. Several clinical investigations have also found a link between the number of affected axillary lymph nodes and a greater risk of distant recurrence in breast cancer patients ^{121,122}. Pereira et al. ¹²³ mice studies corroborate these findings by demonstrating that lymph node metastases can serve as a source of cancer cells for distant metastases. Their findings are consistent with those reported separately by Brown et al. in mouse models using various methods ¹²⁴. More research is needed to establish whether cancer cell spread from lymph nodes is a characteristic of human cancer and, if so, whether it should be included in treatment decisions.

1.6 Conclusion

The purpose of this review was to provide a better understanding of breast cancer spread and the underlying lymphatic system processes that aid in disease progression. It provided an overview of the lymphatic system, the lymphatic mechanisms like lymphangiogenesis, tumor microenvironment and immunoediting. It also included a summary of the role of chemokines in different levels of the lymphatic vessels in breast cancer and chemokine regulation by TLR signaling pathway. Characterization of the lymphatic system is essential in order to provide insight into significant predictive associations with metastatic risk. Understanding tumor metastasis via the lymphatic system is a critical step in human cancer therapy. Since the discovery of lymphatic markers, numerous fields have begun to converge in an attempt to identify the roles of lymphatic channels, tumor cells, and products in enabling metastasis to lymph nodes and beyond. Understanding the complexity of lymphatic formation, morphology, and pathophysiology in terms of lymphangiogenic growth factors, receptor signaling, and tumor immunomodulation may reveal plenty of novel therapeutic options for cancer treatment.

CHAPTER 2. LYMPH-CIRCULATING TUMOR CELLS SHOW DISTINCT PROPERTIES TO BLOOD-CIRCULATING TUMOR CELLS AND ARE EFFICIENT METASTATIC PRECURSORS.

THIS IS A PUBLISHED JOURNAL ARTICLE. Reprinted with permission from: Molecular Oncology Journal. **Lymph-circulating tumor cells show distinct properties to blood-circulating tumor cells and are efficient metastatic precursors.** Mol Oncol. Mohammed SI, Torres-Luquis O, Walls E, Lloyd F. 2019 Jun;13(6):1400-1418. doi: 10.1002/1878-0261.12494. Epub 2019 May 23. PMID: 31026363

Abstract

The leading cause of breast cancer-associated death is metastasis. In 80% of solid tumors, metastasis via the lymphatic system precedes metastasis via the vascular system. However, the molecular properties of tumor cells as they exit the primary tumor into the afferent lymphatics en route to the sentinel lymph nodes (SLNs) are not yet known. Here, we developed an innovative technique that enables the collection of lymph and lymph-circulating tumor cells (LCTCs) en route to the SLN in an immunocompetent animal model of breast cancer metastasis. We found that the gene and protein expression profiles of LCTCs and blood-circulating tumor cells (BCTCs) as they exit the primary tumor are similar, but distinct from those of primary tumors and lymph node metastases (LNMs). LCTCs, but not BCTCs, exist in clusters, display a hybrid epithelial/mesenchymal phenotype and cancer stem cell-like properties, and are efficient metastatic precursors. These results demonstrate that tumor cells that metastasize through the lymphatic system are different from those spread by blood circulation. Understanding the relative contribution of these cells to overall peripheral blood-circulating tumor cells is important for cancer therapy. Whether these two types of cell occur in cancer patients remains to be determined.

2.1 Introduction

Breast cancer is the most common malignancy in women. The leading cause of breast cancer-associated death is metastasis¹²⁵. Although advances in early diagnosis and systemic adjuvant therapy targeting primary tumors have significantly improved survival in women with breast cancer, treatments for metastatic disease remain less effective. The problem in identifying therapies targeting metastatic disease is our incomplete understanding of tumor biology during the

metastatic process. During metastasis, tumor cells detach from the primary tumor and may intravasate into and disseminate through the blood circulation or lymphatic system; either route of dissemination can lead to the venous circulation, as the lymphatics drain into the blood¹²⁶. In 80% of solid tumors, metastasis via the lymphatic system precedes metastasis via the vascular system. In many of these tumors, the lymph nodes are the first organ to develop metastasis. As a result, the tumor-draining lymph node, which is the sentinel lymph node (SLN), is accepted universally as the most powerful prognostic tool available for early-stage breast cancer and is often used in disease management⁵⁹. Despite the clinical implications of tumor cell lymphatic spread and lymph node metastasis in breast cancer patient care and management, little is known about the cellular and molecular communication that takes place between the primary tumor and the sentinel node. In addition, lymphatically disseminated tumor cells in transit from the primary tumor to the local lymph node have never been characterized and compared to blood-borne tumor cells in the same host. Several studies have examined tumor cells discharged into the tumor venous drainage¹²⁷, but to our knowledge, there have been no experimental studies of LCTCs in transit from the primary tumor to the local draining SLN. The major reasons for this lack of knowledge have been the microscopic size of the afferent lymphatic vessels, the fragile nature of these vessels, the loss of pressure that occurs as soon as the vessels are punctured, and the difficulty in identifying and cannulating the lymphatic vessels en route to the SLN¹²⁸. The characterization of LCTCs and BCTCs may provide important information about the cascade of metastatic events. Recently, accumulating evidence suggested that the microenvironment of the SLN is greatly influenced at a distance by the primary tumor, which secretes factors such as cytokines, exosomes, or enzymes that pre-condition the lymph node microenvironment, making the lymph nodes supportive metastatic niches for disseminating tumor cells (soil and seed hypothesis)^{129,130}. According to this understanding, the lymphatic fluid draining a primary tumor is expected to be rich in these premetastatic conditioning materials and can serve as discriminating indicators of the tumor metastatic potential. The identification and monitoring of these pre metastatic niche-inducing materials in situ in lymph draining a primary tumor can provide insights about immune recognition or immune priming in the SLN that are highly relevant to tumor treatment. Here, we developed a unique microsurgical technique to collect lymph draining from a primary tumor. We have used an approach that is routinely practiced for the identification and mapping of the draining lymph nodes during the SLN dissection procedure in women diagnosed with breast cancer. The SLN concept

implies that the tumor cells migrating from a primary tumor metastasize to a single lymph node in the relevant lymph node basin¹³¹. The injection of lymphazurin in the breast tissue around the area of the tumor permits the identification of one or more SLNs in the majority of patients. Taking advantage of this concept, we developed a technique to intercept the migration of tumor cells from the primary tumor to the SLN and collect both the lymph and the tumor cells therein. We collected a large enough volume of afferent lymph for adequate analysis. The sample of lymph provides an in situ molecular portrait of the lymph and the lymph-circulating tumor cells (LCTCs). We were able to dissect the critical properties of LCTCs that orchestrate their dissemination and survival in comparison with those of BCTCs from the same animal as they exit the primary tumor. We found that in contrast to BCTCs, LCTCs exist in clusters, display a hybrid epithelial/mesenchymal (E/M) phenotype and cancer stem cell-like properties, and constitute extraordinarily efficient metastatic precursors. In addition, we found that EGF is the major tumor-derived factor in the lymph from metastatic tumor-bearing animals compared to non-metastatic tumor-bearing animals and that the receptor for EGF is expressed in LCTCs but not BCTCs.

2.2 Materials and Methods

2.2.1 Cell lines and culture conditions.

The cell lines used in this study were rat metastatic MTLn3 and nonmetastatic MTC cells kindly provided by Segall (Albert Einstein College of Medicine, Bronx, NY, USA). MTLn3 cell line was clonally derived from a lung metastasis of the 13762NF rat mammary adenocarcinoma (Neriet al., 1982). Both MTLn3 and MTC cell lines were cultured in Minimal Essential Medium, Alpha (MEM; Sigma, St. Louis, MO, USA), containing nonessential amino acids (Sigma), and supplemented with 5% fetal bovine serum (FBS; HyClone, Logan, UT, USA). LCTCs and BCTCs were established in our laboratory from the lymph or the blood, respectively, from rats with metastatic mammary tumors

2.2.2 Animal model.

All experiments involving rats were conducted in accordance with National Institutes of Health regulation on the care and use of experimental animals. Purdue University Animal Use and Care Committee approved the study. Immunocompetent syngeneic female Fisher 344 rats (n=120)

were purchased from Harlan (Indianapolis, IN, USA). The rats were housed in the Purdue Animal Facility and received standard rodent chow and water *ad libitum* and kept at a 12-h light–dark cycle.

2.2.3 Spontaneous metastasis.

To develop spontaneous metastases, rats were injected with MTLn3 or MTC cells or only PBS (vehicle control). Briefly, MTLn3 or MTC cells were grown to 70–80% confluence, trypsinized, washed with PBS, and counted. 1×10^6 cells in 0.1 mL PBS were injected into the two-left caudal- and rostral-most mammary fat pads to establish primary (MTLn3 and MTC) and metastatic tumors (MTLn3).

2.2.4 Lymph fluid and blood collection.

Development of the primary tumors followed by the lymph node and lung metastasis was observed after 14 days post cell implant of MTLn3 cells in rats. Tumor metastasis to the draining lymph node is grossly apparent in MTLn3 tumor-bearing rats. MTLn3 tumor-bearing, MTC tumor-bearing, and PBS-injected animals (no tumor) were then anesthetized with Ketamine/Xylazine at 60 mg per kg⁻¹ of Ketamine/HCl and 5–10 mg per kg⁻¹ Xylazine/HCl by I.P. injections. Lymphatic vessels of tumor-bearing animals and non-tumor-bearing animals were visualized by injecting Lymphazurin dye (1%, isosulfanblue) (United States Surgical Corporation, Ben Venue Laboratories Inc., OH, USA). Routinely, we can collect about 80–100 uL of lymph per animal. From each animal, blood was collected from blood vessels exiting the primary tumor as well; in addition, 3 mL of blood was collected by cardiac puncture. The primary tumor and the draining lymph node tissues were collected and processed for histopathology to confirm metastasis. Five microliters of collected lymph (80–100uL) from each animal was immediately smeared onto a glass slide and examined under a microscope. A portion of the lymph used to grow LCTCs and another portion was used for other analysis. A portion of the blood was used to grow BCTCs.

2.2.5 Tumor histology and assessment of metastasis.

The primary tumors, lymph nodes, and lung tissues from metastatic tumor-bearing rats (implanted with MTLn3 cells), nonmetastatic tumor-bearing rats (implanted with MTC cells) or the primary site of inoculation, lymph node, and lung tissues from the control rats (injected only with PBS) were used for histopathological analysis. Tissues were fixed in formalin, embedded in paraffin, and 5µm sections were stained with H&E.

2.2.6 Lymph- or blood-circulating tumor cells' isolation and propagation.

To isolate and propagate the lymph- or the blood-circulating tumor cells, lymph (~50µL) was mixed with Stem Cell medium EpiCult (STEMCELL, Seattle, WA, USA) in tissue culture dishes and incubated for 5–7 days. Plates were washed several times with PBS, and a fresh stem cell medium was added. To grow cells in 3D culture, cells were transferred to ultralow attachment plates (Corning, Fisher Scientific, Waltham, MA, USA) and were slowly adapted and cultured in Minimal Essential Medium, Alpha (MEM; Sigma), containing nonessential amino acids (Sigma), and supplemented with 5% fetal bovine serum (FBS; HyClone, Logan, UT, USA). After which their epithelial nature was determined by staining with cytokeratin (AE1/AE3+8/18), and CD45 (BD Pharmingen (554875) from BioCare (Pacheco, CA, USA) to exclude the white blood cells using the rat white blood cells as a positive control (purified from the same rat blood cells using Ficoll gradient). Negative controls were prepared by omitting the primary antibodies.

2.2.7 Activsignal IPAD assay.

The cells from lymph allowed to grow were collected and lysed in PBS + 1% NP40 lysis buffer. The lysates were sent to ActivSignal for further processing (<http://www.activsignal.com>). ActivSignal IPAD platform is a proprietary technology for analyzing the activity of multiple signaling pathways in one reaction. Activities of more than 20 signaling pathways are monitored simultaneously in a single well through assessing expression or protein phosphorylation of 70 target human proteins. The technology allows detection of targets with high specificity and sensitivity due to combination of two distinct antibodies per each target. Each pathway is covered by multiple targets.

2.2.8 NanoString nCounter analysis.

RNA from cells and tissues was harvested using an RNA Isolation Kit (Roche, Basel, Switzerland) as per the manufacturer's instructions. All RNA quantified used the DeNovix DS-11 spectrophotometer. Samples were processed for analysis on the Nano-String nCounter Flex system using the 770 gene Pan Cancer Pathways Plus panel (606 critical genes from 13 canonical cancer pathways, 124 cancer driver genes, and 40 reference genes) and nCounter PanCancer Immune Profiling Panel from NanoString Technologies (Seattle, WA, USA), as per manufacturer's instructions.

2.2.9 RNA expression analysis

Resource compiler (RCC) data files were imported into NanoString nSolver 3.0 and further analyzed using the PanCancer Pathways Advanced Analysis Module, which normalizes gene expression to a set of positive and negative control genes built into the platform. Using the nCounter analysis software, we identified a list of genes with significantly altered expression between LCTC, BCTC, LMNs, and primary tumors. The fold change and P-values were calculated using nCounter default settings. As recommended, genes whose expression levels were below the level of the negative controls were removed from the analysis. With the remaining list of genes on the PanCancer panel, a filter cutoff of foldchange $\geq \pm 1.5$ or $\geq \pm 2$ and P -value < 0.05 were used to identify the significant gene expression changes based on the nCounter analysis. A pathway score was calculated using nSolver Advanced Analysis from the expression levels of the relevant genes in 13 canonical pathways using measurements of pathway activity values derived from singular value decompositions. This method uses metagenes to represent pathway activity and aims to capture not only over-represented significantly altered genes but also smaller but cumulatively impactful changes within a pathway.

2.2.10 Lymph chemokine/cytokine determination.

Chemokine/cytokine levels in the lymph collected from metastatic tumor-bearing rats, nonmetastatic tumor-bearing rats, and normal control rats (total $n=30$) and supernatant from cells cultures were measured using MILLIPLEX Rat Expanded Cytokine/Chemokine Magnetic Bead Premixed 27 Immunology Multi-plex Assay (EMD Millipore, Billerica, MA, USA) as per the

manufacturer's instructions. Standard curves were generated from known concentrations of each cytokine and then used to determine the quantity of cytokine in each sample based on the level of spectrophotometric absorbance of the sample using regression analysis. Each assay was performed in triplicate and each value shown in the figures is the mean of the triplicate. Quantification of real-time PCR Total RNAs were extracted from LCTCs and BCTCs, using TRIzol RNA Isolation Reagents as per the manufacturer's instructions (Invitrogen, Carlsbad, CA, USA). RNAs were reverse-transcribed by oligo(dT)primer using Superscript RT-PCR kit from Roche, according to the manufacturer's instructions. PCR was performed under the following conditions: 94°C for 3 min; 94°C for 30 s; 58°C for 30 s; 72°C for 30s for 40 cycles; and 72°C for 10 min, using IQ SYBR Green Supermix Kit from Roche. Results were analyzed by the relative quantification method and expressed as relative RNA levels (ΔCT , difference of cycling threshold). ΔCT values represent $CT [gene]-CT [GAPDH]$; thus, higher values indicate relatively lower expression levels.

2.2.11 Western blot analysis.

Cells were grown in 3D cultures, and proteins were isolated using RIPA buffer (0.5M Tris/HCl, pH 7.4, 1.5M NaCl, 2.5% deoxycholic acid, 10% NP-40, 10 mM EDTA). Protein concentrations were determined using Pierce BCA Protein Assay Kit according to the manufacturer's instructions (Thermo Fisher Scientific). Ten micrograms of each sample protein were subjected to SDS/PAGE and transferred to nitrocellulose paper. The blots were reacted sequentially with primary antibodies: HRP-conjugated goat anti-rabbit IgG or goat anti-mouse IgG and visualized with diaminobenzidine. Immunocytochemistry cells were fixed with 1:1 methanol:acetone and pre-blocked with 1% bovine serum albumin in PBS. Cells were then incubated with the following anti-primary antibodies: E-cadherin, N-cadherin, CXCR3, CX3CR1 and CXCR4 (Novus, Littleton, CO) at 4°C overnight, followed by the secondary antibody conjugated with Alexa Fluor 594 or FITC (Jackson ImmunoResearch, West Grove, PA, USA). The cells were mounted with mounting medium containing 1 $\mu\text{g per mL}^{-1}$ DAPI (4', 6'-diamidino-2-phenylindole; Sigma).

2.2.12 Statistical analysis.

All data are presented as means standard deviation (SD). Statistical calculations were performed with Microsoft Excel analysis tools. Differences between individual groups were analyzed by paired t-test. *P*-values of <0.05 were considered statistically significant.

2.3 Results

2.3.1 Visualization and mapping of lymphatic vessels allow the isolation of LCTCs before they reach the regional lymph nodes.

We developed a novel microsurgical technique for the collection of lymph draining a primary tumor prior to its entry into the SLN. We used metastatic MTLn3 and nonmetastatic MTC cell lines that were transplanted orthotopically into the mammary fat pads of immunocompetent female Fisher 344 rats for the syngeneic model. These two cell lines were isolated from the same parent tumor, 13762NF mammary adenocarcinoma, but differed in their ability to metastasize¹³². Approximately 10–14 days after injecting the cells, tumors developed in all MTLn3- and MTC-implanted rats. The PBS injection site was free of tumors (negative controls). To visualize and map the afferent lymphatic vessels prior to entering the draining SLNs to make it possible to collect the lymph, we injected approximately 10 uL of lymphazurin dye around the circumference of the primary tumor or the control injection site. After careful dissection of the skin over the tumor and lymph node area, the SLNs and afferent lymphatic vessels were identified by their green color (Fig. 1A, B) and cannulated. This procedure is similar to the procedure that is routinely performed for SLN dissection in women with breast cancer. Routinely, 20–80 uL of lymph per rat was collected before the lymph vessels collapsed. The outcome of this innovative work showed that the collection of lymph draining a primary tumor prior to its entry into the draining SLN was reliable and reproducible and yielded an adequate volume for analysis.

2.3.2 Lymph node metastasis was confirmed in MTLn3 tumor-bearing animals.

Histologic evaluation was used to verify the presence, number, and size of metastases in the SLNs and lungs. Gross whitish colonies of tumor cells were observed in the lymph nodes and lungs of MTLn3 tumor-bearing rats but not in the lymph nodes or lungs of MTC tumor-bearing

rats. The metastatic colonies were confirmed to be malignant tumor cells by histopathology (Fig. 1C).

2.3.3 LCTCs existed in clusters and could be reliably harvested in the MTLn3 tumor-draining lymph prior to their entry into the SLN.

In this study, we successfully identified, cannulated, and collected the lymph and LCTCs on their way to the SLN. To ensure that the lymph contained tumor cells, we smeared 5 μ L of the collected lymph from each animal onto a microscope glass slide for cytopathologic staining and immunohistochemistry. LCTCs were found in clumps (50–75 cells), and a subset of LCTCs was arranged in pseudo acini (Fig. 1D, E). Blood-circulating tumor cells (BCTCs) were collected in a similar way from blood vessels (data not shown). Both cells in the lymph and the blood were cultured first in 2-dimensional (2D) mono-layer cell culture plates (to separate them from white blood cells which do not attach to the bottom of the plate or survive for a long period of time), and the attached tumor cells were washed thoroughly and then propagated in ultralow attachment cell culture plates (Fig. 1F). To confirm the epithelial origin of the cells and exclude an immune cell origin of the propagated cells, we used the accepted CTC characteristics, which include the presence of a nucleus, visible cytoplasm, and the expression of cytokeratin and the absence of CD45 expression¹³³, using both hematoxylin and eosin (H&E) and immunostaining. Both LCTCs and BCTCs are large in size, grow well in vitro in 3D cultures, and stain positive for cytokeratin and negative for CD45, confirming their epithelial origin (Fig. 1G). Together, these data confirmed that it is possible to collect LCTCs and BCTCs as they exit the primary tumor and that these cells can be readily propagated and identified. To avoid the effects of in vitro culture, all LCTC characterizations were performed on cells smeared directly from the lymph, and tumor cells were then collected from the slides or by using the first passage of cells before splitting.

2.3.4 LCTCs and BCTCs share similar gene profiles that are distinct from those of the primary tumor and LNMs.

We then determined whether LCTCs, BCTCs, primary tumors, and synchronous LNMs share similar gene expression profiles indicative of the same origin. RNA was collected from cells directly from the lymph. Gene expression analysis was performed using the 770 known cancer genes from 13 canonical cancer-associated pathways that include MAPK, STS, PI3K, RAS, cell

cycle, apoptosis, Hedgehog, Wnt, DNA damage control, transcriptional regulation, chromatin modification, and TGF- β in the NanoString PanCancerPathways Panel (NanoString Technologies). The principal component analysis was conducted to assess overall gene expression similarity across samples. LCTCs and BCTCs clustered together, while primary tumors and LNMs clustered together, suggesting that gene expression was similar between LCTCs and BCTCs and differed from that of the primary tumor and LNMs despite the same parent cell origin (MTLn3). The differentially expressed genes in LCTCs, BCTCs, and LNMs that exhibited a log₂-fold change > 2.0 or < 2.0 and $P \leq 0.05$ compared to primary tumors are shown in Fig. 2A–C. In total, 122 and 116 genes exhibited altered expression in LCTCs vs primary tumors and BCTCs vs primary tumors, respectively. Relative to the primary tumor, LCTCs exhibited an increase in log₂-fold expression for GADD55a, BAMBI, STRP4, TSPAN7, DDIT3, IL1a, and CSF3 and a decrease in log₂-fold expression for COL1A2, COL5A1, COL5A2, PDGFRB, CARD11, GAQS1, IGF1, SFRP2, and COL3A1. Compared to the primary tumor, BCTCs exhibited increased expression of CSF3, WNT5B, BAMBI, MGMT, MLF1, GADD45A, HSPB1, PLAT, DUSP, and TSPAN7 and decreased expression of COL1A1, PDGFRB, COL3A1, COL5A1, IGF1, COL5A2, CARD11, GAS1, SFRP2, and COL1A2. However, only three genes were upregulated ($P < 0.05$; $> 2 \log_2$) in BCTCs compared to LCTCs (Fig. 2D, E), given that these cells originated from the same primary tumors, with one cell type found in the blood and the other cell type found in the lymph fluid. These three genes were FUBP1, which plays a role in glucose metabolism, PLAT or tPA, which is a plasminogen activator that maintains blood and lymph fluidity, and FGFR2, which mediates a wide spectrum of cellular responses that are crucial for the development and wound healing. Altered expression of these genes was shown to be associated with cancer progression, survival and death, and migration^{134–136}. To examine our differential gene expression analysis from a pathway perspective rather than the level of individual genes, we performed pathway score analysis, which summarizes the data from the genes in a pathway with a single score. This approach helps in understanding which pathway scores cluster together and which samples exhibit similar pathway scores. A heatmap of pathway scores that provides a high-level overview of how the pathway scores change across samples is presented in Fig. 3A. All 13 pathways examined had lower scores in BCTCs and LCTCs than in the primary tumor and LNMs (Fig. 3A). Figure 3B shows box-and-whisker plots comparing the scores of some selected pathways. We then used gene set analysis to assess the importance of the 13 examined canonical pathway activities in LCTCs,

BCTCs, and LNMs relative to primary tumor cells. Global significance statistics were used to analyze cumulative evidence for the differential expression of genes in each pathway. Among the significantly ($P < 0.05$) altered pathways were WNT and PI3K, which had the lowest scores in both LCTCs and BCTCs compared to primary tumors (Fig. 3C). In contrast, the TGF- β , apoptosis, cell cycle, and DNA damage repair pathways had upregulation in both LCTCs and BCTCs compared with those in primary tumors (Fig. 3C). Volcano plots displaying each gene's $-\log_{10}$ (P-value) and \log_2 -fold change for the selected covariate were used. Figure 3D1 shows volcano blots for TGF-beta, and Fig. 3D2 shows volcano blots for PI3K signaling pathways.

2.3.5 LCTC and BCTC protein expression and phosphorylation status.

To confirm the expression of the above signaling pathways at the protein level, we used the immuno-paired-antibody detection (IPAD) system provided by ActivSignal, Inc. (Natick, MA, USA). This analysis provides information on the phosphorylation states, protein levels, and cleavage of more than 60 signaling factors that cover more than 20 major signaling pathways. IPAD analysis revealed the significant upregulation of proteins that affect the DNA damage response, the cell cycle, apoptosis, epithelial–mesenchymal transition (EMT), and the TGF β and EGFR pathways in LCTCs and BCTCs (Fig. 4), confirming our gene expression data. Specifically, we show changes in cell cycle progression (the upregulation of p27) (Fig. 4A), the activation of DNA damage repair (decreased phosphorylation of histone H2AX and Chk2) (Fig. 4B), and the activation of apoptosis, EGFR, TGF- β , and JAK/STAT (increased phosphorylation of Smad, Mek-1, and p-44) (Fig. 4C–F) and EMT (the upregulation of Mek-1 and p-44) (Fig. 4G). However, we observed lower expression and phosphorylation of p-27, Mek-1, and p-44 in lymph node metastases (LNMs) than in the other cell types. In addition, the IPAD analysis revealed other pathways that were not shown to be altered in our gene expression analysis. These pathways include NF- κ B, the heat shock response, and the unfolded protein response, which were similar in all samples, and signaling pathways that were upregulated only in LCTCs and BCTCs, such as mTOR, insulin receptors, and IGF1R. Collectively, the gene and protein expression data indicate the upregulation of signaling pathways involved in cell motility (EGFR, EGF, ErbB2, IGF-IR, and tPA) and signaling pathways involved in angiogenesis (VEGFR and PDGFR) (Fig. 4H), cell-proliferation, and DNA repair.

2.3.6 LCTCs display a hybrid E/M phenotype.

Because our transcriptional and translational analyses showed upregulation of the TGF- β pathway and EMT inducer, in LCTCs and BCTCs, we assessed the E/M phenotypes of LCTCs and BCTCs by measuring E/M markers. During the EMT process, cells lose the epithelial markers E-cadherin and cytokeratin and gain the mesenchymal markers vimentin and N-cadherin¹³⁷. The loss of these intercellular adhesion molecules allows cells to become motile and enter the bloodstream or lymphatic system¹³⁸. BCTCs exclusively expressed the mesenchymal markers N-cadherin and vimentin, whereas LCTCs expressed vimentin and the epithelial phenotype markers E-cadherin and N-cadherin (Fig. 5A and C). LCTCs and BCTCs expressed similar levels of the EMT transcriptional factors TWIST1, ZEB1, ZEB2, SNAI1, SNAI2, and BMI1 (Fig. 5B), which organize entrance into a mesenchymal state by suppressing the expression of epithelial markers and inducing the expression of other mesenchymal markers¹³⁸. These LCTC phenotypic characteristics were consistent with the hybrid E/M state, which represents a partial or intermediate E/M phenotype¹³⁹. Cells with the hybrid E/M phenotype have both epithelial properties, such as adhesion, and mesenchymal properties, such as migration¹⁴⁰. These properties allow these cells to move collectively as clusters. Cells in clusters can exit the bloodstream more efficiently, are more resistant to apoptosis, and can be up to 50 times more metastatic than individually migrating cells¹⁴⁰. Furthermore, EMT has been associated with epithelial and carcinoma stem cell properties¹⁴¹.

2.3.7 LCTCs display cancer stem cell properties and have a higher propensity than BCTCs to form mammospheres in culture and to form tumors in vivo.

The induction of EMT in immortalized human mammary epithelial cells results in the acquisition of mesenchymal traits and the expression of stem cell markers, resulting in an increased ability to form mammospheres, a property associated with mammary epithelial stem cells¹⁴¹. Therefore, we reasoned that cancer stem cells (CSCs) or tumor-initiating cells must be a component of LCTCs and BCTCs. Using immunohistochemistry and immunofluorescence, we examined the CSC properties of LCTCs and BCTCs using the accepted breast cancer stem markers CD29, CD44, and CD24^{142–145}. LCTCs were enriched in cells that are CD29⁺, CD44⁺, and CD24⁺, whereas BCTCs were enriched in cells that express CD29⁺ and CD44⁺ but are CD24⁻ or CD24^{low} (Fig. 6A). Compared to BCTCs and MTLn3 cells, LCTCs also expressed high levels of additional CSC markers, such as NANOG, MMP9, and ALDH1¹⁴⁶ (Fig. 6B, C). These data suggest that

LCTCs have CSC-like properties, as demonstrated by the expression of CD29⁺/CD44⁺/CD24⁺ surface markers and high levels of ALDH1, which have been shown to increase in cells with stem/progenitor properties ¹⁴⁶. By contrast, BCTCs included cells that had the phenotype CD29⁺/CD44⁺/CD24^{low}. To further assess the self-renewal properties of LCTCs and BCTCs, we performed two assays that are routinely used to assess cancer cell stemness, *in vitro* spherical colony or mammosphere formation ¹⁴⁷ and *in vivo* tumor formation in immunocompromised mice ¹⁴⁸. Both LCTCs and BCTCs grew as nonadherent mammospheres in ultralow attachment plates; however, LCTCs formed ten times more mammospheres than BCTCs, showing the unique self-renewal ability of LCTCs (Fig. 6D). Next, we examined the tumor-initiating capacities of LCTCs, BCTCs, and the parent MTLn3 cells. To this end, we transplanted cells, after sorting using fluorescence-activated cell sorting (FACS) in limiting dilutions, into the mammary fat pads of female immunocompetent rats. We observed that 1x10⁶ cells were the threshold concentration for successful colonization and tumor formation for MTLn3 cells and BCTCs (Fig. 6E). BCTCs and MTLn3 cells at concentrations of 1x10³ or 2x10⁵ cells, respectively, failed to form tumors during the 6 weeks following implantation. In contrast, the injection of 2x10³, 2x10⁵, or 1x10⁶ LCTCs resulted in visible, large tumors within 2 weeks in all three rats (Fig. 6E). These data demonstrated that in contrast to BCTCs, LCTCs possess stem-like properties and have the ability to self-renew and efficiently form tumors.

2.3.8 LCTCs and BCTCs downregulate antigen presentation pathways to escape the immune response.

We next examined the immune profiles of LCTCs, BCTCs, and LNMs compared to that of the primary tumor to understand why these cells are not detected by the immune system, either in the blood or in the lymph. We performed targeted gene expression profiling using a custom 795-gene NanoString Panel composed of immune-related genes and genes pertaining to common cancer signaling pathways (NanoString Technologies). Our undirected and directed global significance analyses (Fig. 7A) showed that the tumor necrosis factor (TNF) superfamily pathway was upregulated in LCTCs and BCTCs but not in LNMs compared with primary tumors. Although TNF is mainly produced by lymphocytes, it is also produced by tumor cells ^{149,150} and affects cellular processes such as apoptosis, necrosis, angiogenesis, immune cell activation, differentiation, and cell migration ¹⁵¹. On the other hand, the antigen presentation, pathogen

response, and major histocompatibility complex (MHC) were among the significantly downregulated immune pathways in LCTCs and BCTCs compared to primary tumors. These data suggest that LCTCs and BCTCs undergo immune escape and become invisible by downregulating the antigen-processing machinery. This work, for the first time, shed light on how circulating tumor cells in the lymph evade the immune system.

2.3.9 The lymph immune microenvironment.

We next examined the cytokines/chemokines and growth factors in the primary tumor-draining lymph (tumor-derived factors) prior to lymph node entry to determine which factors may protect LCTCs, promote their migration to the lymph nodes, and aid in premetastatic niche formation. A multiplex assay consisting of 27 cytokines, chemokines, and growth factors was used to profile these factors in lymph from metastatic tumor-bearing, nonmetastatic tumor-bearing, and non-tumor-bearing control rats. Of the 27 cytokines/chemokines examined, 18 had > 2-fold increases in the metastatic lymph relative to the normal lymph (Fig.7B). EGF, TNF- α , IFN- γ -induced protein 10 (IP-10 or CXCL10), vascular endothelial growth factor (VEGF), and fractalkine (CX3CL1) showed >10-fold increases, and interleukin 18 (IL-18) showed a >70-fold increase in the metastatic lymph compared to the normal lymph (Fig. 7B). These cytokines/chemokines and growth factors play an important role in stimulating immune responses, immune cell chemotaxis, and tumor cell migration, invasion, and metastasis¹⁵²⁻¹⁵⁵.

Comparing the lymph from animals with tumors and metastases to that of animals with tumors but without metastases, EGF, and keratinocyte chemoattractant/human growth-regulated oncogene (GRO KC or CXCL1) showed >10-fold increases in the metastatic lymph compared to the nonmetastatic lymph (Fig. 7C). EGF is released by cells and then binds to its receptor (EGFR) on either the cell itself, stimulating its own growth, or on neighboring cells, stimulating the ability of the cells to divide¹⁵⁶, while CXCL1 (bind to CXCR2) plays a role in the immune response, attracts CD11b⁺Gr1⁺ myeloid cells into the tumor, and enhances the survival of tumor cells facing the challenge of invading new microenvironments, tipping the balance from immune protection to tumor promotion^{157,158}. Moreover, IL-12p, which stimulates IFN- γ production and activates both innate (NK cells) and adaptive (cytotoxic T lymphocytes) immunity^{159,160}, IFN- γ , and other cytokines involved in T-cell stimulation and differentiation, macrophage activation, and class II MHC expression^{161,162} were not detected in the metastatic lymph in appreciable amounts relative

to the those in the nonmetastatic lymph (Fig. 7C). These data suggest that the metastatic lymph microenvironment is enriched in molecules that stimulate immune responses, immune cell chemotaxis, and tumor cell migration, invasion, and metastasis but is not enriched in molecules that stimulate T lymphocyte activation and gene processing and presentation, favoring the formation of an immunosuppressive microenvironment.

2.3.10 Primary tumor-derived factors in the lymph are also produced by LCTCs and act in a paracrine manner.

To determine whether the primary tumor-derived factors produced in the lymph fluid were also produced by LCTCs and BCTCs, we performed the same multiplex assays using growth medium from LCTCs, BCTCs, and the MTLn3 cell line. The LCTCs produced > 10-fold higher fractalkine (CX3CL1), IP-10 (CXCL10, which binds to CXCR3), macrophage inflammatory protein 2 (MIP-2, CXCL2/CXC11), and VEGF levels than the BCTCs (Fig. 7D). However, none of the cells produced detectable EGF levels (Fig. 7D). Finally, we examined LCTCs and BCTCs for the receptors of these factors and found that LCTCs expressed the EGFR protein, while BCTCs did not express EGFR (Fig. 7F). Compared to BCTCs, LCTCs expressed high levels of the CX3CR1 protein (CX3CL1 receptor) but similar protein levels of CXCR3 (CXCL10 receptor) (Fig. 7E, F). Additionally, we compared our data for CXCR4, which is known to be expressed in peripheral blood CTCs from breast cancer patients¹⁶³. We found that both LCTCs and BCTCs expressed CXCR4 (Fig. 7E, F). These data suggest that the cytokines and chemokines found in the lymph are partly produced by LCTCs and may function in a paracrine manner. In addition, our data may provide some evidence that interactions between LCTCs and the tumor-associated lymph microenvironment could establish a potential positive-feedback loop that contributes to lymph node metastasis. This result also suggests that BCTCs differ from LCTCs and may produce different factors to survive in the blood microenvironment.

2.4 Discussion

Analyzing the phenotypic and molecular characteristics of LCTCs and BCTCs as they exit the primary tumor and identifying the factors that orchestrate their metastatic potential is an important step for understanding the biology of these cells and the metastasis process. These characteristics may not be evident through an analysis of bulk primary or metastatic tumor

populations ¹⁶⁴ or even peripheral CTCs (P-CTCs) alone ¹⁶⁵. P-CTCs are derived from many sources that include primary tumors, metastatic lesions in different organs, and tumor cells existing in the lymph nodes; therefore, these cells may have altered phenotypes/genotypes depending on their organ of origin ¹⁶⁶. Here, we demonstrated that it is possible to identify the afferent lymphatic vessels and collect the lymph fluid and tumor cells therein before they reach the regional lymph nodes, as well as BCTCs as they exit the primary tumor. Thus, examining the intercellular and extracellular properties and microenvironments of tumor cells (LCTCs and BCTCs) as they exit the primary tumor in comparison with each other, the primary tumor and LNMs may provide critical information about cancer biology and the metastatic process, which has important clinical implications.

To our knowledge, our study is the first to study tumor cells as they exit the primary tumor into the lymph en route to the lymph node. Here, we accurately identified LCTCs and BCTCs and found that LCTCs exist in clusters or clumps of 10–75 cells (Fig. 1C). Given the short distance between the tumor and the SLN and the one-way nature of cell traffic, we believe these clusters originated from the primary tumor and were not a result of multidirectional movement ¹⁶⁷; therefore, these cells represent pure cells coming from the primary tumor and not a mixture of cells from the primary tumor and metastases, as is the case for P-CTCs. Clumps of tumor cells in the blood were initially observed by Liotta et al. ¹²⁷ and were suggested to arise from oligoclonal tumor cell groupings and not from intravascular aggregation ¹⁶⁴. We observed that LCTCs exist as clumps along the lymphatic vessels (data not shown), suggesting that they move as cohesive clusters. This observation is supported by intravital imaging studies that showed that cell clusters rather than single cells invaded through the lymphatic system instead of the blood circulation ¹⁶⁸, suggesting that single cell motility is essential for blood-borne metastasis, while cohesive invasion is involved in lymphatic spread ¹⁶⁸. Unlike LCTCs, large P-CTC clusters are rare in the peripheral venous circulation and constitute only approximately 2.6% of the total P-CTC population ¹⁶⁴. P-CTC clusters have been known for many years to seed colonies with greater efficiency and were recently reported to have 50 times greater metastatic potential than individual P-CTCs ^{164,169}. This behavior of cell clusters was reported to be due to a number of factors, including protection against anchorage-dependent apoptosis ¹⁷⁰ and shielding from assault by immune cells ¹⁷¹.

We then investigated the molecular characteristics (transcriptome, proteome, and immune landscapes) of these living tumor cell clusters as they exit the primary tumor en route to the lymph

node and compared them to those of LNMs, the primary tumor, and BCTCs. Although in our study, all tumor cells (primary tumor, LNMs, LCTCs, and BCTCs) originated from a single parent tumor cell line (MTLn3), we found striking differences in the gene expression and pathway scores of tumor cells engaged in their microenvironments (primary tumor and LNMs) and those of lymph- or blood-circulating cells (LCTCs and BCTCs). Our findings are consistent with those of studies that reported that P-CTCs are biologically different from primary tumors^{172,173}. The detachment of cancer cells from primary tumors and their ability to survive outside their natural extracellular matrix niches may lead these circulating cells to undergo dramatic biological changes¹⁷⁴. These findings have tremendous implications for cancer treatment because primary tumor molecular characterization currently plays an important role in the treatment strategies as well as the prognosis of breast cancer; therefore, reliance on the primary tumor characteristics can be misleading^{172,173,175–177}.

Our data also showed that most of the pathways examined were downregulated in LCTCs and BCTCs compared to primary tumors and LNMs, except for pathways that control DNA repair, the cell cycle, apoptosis, and TGF- β . The upregulation of apoptosis, cell cycle, and DNA damage repair pathways may constitute strategies by which LCTCs and BCTCs survive stressful conditions by initiating complex signaling networks to monitor the integrity of the genome during replication and initiate cell cycle arrest, repair, or apoptotic responses if errors are detected¹⁷⁸. Enhanced DNA repair capabilities were reported previously in CTCs from breast cancer compared to primary tumors. This finding is important and has clinical implications, especially when treating cancer patients with DNA-damaging therapies, such as anthracyclines and platinum, which are known DNA-damaging drugs that are routinely used for breast cancer treatment¹⁷⁹.

Our data also showed that there were striking differences between LCTCs and BCTCs. LCTCs but not BCTCs exhibited altered TGF- β and EMT pathways and were found in clusters. One of the characteristics of these cell clusters is the coexpression of E/M markers, which is known as hybrid or partial EMT¹⁸⁰. In fact, LCTCs but not BCTCs exhibited a hybrid EMT phenotype, which indicates that LCTCs have mixed epithelial and mesenchymal properties, thereby allowing them to move collectively as clusters¹⁸¹.

As we mentioned earlier, cells in clusters were characterized by a higher metastatic potential than cells that were not in clusters and could predict a poor prognosis in breast cancer patients¹⁸². It was also shown that these clusters are more capable of initiating metastatic lesions than cancer

cells that are moving individually with a wholly mesenchymal phenotype, having undergone complete EMT^{181,182}. This tumor-initiating capability is an attribute of stemness-like properties that drive metastasis and reoccurrence¹⁴⁸. The CSCs were shown to coexpress epithelial markers (CD24 or ALDH1) and mesenchymal markers (CD44)^{142,183}, as we have shown that LCTCs coexpress the CSC markers CD24, CD44, and ALDH1 (Fig. 7A), and BCTCs express only CD44 and ALDH1. This result is supported by a few recent studies that suggested that cells in a hybrid or partial EMT state are most likely than cells in a pure epithelial or pure mesenchymal state to exhibit stemness¹⁴⁸. Furthermore, the co-expression of both epithelial and mesenchymal genes in the same cell promotes mammosphere formation and stemness¹⁴⁸. Collectively, our findings showed that compared to BCTCs, LCTC clusters exhibit hybrid E/M and stemness properties and therefore constitute extraordinarily efficient metastatic precursors in breast cancer. These data comparing LCTCs to BCTCs as they exit the primary tumor allowed for the identification of a specific signature of LCTCs that provides crucial information on their stem cell properties, as well as their ability to initiate and support the formation of LNMs. More studies are needed to further elucidate the characteristics of these cells and investigate the specific molecular mechanisms involved in breast cancer progression and the development of new drugs to inhibit metastasis.

Despite the immunological power of lymph nodes, tumor cells are able to avoid immune surveillance in the lymph fluid and the lymph node, colonize the lymph node, and then migrate to distant sites. Innate and adaptive immune responses that include macrophages, natural killer cells, interferon- γ (IFN- γ) secretion, and CD8⁺ cytotoxic T lymphocytes (CTLs) constitute the immunosurveillance mechanisms by which transformed cells are eliminated¹⁸⁴. Under this immunosurveillance mechanism, tumor cells in the lymph may develop a phenotype that helps them avoid recognition by the immune system. Consistent with this understanding, we found that LCTCs exhibit a distinct nonimmunogenic phenotype by downregulating gene processing and presentation and MHC pathways, which may significantly impair the ability of CD8⁺ CTLs to recognize these cells, allowing LCTCs to survive undetected despite the presence of immune cells and supporting progression and the colonization of the lymph node¹⁸⁵. The evasion of the immune response is a significant event in tumor development and is considered one of the hallmarks of cancer. Therefore, distinct therapeutic strategies, which depend on the biology and mechanism of immune evasion exploited by tumor cells in the lymph, may be required for restoring productive cancer immunosurveillance.

Furthermore, accumulating evidence suggests that the primary tumor releases molecules that influence the microenvironment of the SLN and make them a permissive site, known as the premetastatic niche, for receiving disseminated tumor cells and thus promoting cell proliferation and subsequent metastases⁶². We reasoned that the analysis of the tumor-draining lymph may help us identify some of these factors. We showed that the metastatic lymph contains secreted factors that differ in type and expression levels from those found in the normal and nonmetastatic lymph. Specifically, the metastatic lymph had high levels of EGF, while this growth factor was not detected in the nonmetastatic lymph. Moreover, we showed that LCTCs but not BCTCs express EGFR. EGF/EGFR-induced signaling is associated with organ morphogenesis, maintenance, and repair, as well as tumor invasion and metastasis^{186,187}. Collectively, our data showed that the activation of EGF/EGFR signaling in the lymph and LCTCs may create a microenvironment that is conducive to metastasis, providing a rationale for efforts to inhibit EGFR signaling in lymph metastases. However, the significance of EGFR signaling in BCTCs may need to be re-evaluated.

We then assessed whether LCTCs contributed to the cytokine/chemokine pool found in lymph fluid. We showed that LCTCs released the IP-10 (CXCL10), VEGF, fractalkine (CX3CL1), and MIP-2 (CXCL2) cytokines, which were produced at high levels in the metastatic lymph (Fig. 7B). In addition, LCTCs expressed the receptors for the cytokines CX3CL1, CXCL10, CX3CR1, and CXCR3. Our data suggest that cytokines and growth factors released by the tumor microenvironment in the lymph and LCTCs themselves may represent extracellular triggers that control the migration programs of LCTCs¹⁸⁸. The CX3CR1/CX3CL1 and CXCR3/CXCL10 axes have been demonstrated to be involved in the proliferation, survival, and metastasis of various malignant tumor types, including breast cancer, and were suggested to predict the site of metastatic relapse^{189,190}. These studies support the continued examination of the CX3CR1/CX3CL1 and CXCR3/CXCL10 axes as potential therapeutic targets in patients with breast cancer.

2.5 Conclusion

In conclusion, we now have the capability to routinely characterize the molecular and cellular composition of tumor-derived native lymph in transit to the draining SLN. This approach will provide a new level of information that is highly relevant to our understanding of metastasis. Moreover, the contribution of LCTCs to the overall metastatic process is not fully understood, and the percentage of tumor-draining lymph cells that enter the general hematogenous circulation is

unknown. The answers to these questions will provide important insights into the molecular characteristics of metastasis.

2.6 Acknowledgements

The work was supported by DOD concept award # W81XWH-04-1-0747 and NIH/NCI grant # 1R21CA199621-01A1. We thank Dr. Chun-Ju Chang and Mi Ran Kim for their help with EMT confocal image and Dr. Segall from Albert Einstein College of Medicine, Bronx, NY, for providing the MTLn3 and MTC cell lines.

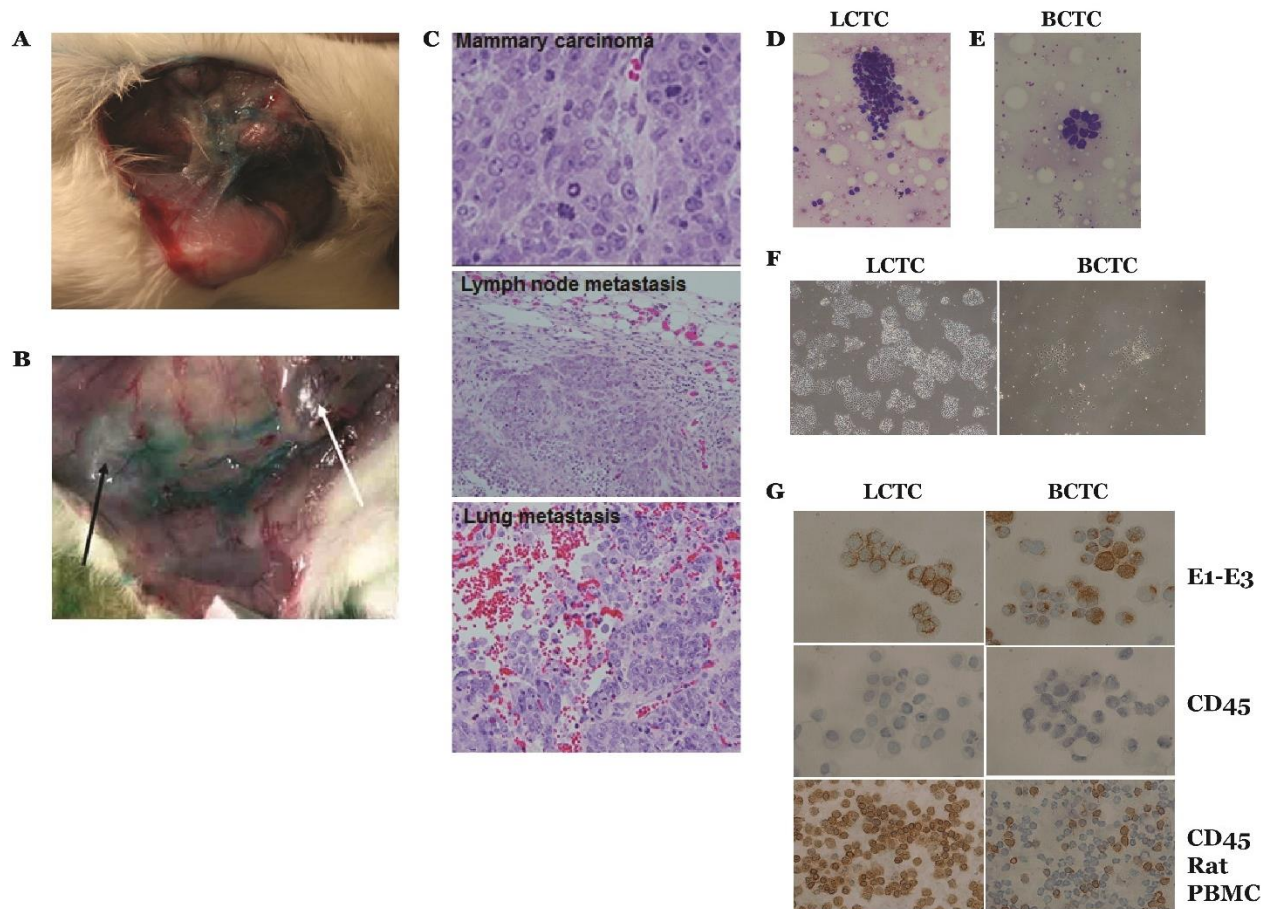


Figure 2.1: Lymph vessel visualization, lymph and LCTC collection, identification, and growth.

(A) Female rats were implanted with metastatic cell line MTLn3, and after tumor formation, lymphazurin dye was injected around circumference of the tumor, and the skin over the tumor and lymph node area was carefully dissected away to expose the lymphatic vessels. The exposed lymphatic vessels draining from the primary tumor are shown in blue due to staining with the lymphazurin dye. (B) The exposed primary tumor (white arrow) and the nearest lymph node (black arrow). (C) Representative images of H&E-stained histopathology showing the primary mammary tumor, and tumor cell metastases on the lymph node and lung of MTLn3 tumor-bearing rats (40×). (D) Cluster of LCTCs in directly smeared lymph on glass slides. (E) LCTC acini in directly smeared lymph. (F) LCTC and BCTC growth in culture (10×). (G) LCTCs and BCTCs stained for pan-cytokeratin (AE1-AE3) and CD45. To confirm their epithelial origin, rat white blood cells were used as a control.

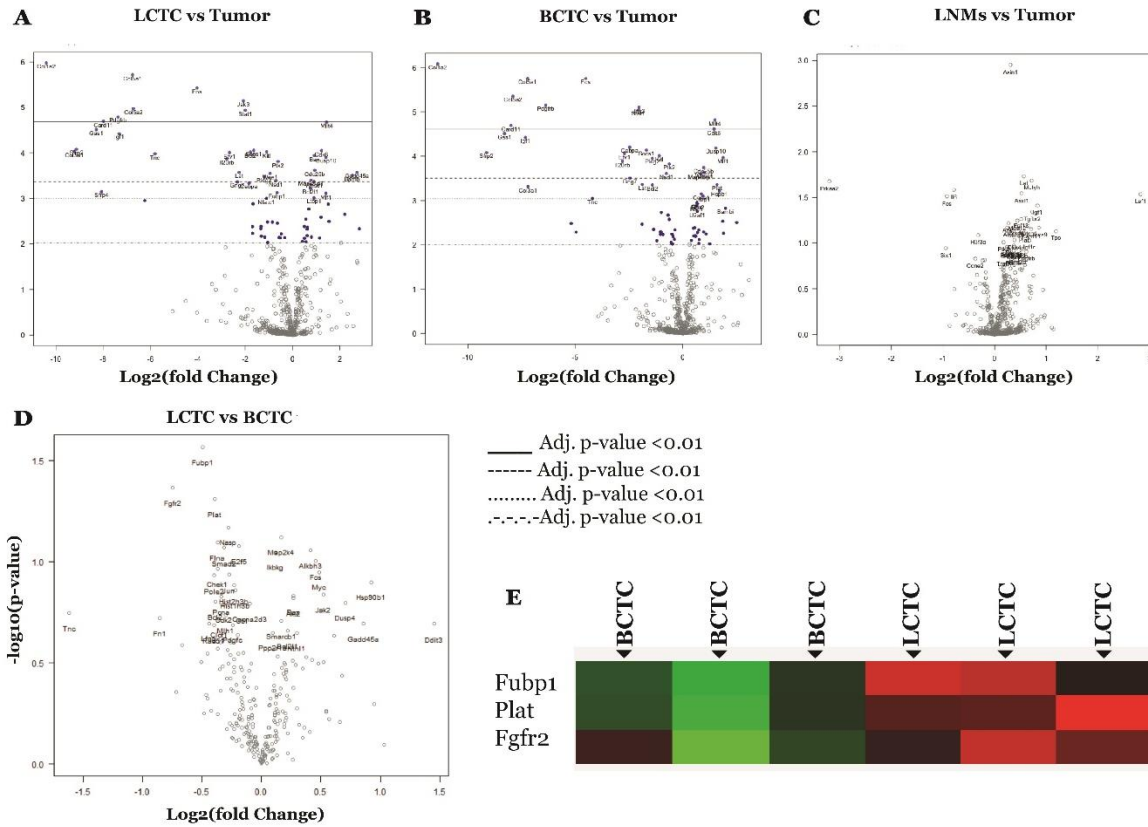


Figure 2.2: Volcano plot displaying differentially expressed genes between LCTC, BCTC, and LNMs (using the primary tumor as reference).

The y-axis corresponds to the mean expression value of $\log^{10}(P\text{-value})$, and x-axis displays the \log_2 -fold change value. Highly statistically significant genes appear at the top of the plot above the horizontal lines (various P -values threshold indicated): $P < 0.05$, $P, 01$, $P < 0.5$, and highly differentially expressed genes are plotted at either side of zero. Genes were considered significant as indicated in the figure. Only genes in significant range are colored and named. The 40 most statistically significant genes of LCTCs vs. primary tumor are shown in (A), BCTCs vs. primary tumor are shown in (B), LNMs vs. primary tumor are shown in (C), and LCTCs vs. BCTCs are shown in (D) are labeled in the plot. (E) Differentially expressed genes between LCTC and BCTC. Green = overexpressed gene; Red = underexpressed genes; black = no change in expression.

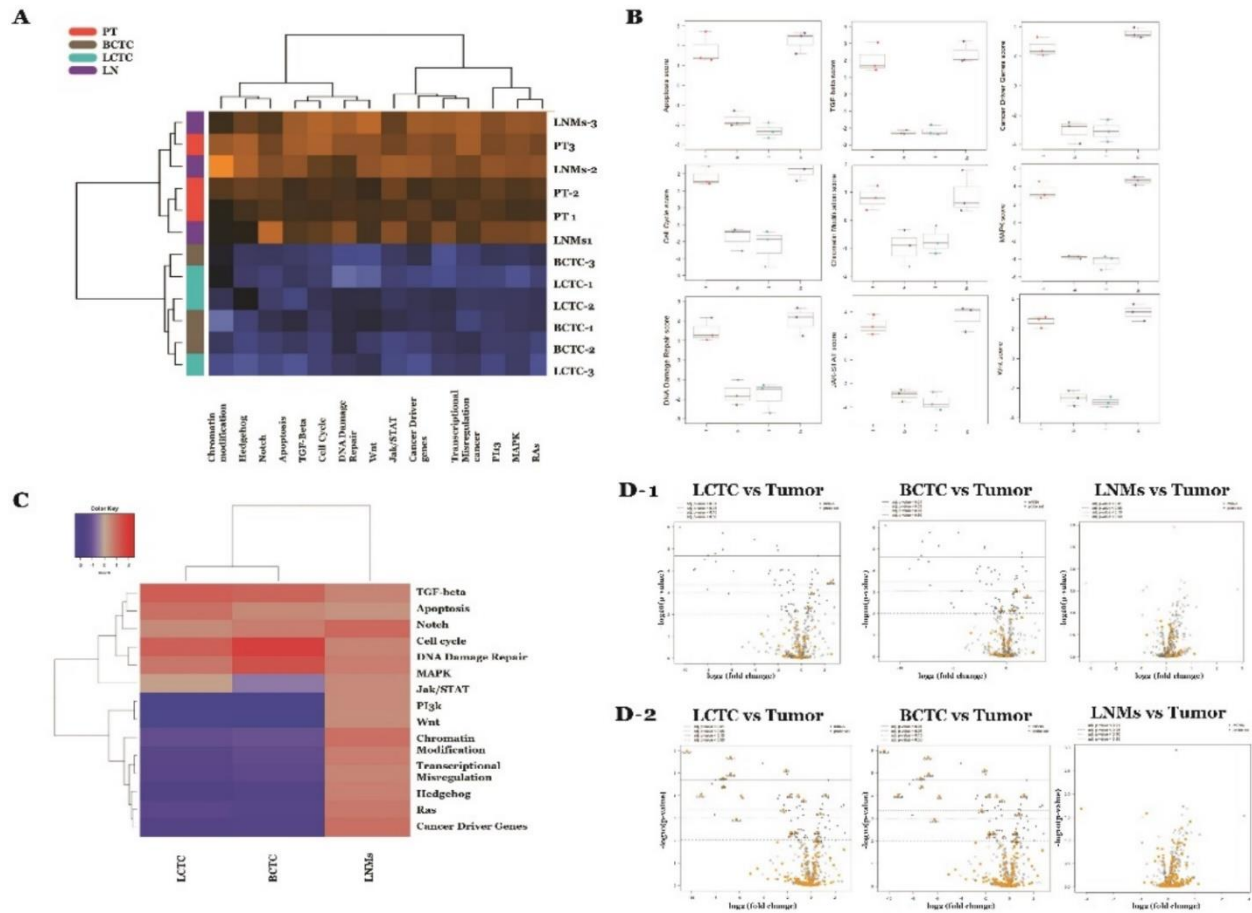


Figure 2.3: Pathway activation scores for LCTC, BCTC, LNMs, and primary tumor were compared to identify the pattern of pathway activation in each.

(A) LCTC and BCTC exhibit a common profile of pathway activation, while primary tumor and LNMs exhibit a common profile of pathway activation. Pathway activation score was calculated using the cumulative increase or decrease in abundance of all genes which mapped to that functional pathway. Orange indicates high scores; blue indicates low scores. Scores are displayed on the same scale via a Z-transformation. (B) Box-and-whisker plots showing apoptosis pathway score levels in LCTC (l), BCTC (b), primary tumor (t), and LNMs (ln). (C) Gene set analysis showing the variations in global significance scores among the gene sets in each sample. (D) Volcano plots displaying each gene's $-\log_{10}(P\text{-value})$ and $\log_2\text{-fold change}$ for the selected covariate (Fig. 3D1). Showing volcano blots for TGF-beta and (Fig. 3D2) showing volcano blots for PI3K. Highly statistically significant genes fall at the top of the plot, and highly differentially expressed genes fall to either side. Genes within the selected gene set are highlighted in orange. Horizontal lines indicate various P -value thresholds.

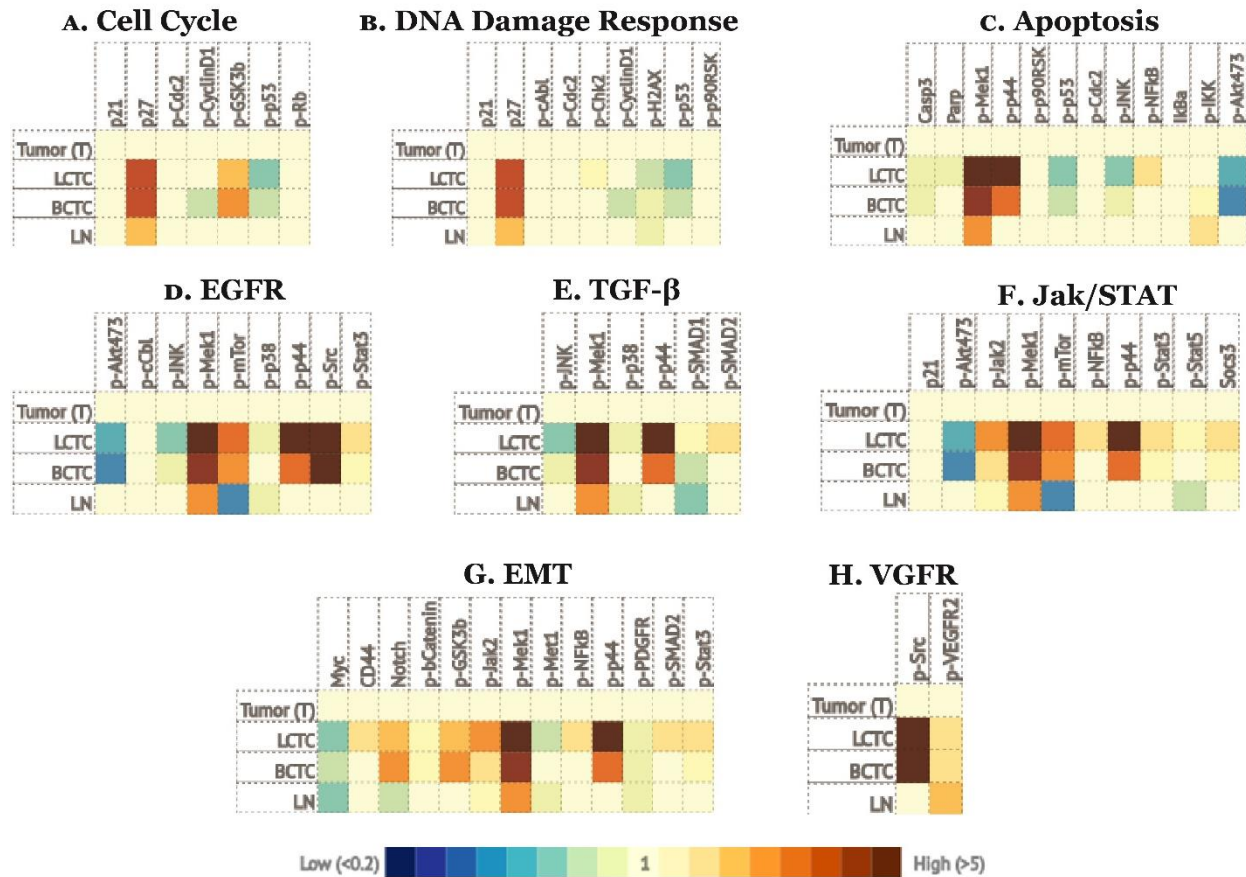


Figure 2.4: Signaling pathways alerted in LCTCs, BCTCs, and LNMs relative to primary tumor. Heat maps demonstrating changes.

(A) Cell cycle, (B) DNA damage response, (C) apoptosis, (D) EGFR, (E) TGF- β , (F) JAK/STAT, (G) EMT, (H) VGFR signaling pathways in LCTC, BCTC, and LNMs relative to primary tumor. The analysis was performed using IPAD technology by ActivSignal, Inc. The graph shows the major proteins involved in each pathway. The heat map presents three gradations of color intensities corresponding to 1.2, 1.8, and 2.4 and higher fold increase or decrease in IPAD values over primary tumor. Translation of the IPAD values to actual change in the activity of signaling molecules depends on the target. On average, 1.8-fold change in IPAD values corresponds to threefold change in the target activity. Each heat map represents three samples from three independent animals.

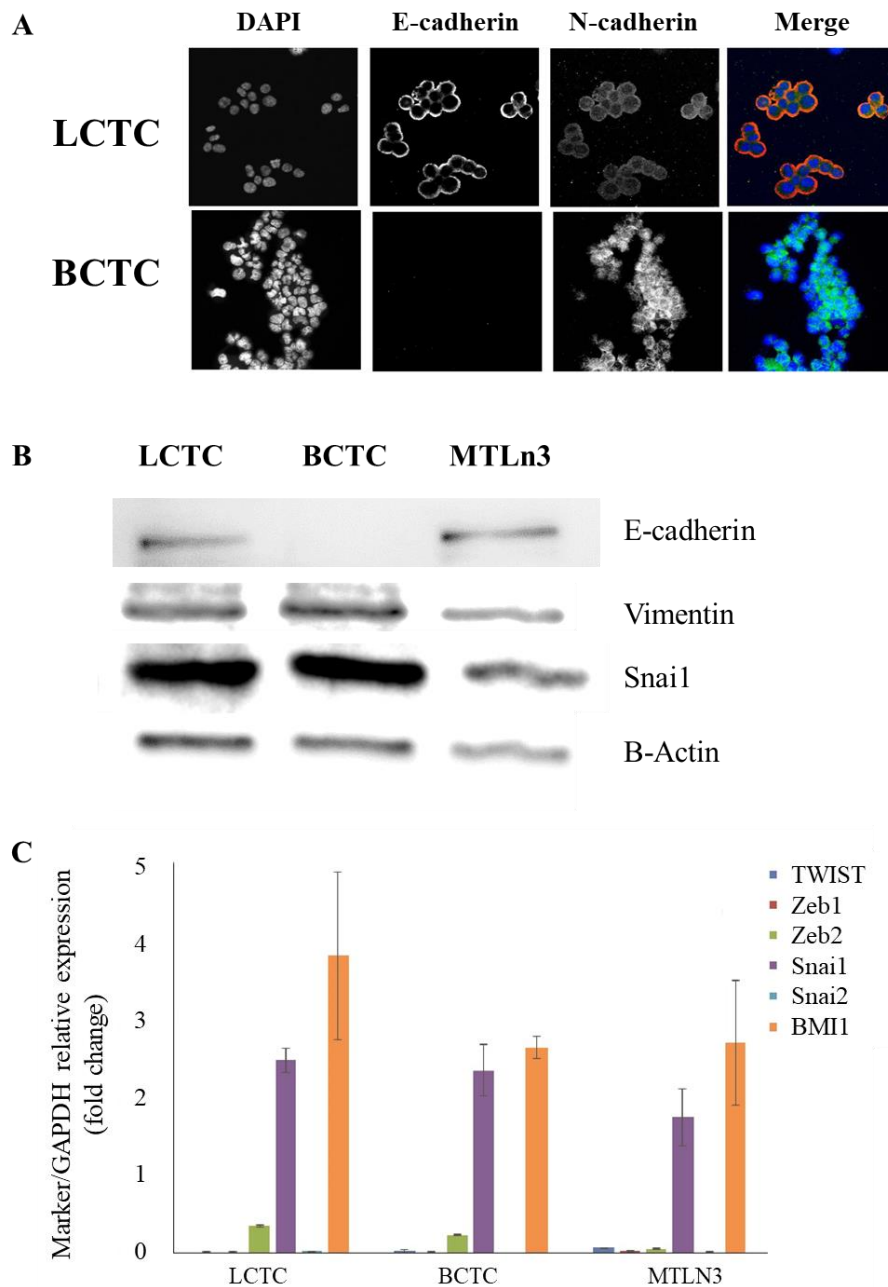


Figure 2.5: Epithelial–mesenchymal transition phenotype and markers expressed by LCTCs, BCTCs, and MTLn3.

(A) EMT was recorded through immunofluorescence after cells were fixed and stained with anti-E-cadherin (red) and anti-N-cadherin (green) antibody visualization through confocal microscopy with 40 \times . (B) Fold change of mRNA expression relative to GAPDH of selected EMT markers (mean of three samples from different three animals, error bars denote \pm SD). (C) Immunoblotting analysis of EMT markers. β -actin was used as a loading control.

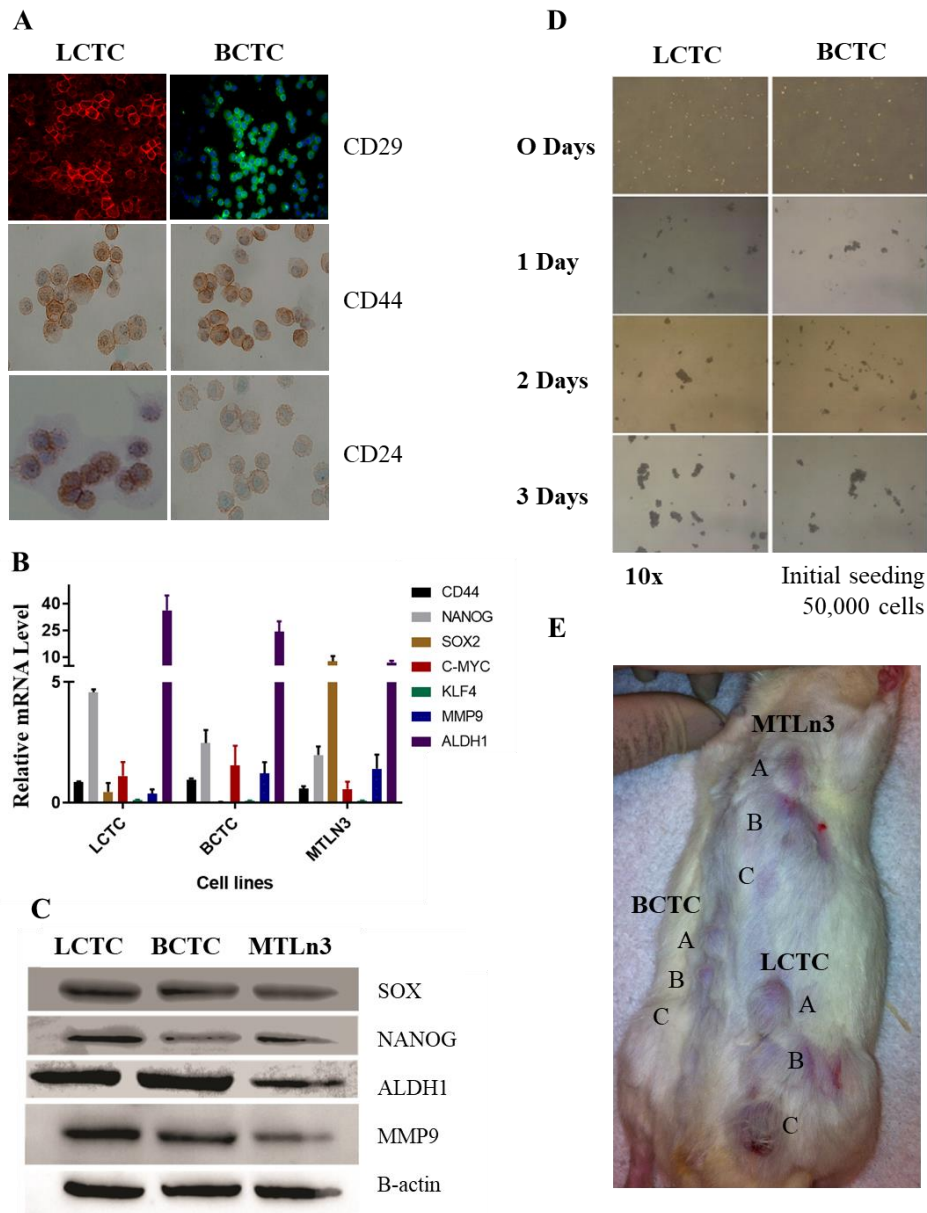


Figure 2.6: Cancer stem cell signatures of LCTCs and BCTCs.

(A) Immunofluorescence analysis of CSC markers CD29 (20X), CD44, and CD24 (40×) in LCTC and BCTC. (B) RT-qPCR analysis of stem cell transcriptional factor mRNA levels relative to GAPDH (mean of three samples from three different animals, error bars denote \pm SD). (C) Immunoblotting analysis of selected stem cell markers. (D) Representative images of mammospheres at 14 days post seeding of LCTC and BCTC (magnification 10×). (E) Representative image of tumor formation in rat implanted with various numbers A = 1×10^6 , B = 2×10^5 , C = 1×10^5 of LCTCs, BCTCs, and MTLn3 cells. Three independent samples from three different animals.

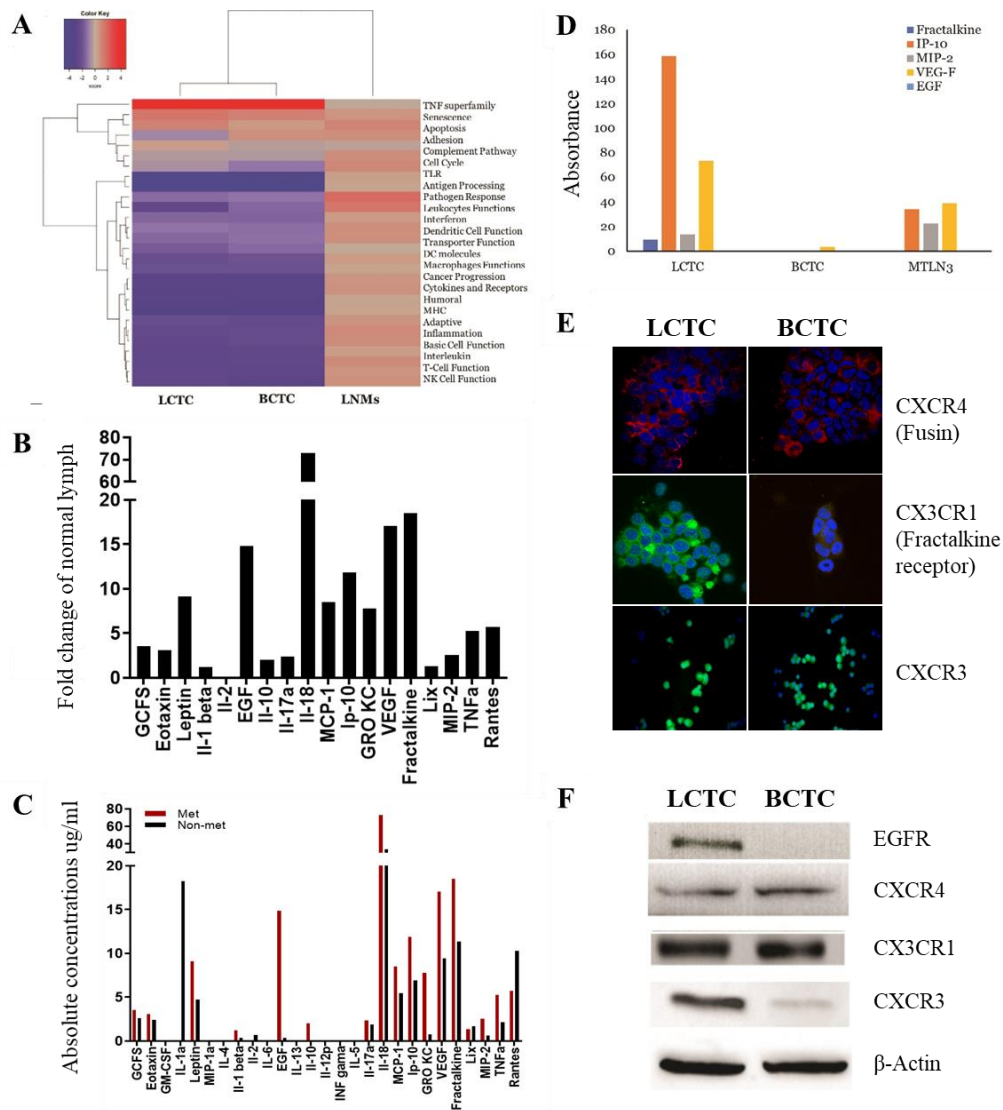


Figure 2.7: Heat map plot of directed global significance score and multiplex quantification of cytokines and chemokines using the multiplex map rat cytokine/chemokine magnetic bead 27-plex immunoassays.

(A) The map displays the extent to which a gene set's genes are up- or downregulated with the variables showing the significantly expressed immune pathways in LCTCs, BCTCs, and LMNs compared to primary tumors. (B) A panel of cytokines, chemokines, and growth factor were measured in lymph from metastatic tumor-bearing animals relative to that of the lymph from normal animals. (C) Absolute mean concentration $\text{pg}\cdot\text{mL}^{-1}$ of cytokines, chemokines, and growth factors in the lymph of metastatic tumor-bearing and nonmetastatic tumor-bearing animals. (D) Absolute mean concentration $\text{pg}\cdot\text{mL}^{-1}$ of cytokines and chemokines released by LCTCs, BCTCs, and MTLn3 cells detected in 3D culture medium supernatants. (E) CXCR4, CX3CR1, and CXCR3 expression in LCTCs and BCTCs was detected by immunocytochemistry, and the results were visualized by confocal microscopy. (F) Immunoblotting of EGFR, CXCR3, CX3CR1, and CXCR4. β -actin used as loading control. $n=$ three samples from three animals.

CHAPTER 3. TUMOR-DRAINING LYMPH SECRETOME EN ROUTE TO THE REGIONAL LYMPH NODE IN BREAST CANCER METASTASIS.

THIS IS A PUBLISHED JOURNAL ARTICLE. Reprinted with permission from: Dove Med Press. **Tumor-Draining Lymph Secretome En Route to the Regional Lymph Node in Breast Cancer Metastasis. Breast Cancer (Dove Med Press).** Mohammed SI, Torres-Luquis O, Zhou W, Lanman NA, Espina V, Liotta L. 2020 Mar 25;12:57-67. doi: 10.2147/BCTT.S236168. eCollection 2020. PMID: 32273752

Abstract

During metastasis, tumor cells metastasize from primary tumors to distant organs via the circulatory and the lymphatic systems. There is a plethora of information about metastasis through the circulatory system, however not much information is available about the tumor cells dissemination through the lymphatic system or the lymphatic microenvironment that aids in this process in breast cancer metastasis. The study designed to examine the tumor-derived secretome in lymph before reaching the draining lymph nodes. Using a microsurgical technique, we have collected the lymph in transit from the primary tumor en route to the regional lymph node in animals with metastatic and non-metastatic mammary carcinoma and healthy controls. The lymph samples were subjected to LC-MS/MS analysis, bioinformatics, and pathway analysis. The metastatic tumor-draining lymph before its entry into the closest regional lymph node contain 26 proteins with >175-folds in abundance compared to lymph from non-metastatic tumor-bearing animals. Among these proteins were biliverdin reductase B, heat shock protein, coagulation factor XIII, lymphocytes cytosol protein 1, and aldose reductase. These proteins were not identified in the lymph from healthy animals. Pathway analysis revealed that cadherin-mediated endocytosis, acute phase response, junction signaling, gap junction, VEGF signaling, and PI3K/AKT signaling pathways are overrepresented in the lymph from metastatic tumor-bearing compared to the lymph from non-metastatic tumor-bearing animals. Among the significantly up-regulated proteins in the lymph from metastatic tumor-bearing animals were proteins that identified in exosomes include heat shock protein, enolase 1 alpha, S100, and biliverdin reductase B. One of the proteins significantly downregulated in lymph from animals with metastasis is Kininogen, a known metastasis inhibitor protein. Proteins and exosomal proteins in lymph draining a metastatic tumor

are different from those in lymph draining non-metastatic tumors, and these proteins involved in pathways that regulate tumor cells migration and invasion.

3.1 Introduction

Early diagnosis and systemic adjuvant therapies have improved survival rates in many women with breast cancer; unfortunately, these treatments often fail to treat women with metastatic disease effectively. During metastasis, tumor cells spread from the primary tumor to distant organs forming secondary tumors that results in patient death. The tumor cells spread via the circulatory and lymphatic systems¹⁹¹. Although there is a plethora of information about the tumor cells spread through the circulatory system, little information is available regarding the tumor cells spread through the lymphatic system or the lymphatic microenvironment that aid in this process in breast cancer.

The tumor-draining lymph is shed predominantly at the interstitial periphery of the tumor and collected into lymphatic capillaries that merge into progressively larger vessels, afferent lymphatic vessels, which drain the lymph into the regional lymph node. Upon filtration of proteins and particulate uptake of the lymph by the immune cells in the regional lymph nodes, it returns by efferent lymphatic vessels to the venous blood. This journey makes the lymph rich in proteins from tissue growth and remodeling, cellular metabolic/catabolic activities, and cell death. These lymph-collected proteins are organ-specific, suggesting that the lymph proteome reflects ongoing extracellular and intracellular processes in the particular tissue, mirroring the normal or disease conditions^{128,192}. It has been shown that the lymph in the afferent lymphatic vessels has different proteins from that of the plasma, interstitial fluid, and efferent lymph¹⁹³. Accordingly, the proteome (including exosomal proteins) and cellular composition of the tumor-draining afferent lymph before its entry into the draining lymph node differ from that of the efferent lymph or plasma and play a significant role in metastasis. Furthermore, the tumor microenvironment is known to influence metastasis to the lymph node. The tumor secretes factors such as cytokines, exosomes, and enzymes that pre-condition the microenvironment of lymph nodes, making them a welcoming and supportive metastatic niche for disseminating tumor cells^{129,194}. Thus, the secreted protein profile, including the tumor-derived factors and exosomes of the afferent lymph, may provide information regarding the physiological and pathological states of the primary tumor and its potential to form metastasis which may provide means to design therapy. To determine the protein

composition and tumor-derived factors of tumor-draining lymph, we have developed and employed a novel microsurgical technique to successfully collect the lymph from the lymphatic vessels exiting the primary tumor before their entry into the draining lymph node in an immunocompetent rat model of breast cancer metastasis. The afferent lymph protein composition of metastatic tumor-bearing, non-metastatic tumor-bearing, compared to no tumor-bearing rats, were characterized, and studied to determine unique tumor-derived factors that can serve as discriminating indicators of the metastatic tumor potential

3.2 Materials and methods

3.2.1 Cell Lines and Culture Condition

The rat metastatic MTLn3 and non-metastatic MTC cells were kindly provided by Dr. Segall (Albert Einstein College of Medicine, Bronx, NY) and approved by Purdue Biosafety Committee. The MTLn3 cells were clonally derived from a lung metastasis of the 13762NF rat mammary adenocarcinoma¹⁹⁵. Both MTLn3 and MTC cells were cultured in Minimal Essential Medium, Alpha (MEM; Sigma, St. Louis, MO), containing nonessential amino acids (Sigma, St Louis, MO), and supplemented with 5% fetal bovine serum (FBS; Hyclone, Logan, UT).

Orthotopic Tumor Growth and Metastasis.

All experiments involving rats were conducted according to the National Institutes of Health regulation on the care and use of experimental animals. Purdue University Animal Use and Care Committee approved the study. Immunocompetent syngeneic female Fisher 344 rats were purchased from Harlan (Indianapolis, IN). MTLn3 and MTC cells were grown to 70-80% confluence, and 1X10⁶ cells in 0.1 mL PBS or PBS (vehicle control) were injected into the two left caudal- and rostral-most mammary fat pads to establish primary (MTLn3 and MTC) and lymph node and lung metastasis (MTLn3).

3.2.2 Collection of Lymph and Blood from Tumor-Bearing and Non-Tumor-Bearing Rats

Lymph and blood were collected as previously described by Mohammed et al.⁸⁸. Briefly MTLn3- and MTC-tumor bearing, and PBS-injected animals (no tumor) were anesthetized, and the tumor-draining lymphatic vessels were visualized by injecting Lymphazurin dye (1%, isosulfan blue; United States Surgical Corporation, Ben Venue Laboratories Inc, Ohio). A heparin-

treated polyethylene catheter was used to cannulate the afferent vessel at a site distal to the tumor and proximal to the vessel entry site on the sentinel lymph node and taped in place. The lymph from the four tumor cells-injected mammary fat pad sites was collected and pooled for each animal. Blood was collected similarly. The primary tumor, the draining lymph node, and lung tissues were collected and processed for histopathology to confirm metastasis.

3.2.3 Mass Spectrometry (MS) Data Acquisition and Analysis

Lymph and the blood samples were centrifuged, and subsequently, 200 μ L of 8 M urea and 10 mM dithiothreitol (DTT) was added to the supernatant, which was then incubated for 30 min at 37°C and then alkylated with 50 mM iodoacetamide for 20 min at room temperature. The urea concentration was adjusted to 2 M, and proteins were digested by trypsin at 37°C for 6h in a buffer containing ammonium bicarbonate (50 mM, pH 9). The digestion mixture was then acidified by adding glacial acetic acid to a final concentration of 2% and desalted by ZipTip (Millipore). We used high sensitive reversed-phase liquid chromatography coupled nanospray tandem mass spectrometry (LC-MS/MS) using an LTQ-Orbitrap mass spectrometer (Thermo Fisher) ¹⁹⁶ to analyze the resultant peptides. The reversed-phase LC column was slurry-packed in-house with 5 μ m, 200 Å pore size C18 resin (Michrom BioResources, CA) in a 100 μ m i.d. \times 10 cm long piece of fused silica capillary (Polymicro Technologies, Phoenix, AZ) with a laser-pulled tip. After packing, the new column, the HPLC system (Surveyor MS Pump Plus from ThermoFisher) and the LTQ-Orbitrap were tested by analyzing 100 fmol “Yeast Enolase Standard & Tryptic Digestion” from Michrom Bioresources, Inc. (catalogue number PTD/00001/46) to ensure obtaining stable ESI, desired mass accuracy, peak resolution, peak intensity and retention time. Additional iterations were performed to ensure reproducibility. We spiked a total of 100 fmol of standard peptide angiotensin I (Ang I) into the sample as an internal standard. After sample injection, we washed the column for 5 min with mobile phase A (0.1% formic acid), and peptides were eluted using a linear gradient of 0% mobile phase B (0.1% formic acid, 80% acetonitrile) to 50% B in 120 min at 200 nL/min, then to 100% B in an additional 10 min for the proteomics analysis. Before and after analyzing one sample, the column was washed with HPLC mobile phase B for 30 min, then mobile phase A for 20 min at a high flow rate (1 μ L/min) to reduce potential carryover. The LTQ-Orbitrap mass spectrometer was operated in a data-dependent mode in which eight MS/MS scans followed each full MS scan (60,000 resolving power), and the eight most

abundant molecular ions were dynamically selected and fragmented by collision-induced dissociation (CID) using a normalized collision energy of 35%. The Dynamic Exclusion Time was 30 s, and the Dynamic Exclusion Size was 200. The “FT master scan preview mode,” “Charge state screening,” “Monoisotopic precursor selection,” and “Charge state rejection” were enabled so that only the 1+, 2+, and 3+ ions were selected and fragmented by CID.

Tandem mass spectra collected by Xcalibur (version 2.0.2) were searched against the NCBI rodent protein database using SEQUEST (Bioworks software from ThermoFisher, version 3.3.1) with full tryptic cleavage constraints, static cysteine alkylation by iodoacetamide, and variable methionine oxidation. Mass tolerance for precursor ions was 5 ppm, and mass tolerance for fragment ions was 0.25 Da. The SEQUEST search results of proteomics data were filtered by the criteria “Xcorr versus charge 1.9, 2.2, 3.0 for 1+, 2+, 3+ ions; $\Delta C_n > 0.1$; probability of randomized identification of peptide < 0.01 ”. Positive peptide identifications were determined using these stringent filter criteria for database match scoring, followed by manual evaluation of the results. The false discovery rate (FDR) was estimated by searching a combined forward-reversed database as described by Elias ¹⁹⁷. The SEQUEST search results were exported to Excel files and compared.

3.2.4 Bioinformatic Analysis

For annotation analysis, we uploaded the GI protein accession numbers into the DAVID (Database for Annotation, Visualization, and Integrated Discovery) informatics tool (DAVID Bioinformatics Resources 6.7. ¹⁹⁸ For GO Term (Gene Ontology) analysis, we studied the Biological Process categories using the GO FAT default settings. For functional annotation searches, we set the following parameters: threshold count 3, EASE score (enrichment probability) 0.1; medium stringency for functional annotation clusters. For KEGG pathway searches, the parameters were: threshold count 5 (minimal count of proteins mapped to the pathway ≥ 5), enrichment probability ≤ 0.05 (strong enrichment).

Enrichment values (for GO terms), enrichment scores (for annotation clusters), and statistical determinants (for p values and Benjamini coefficients) are those calculated by DAVID software. The Group Enrichment Score is a geometric mean (in $-\log$ scale) of member’s Fisher exact test P-values in a corresponding annotation cluster, where each member’s p-value reflects the probability of enrichment for a particular gene in a given gene list. The Benjamini coefficients

are Benjamini-Hochberg-corrected p values adjusted for multiple comparisons to lower the family-wise false discovery rate and thus are more conservative than Fisher exact p values. ToppCluster was used to perform additional functional analysis of differentially expressed proteins ¹⁹⁹.

3.3 Results

3.3.1 Afferent Lymph Collection from Metastatic Mammary Tumor Syngeneic Model

We developed a novel microsurgical technique for the collection of lymph draining a primary tumor before its entry into the regional lymph node (Figure 1A). We used metastatic MTLn3 and non-metastatic MTC cells transplanted orthotopically in mammary fat pads of immunocompetent female Fisher 344 rats for the syngeneic model (Figure 1B). These two cells were isolated from the same parent tumor, 13762NF mammary adenocarcinoma, but differed in their ability to metastasize ¹³². In approximately 10–14 days after injecting the cells, tumors developed in all MTLn3 and MTC implanted rats, but lymph node and lung metastasis only developed in MTLn3-bearing rats. The PBS injection site was free of tumor (negative controls). Lymph vessels were visualized by using Lymphazurin (Figure 1C), and the lymph and blood were collected as previously described ⁸⁸.

3.3.2 Tumor-Derived Secretome Profiled in Lymph Before Reaching the Draining Lymph Node.

Tumor cells communicate through direct cell-to-cell contact and secretion of soluble protein-based factors such as cytokines and exosomes. To identify these soluble proteins including exosomal proteins in metastatic lymph, we performed liquid chromatography coupled nanospray tandem mass spectrometry (LC-MS/MS) in supernatant of lymph and plasma samples draining the primary tumor before reaching the draining lymph node from metastatic and non-metastatic-tumor bearing, and healthy animals as described by Zhou et al ²⁰⁰. LC-MS/MS analysis identified a total of 598 proteins significantly differentially expressed between lymph samples from animals with metastasis, no metastasis, and healthy control. Of these, 124 proteins were shared between the healthy, non-metastatic, and metastatic lymph samples, while 12 were shared between the metastatic lymph and non-metastatic lymph samples, and 392 proteins were unique to the metastatic lymph samples (Figure 2A). Comparing all proteins found in metastatic lymph to non-

metastatic lymph, we found 70% of the proteins were similar in both groups while 26% were up-regulated, and 3 proteins were down-regulated in metastatic lymph (Figure 2B). Additionally, we found 429 proteins to be differentially expressed between lymph and plasma from metastatic tumor-bearing animals; among these, 20% were down-regulated and 15% were up-regulated in lymph (Figure 2C).

We found 26 proteins were >175-fold higher in abundance (p-value <0.05) in the lymph from metastatic tumor-bearing compared to lymph from non-metastatic tumor-bearing animals. Among these proteins were biliverdin reductase B, heat shock protein, coagulation factor XIII, lymphocytes cytosol protein 1, and aldose reductase. These proteins were not identified in the lymph from healthy animals (Table 1).

3.3.3 Molecular Pathway Analysis of Lymph Proteins Demonstrate Up Regulation of Key Metastatic Pathways and Immunomodulation Network.

To understand how the tumor-derived proteins in the draining lymph interact to communicate signals which contribute to cancer progression, we examined the major biological pathways involved in lymphatic metastasis using Ingenuity Pathway Analysis (IPA, Qiagen Redwood City). The topmost signaling pathways in lymph from metastatic tumor-bearing animals compared to lymph from non-metastatic tumor-bearing animals were BAG2, Cell cycle G2/M DNA damage checkpoint regulation, p70S6K, protein ubiquitination, and unfolded protein response signaling pathways (Figure 3A). These signaling pathways were not identified in plasma from metastatic tumor-bearing or non-metastatic tumor-bearing animals (Figure 3B). These signaling pathways are unique to the lymph from metastatic tumor-bearing animals. We also searched explicitly for pathways overrepresented in metastasis in the IPA and DAVID results. The results showed that pathways that were significantly overrepresented (Fisher's exact test, *P*-value < 0.001) in the metastatic lymph compared to the non-metastatic lymph included cadherin-mediated endocytosis, acute phase response, junction signaling, gap junction, VEGF signaling, and PI3K/AKT signaling (Figure 4A)

Also, a functional analysis performed (Figure 4B) shows the most significantly enriched biological process, and molecular function GO terms associated with the proteins that have extreme relative differences in the range of + 50 or -50. Among the 35 enriched GO terms, 10 are molecular function annotations, and 25 are biological processes. In molecular functions, most

terms were associated with metabolic enzymatic activities and cytoskeleton structures, while the most terms in biological processes were associated with glycolysis and nucleotide synthesis. This analysis indicates that the top 25 metastasis-related proteins with extreme relative differences were mostly involved in metabolism and glycolysis.

Figure 4C shows the top 10 immune-related pathways in lymph from metastatic tumor-bearing animals, and these include IL-12, IL-10, IL-17, IL-6, leukocytes extravasation, and the role of pattern recognition receptors.

3.3.4 Lymph Protein Profile Revealed Exosomal Proteins That Associate with Patients Survival.

Among the significantly up-regulated proteins in the metastatic lymph in our study were proteins identified in exosomes, as indicated in the ExoCarta database <http://www.exocarta.org/>. These proteins include heat shock protein (HSPA8; P -value $3.13e^{-10}$), enolase 1 alpha (ENO1; p -value $1.13e^{-09}$), S100, and biliverdin reductase B (BLVRB; P -value $1.24E-04$). One of the proteins significantly down-regulated in lymph from animals with metastasis is Kininogen (KNG1; p -value $1.00e^{-30}$), a known metastasis inhibitor protein²⁰¹. To determine whether these tumor-derived proteins are expressed in human breast cancer patients as well, we utilized an in silico approach to analyze the following proteins, BLVRB, HSPA8, and KNG1 in breast cancer using the Human Protein Atlas (<http://www.proteinatlas.org>) microarray tissue data. We found that BLVRB and HSPA8 are significantly overexpressed in human breast cancer tissues compared to normal, while the opposite is correct for KNG1 protein using three different antibodies.

Furthermore, the potential significance of these proteins was evaluated against gene expression data of the human breast cancer from TCGA (<https://cancergenome.nih.gov>). Kaplan-Meier survival analysis of gene expression, for example, for HSPA8, BLVRB, and KNG1, revealed that a high expression of BLVRB and HSPA8 correlated significantly with shorter relapse-free survival of patients, while the opposite is exact for KNG1 (Figure 5A–C, respectively). Together, these results suggest that the lymph draining from primary tumors before entry into the nearest lymph node contains exosomal proteins, the relative abundance of which may influence the propensity for lymphatic metastasis and tumor aggressiveness.

3.4 Discussion

Despite the knowledge regarding the importance of cancer cell dissemination through the lymphatic system, to our knowledge, factors in lymph in transit from the primary tumor to the local draining lymph node were previously unknown. A significant reason that lymph has not been sampled in situ from growing tumors is the microscopic size of lymphatics and the difficulty in identifying and cannulating the lymphatics en route to the regional lymph node. The present study uses a unique microsurgical technique to collect and characterize the lymph draining from the primary tumor. Using an immunocompetent rat model of breast cancer transplanted orthotopically with metastatic MTLn3 and non-metastatic MTC cells; we have isolated and characterized the tumor-draining lymph as it drains from the primary tumor in live immunocompetent animal models of breast cancer metastasis ⁸⁸.

In recent years, accumulating evidence suggested that the primary tumor greatly influences the microenvironment of the regional lymph node. The primary tumor secretes factors that include cytokines, exosomes, or enzymes that condition the lymph node, creating an ideal environment for disseminating tumor cells ^{129,194}. It follows then that the primary tumor-draining lymph should be rich in these premetastatic conditioning factors. These factors can serve as discriminating indicators of the metastatic tumor potential. The identification and monitoring of these premetastatic niche-inducing materials in situ in lymph draining from primary tumors can provide insights about immune recognition or immune priming in the sentinel lymph nodes, which are highly relevant to tumor treatment. To determine the protein profiles of these tumor-derived factors, we performed a proteomic analysis of the lymph in transit to the regional lymph node. Our study is the first to study the proteomic profiles of the tumor-draining lymph before its entry into the regional lymph node in live animals. Although the lymph proteome has been examined previously in comparison to the plasma in non-cancer and cancerous diseases, the samples used were obtained either from the subject's legs or mesenteric lymphatic vessels of patients or animals ²⁰²⁻²⁰⁶. Proteomic analysis of exosome in the postoperative lymphatic leak called lymphatic exudate collected after lymphadenectomy inpatient with melanoma was recently examined ²⁰⁷. The drawback of using such lymphatic exudate is the possibility of proteome alteration due to surgery and wound healing. Therefore, our approach is novel and could be applied to breast cancer patients who were undergoing primary and sentinel lymph node dissection comparing women with positive

lymph node to those with negative lymph node metastasis permitting a through a comprehensive analysis of specific tumor predictive biomarker signatures.

We show that lymph from metastatic tumor-bearing animals contains distinct proteins compared to lymph from non-metastatic tumor-bearing animals and that these proteins are involved in pathways that modulate the immune system, gap junctions, angiogenesis, and lymphangiogenesis. Significantly altered pathways include BAG2, cell cycle G2/M DNA damage checkpoint regulation, p70S6K - pathways that were not identified in plasma. Notably, Bag2, is a protein of BCL-2 associated athano gene family, the overexpression of which is associated with poor prognosis in triple-negative breast cancer patients. Inhibition of BAG2 gene expression can completely control the growth and metastasis of triple-negative breast cancer cells to the lungs^{208,209}. Patients with tumors having increased p70S6K phosphorylation had worse disease-free survival and increased metastasis. However, the proteomic profile of extracellular vesicles from lymph node-negative patients' lymphatic exudate was associated with pathways involved in cellular movement, vascularization, extravasation, and adhesion. These pathways are believed to correlate with the early stages of metastasis²⁰⁷. In contrast, the proteomic profile of extracellular vesicles isolated from lymphadenectomy following positive lymph node biopsy show up-regulated signaling pathways connected to cell death, proliferation, and cancer, donating of more advanced disease²⁰⁷.

In contrast, extracellular-derived exosome showed pathways related to antigen presentation, endoplasmic reticulum phagosome, G2/M transition, and IL-12 family signaling²¹⁰. Previously, we have shown that proteomic analysis of tumor cells in lymph draining a tumor enriched in NF-KB, heat shock response, and the unfolded protein response. Also, we have examined the cytokines/chemokines and growth factors in the tumor-derived factors before lymph node entry to determine which factors may protect tumor cells in lymph, promote their migration to the lymph nodes, and aid in premetastatic niche formation. Of the 27 cytokines/chemokines examined, 19 had > 2-fold increases in the metastatic lymph relative to the healthy lymph. EGF, TNF- α , IFN- γ -induced protein 10 (IP-10 or CXCL10), vascular endothelial growth factor (VEGF), and fractalkine (CX3CL1) showed > 10-fold increases, and interleukin 18 (IL-18) showed a > 70-fold increase in the metastatic lymph compared to the lymph from non-metastatic tumor-bearing animals⁸⁸. These cytokines/chemokines and growth factors play an essential role in stimulating

immune responses, immune cell chemotaxis, and tumor cell migration, invasion, and metastasis
152–155,211.

Among the significantly altered proteins in metastatic lymph were proteins that shown to be carried by exosomes. Tumor-derived exosomes were shown to promote progression, invasion, and metastasis of cancer cells and play a significant role in suppressing the immune responses against the tumor. Although we have not explicitly isolated the exosomes, we have analyzed the lymph supernatants, which included exosomes. Among the exosome proteins that we identified in our study is HSPA8, which is known to activate cancer cell motility, migration and metastasis;²¹¹ EnoA, known to promote tumor metastasis²¹² and EMT; and Blvrb, which regulates the insulin/IGF-1/IRK/PI3K/MAPK, and VEGF pathways²¹³. Interestingly, among proteins significantly down-regulated in lymph from metastatic-tumor animals, was a metastasis inhibitor protein Kng1, which is known to inhibit migration and invasion of human prostate cancer and has been shown to have an essential role in suppression of cancer cell adhesion, invasion, and angiogenesis²¹⁴. Therefore, the metastatic lymph contains exosomal proteins that may influence the outcomes of the tumor cell migration and metastasis.

In summary, we now can routinely characterize the molecular and cellular composition of tumor-derived native lymph in transit to the draining regional lymph node. The molecular characterization of lymph would provide a new level of information of high relevance to the understanding of metastasis biology, particularly to the diagnosis and treatment of the lymphatic spread of human cancers.

3.5 Acknowledgements

The authors thank Dr. Mittal for his continuous support. Also, we thank Dr. Segall from Albert Einstein College of Medicine, the Bronx, NY, for providing the MTln3 and MTC cell lines. The work was supported by DOD concept award # W81XWH-04-1-0747 and NIH/NCI grant # 1R21CA199621.

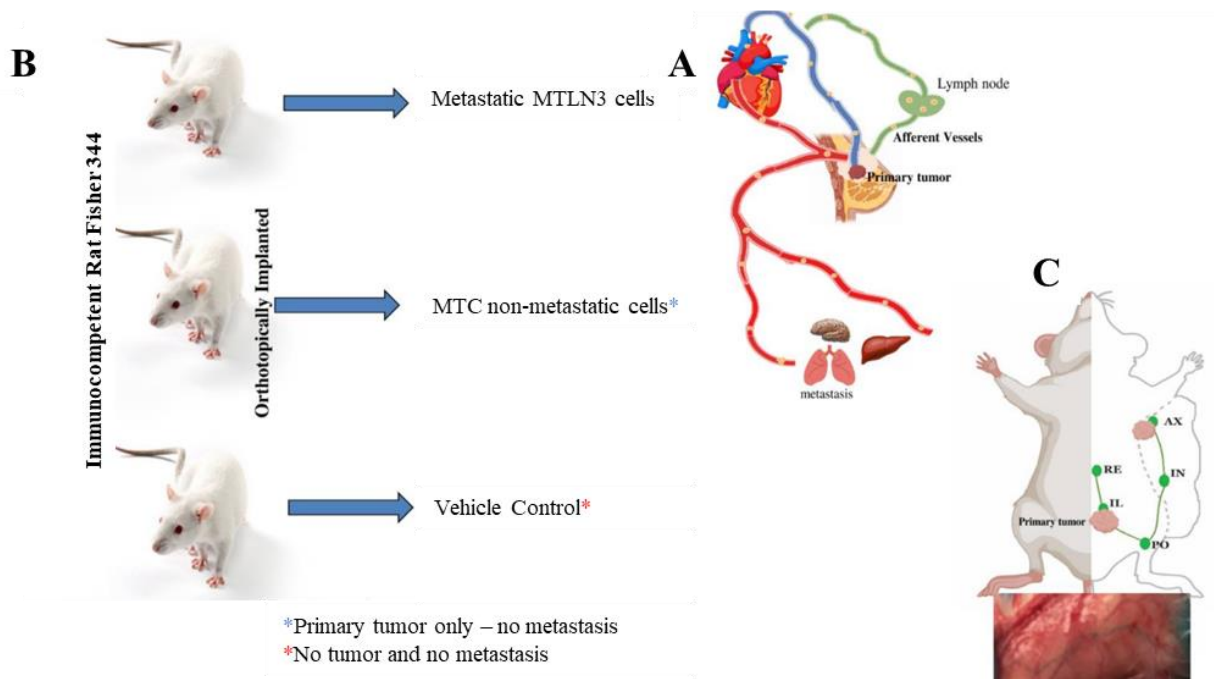


Figure 3.1: Experimental plan and concept of lymph collection.

(A) Scheme illustrating the tumor cells spread through the lymphatic and hematogenous system in women. (B) Outline of the experimental design and tumor implantation. (C) Visualization of afferent lymphatic vessels (green color).

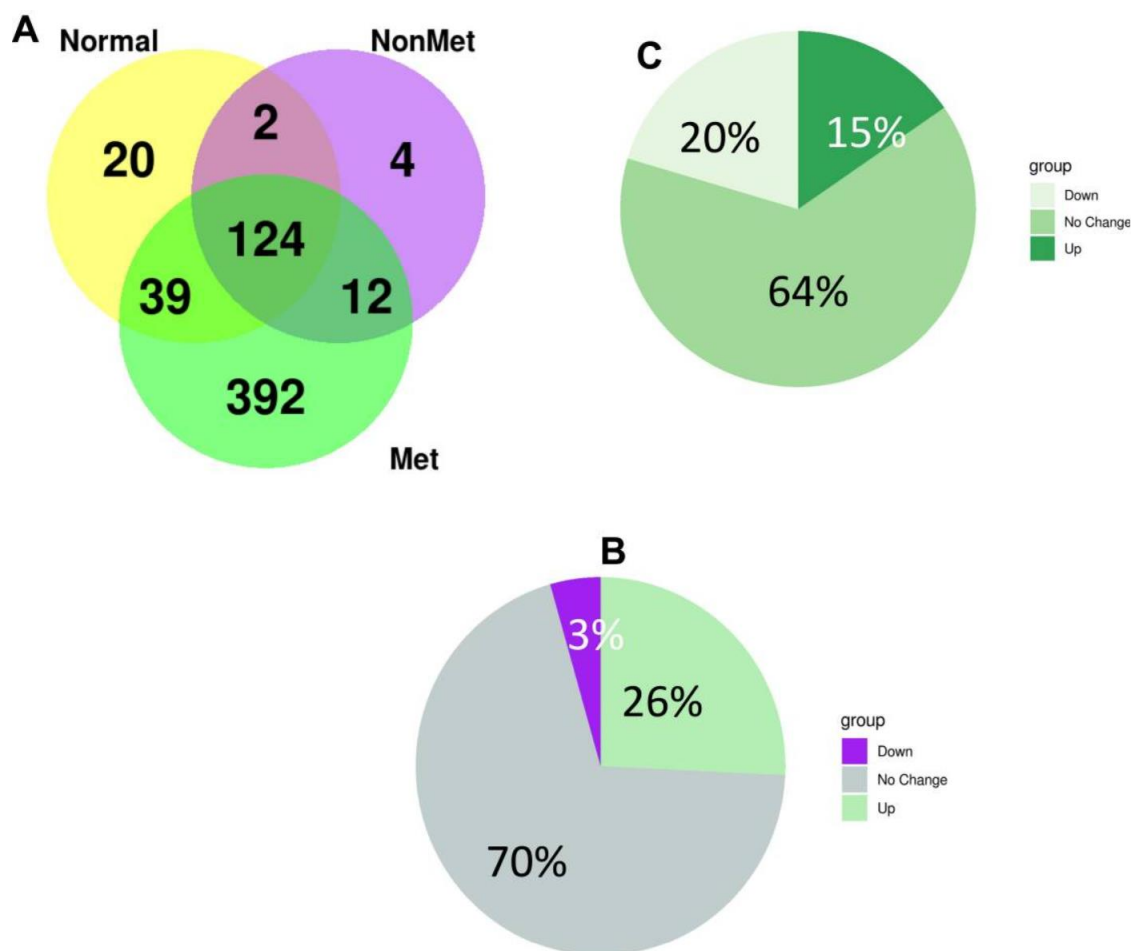


Figure 3.2: Protein expression statistics from metastatic and non-metastatic tumor-bearing animals.

(A) Summary of protein numbers obtained from the lymph from healthy animals, metastatic tumor-bearing and non-metastatic tumor-bearing animals. (B) Differentially expressed proteins between lymph and plasma from metastatic tumor-bearing animals. (C) Differentially expressed protein between lymph from metastatic and non-metastatic tumor-bearing animals.

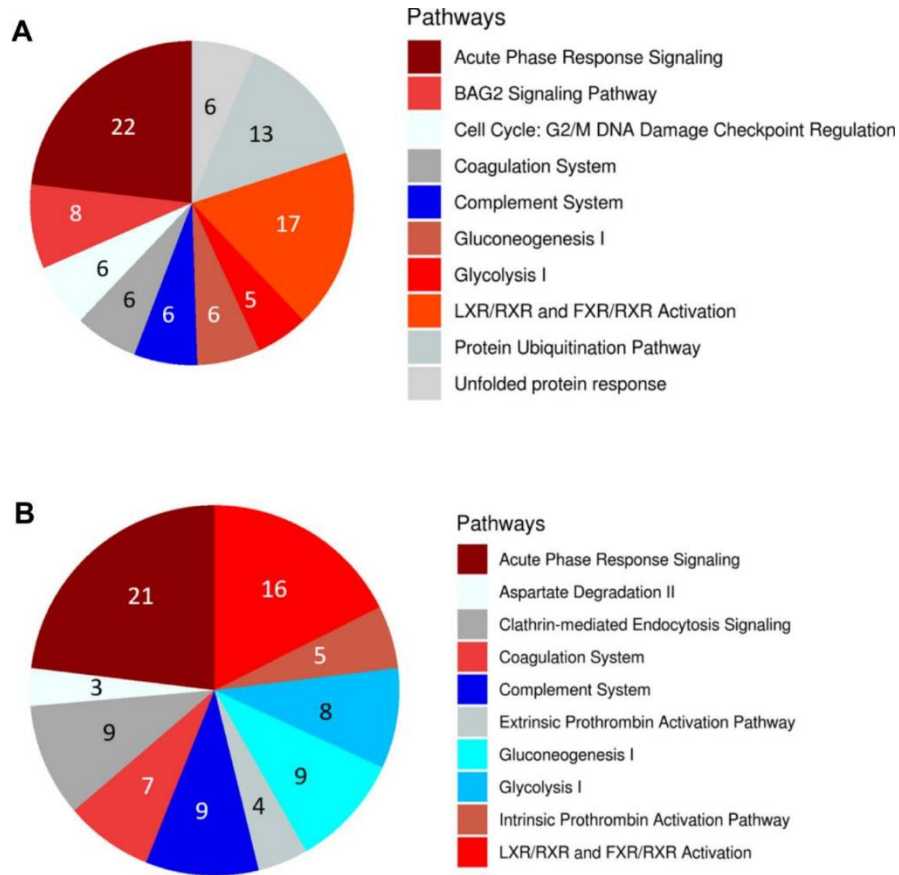
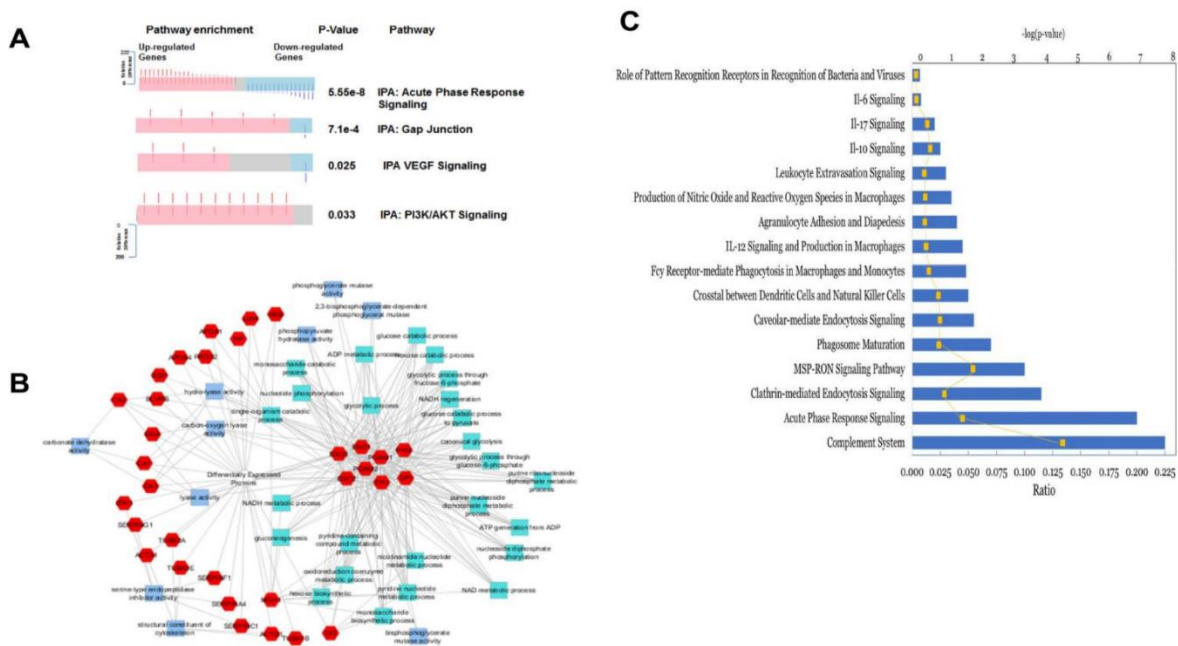


Figure 3.3: Pathways enriched in differentially expressed proteins in lymph.

(A) Top 10 pathways enriched in differentially expressed proteins in lymph from metastatic tumor-bearing animals versus lymph from non-metastatic tumor-bearing animals. (B) Top 10 pathways enriched in differentially expressed proteins in lymph compared to plasma from metastatic tumor-bearing animals. Activation state of the pathway was calculated using an activation z-score. Up-regulated pathways are shown in red, down-regulated are shown in blue, and those in which the activation state could not be determined are shown in grey. Number of proteins in each group is shown for each pathway in the pie chart. All pathways shown have an adjusted p-value < 0.05.



Figures 3.4: Protein expressions in tumor-draining lymph from animals with metastatic tumor and the involvement of signaling pathways.

(A) A spring layout algorithm was used to show the most significant GO terms associated with proteins that had a more extreme relative difference that + or -50. Molecular function GO terms are light blue, biological process GO terms are teal, and proteins are colored in red. A Bonferroni corrected p-value of 0.01 was used as the cutoff, and the top 25 GO terms were selected. (B) Summary of biological pathways indicating the down-regulated and up-regulated genes and the P value of enrichment. (C) Significantly activated 10 top immune-related pathways that in the metastatic lymph compared to non-metastatic lymph.

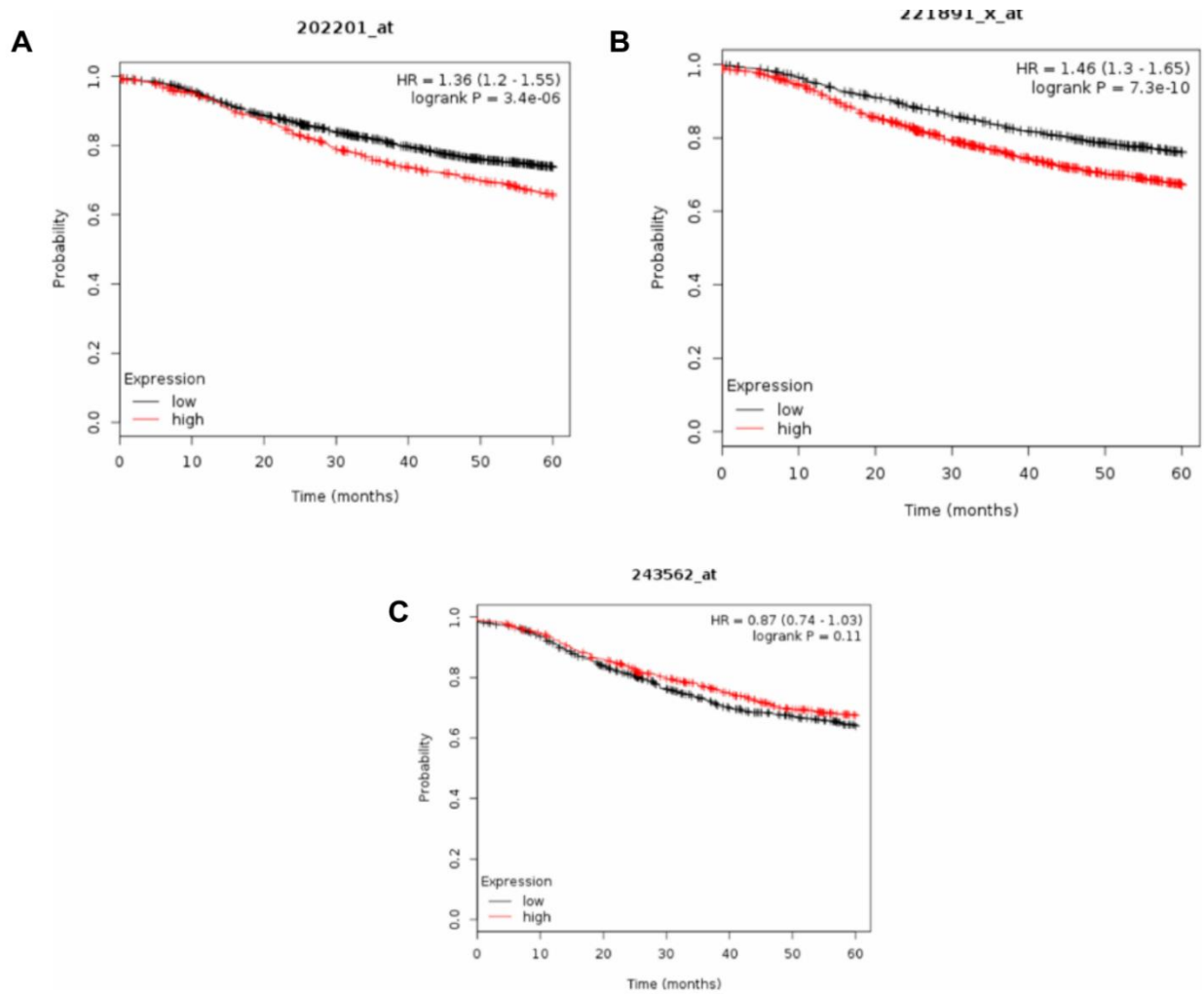


Figure 3.5: Kaplan-Meier survival analysis of human patients (n=3951) with invasive breast cancer divided into two groups based on the expression level of HSPA8.

(A), BLVRB (B), and KING1 (C). Log rank test P-value is displayed. HR, hazard ratio.

Table 3.1: Proteins Differentially (>175 Fold) Expressed in Lymph from Metastatic Tumor-Bearing Compared to Lymph from Non-Metastatic Tumor-Bearing Animals

Protein	P-value	MW	Accession
Serine (or cysteine) proteinase inhibitor, clade G (C1 inhibitor), member 1, (angioedema, hereditary)	9.99E-15	55,576.2	40,018,558
Creatine kinase, muscle	1.11E-15	42,991.8	6,978,661
Enolase 1, alpha	1.13E-09	47,086.3	6,978,809
Pyruvate kinase, muscle	7.54E-12	57,781.0	16,757,994
Guanine deaminase	1.22E-14	50,983.8	13,929,094
PREDICTED: similar to tubulin, beta 2	8.07E-05	49,875.0	109,504,787
Tyrosine 3-monooxygenase/tryptophan 5-monooxygenase activation protein, zeta polypeptide	4.22E-09	27,753.7	62,990,183
Peptidylprolyl isomerase A	2.07E-09	17,862.8	8,394,009
PREDICTED: similar to triosephosphate isomerase	3.42E-07	26,847.8	62,663,437
PREDICTED: similar to biliverdin reductase B (flavin reductase (NADPH))	1.24E-04	22,080.3	109,461,493
PREDICTED: similar to Tubulin alpha-3 chain (Alpha-tubulin 3)	5.66E-13	49,927.7	109,474,238
Solute carrier family 4, member 1	2.56E-13	103,178.4	76,443,687
PREDICTED: similar to Tubulin alpha-2 chain (Alpha-tubulin 2)	5.48E-05	50,247.7	109,481,286
Enolase 2, gamma	4.47E-11	47,111.0	26,023,949
Glucose phosphate isomerase	2.15E-07	62,787.2	46,485,440
Phosphoglycerate mutase 2	1.27E-07	28,736.8	8,393,948
Enolase 3, beta	8.77E-10	46,931.4	6,978,811
Heat shock protein 8	3.13E-10	70,827.3	13,242,237
Coagulation factor XIII, A1 subunit	1.29E-12	82,606.5	11,067,435
Transketolase	1.01E-04	71,141.5	12,018,252
Xanthine dehydrogenase	2.47E-04	146,148.7	8,394,544
Lymphocyte cytosolic protein 1	2.59E-08	70,077.9	58,865,656
Phosphoglycerate mutase 1	3.79E-09	28,627.7	16,757,984
Tyrosine 3-monooxygenase/tryptophan 5-monooxygenase activation protein, theta polypeptide	1.89E-14	27,760.8	6,981,712
Creatine kinase, brain	6.01E-11	42,685.3	31,542,401
PREDICTED: similar to Phosphoglycerate kinase 1	5.93E-10	43,148.3	62,642,907

CHAPTER 4. **ACTIVATION OF TLR3 CONTRIBUTES TO TUMOR CELL MIGRATION AND METASTASIS THROUGH THE LYMPHATIC SYSTEM.**

THIS IS A PUBLISHED JOURNAL ARTICLE. Reprinted with permission from: Molecular Oncology Journal. **Lymph-circulating tumor cells show distinct properties to blood-circulating tumor cells and are efficient metastatic precursors.** Mol Oncol. Mohammed SI, Torres-Luquis O, Walls E, Lloyd F. 2019 Jun;13(6):1400-1418. doi: 10.1002/1878-0261.12494. Epub 2019 May 23. PMID: 31026363

Abstract

Metastasis via the lymphatics is the primary route of metastasis in early breast cancer. However, little is known about how tumor cells migrate to the lymph nodes (LNs.) We hypothesized that Toll-like receptor (TLR) signaling may guide tumor cell migration to the LNs. We developed a technique that enables the collection of lymph-circulating tumor cells (LCTCs) en route to the regional LN, as well as blood circulating tumor cells (BCTCs), in animal model of breast cancer metastasis and examined the role of TLRs in aiding tumor cells metastasis. We identified that LCTCs, not BCTCs, expressed high levels of TLR3 upon stimulation with its ligand Poly (I:C). In consequence, chemokine CXCL10 and its receptor, CXCR3 were also induced, thus increasing LCTCs migration and metastasis in vitro and in vivo. Our data suggest that activation of TLR3 and induction of CXCL10 contribute to tumor cell migration and metastasis through the lymphatics.

4.1 Introduction

The primary cause of death from breast cancer is the spread of tumor cells from the primary tumor and their growth in distant organs affecting their normal physiological functions. The spread of tumor cells occurs via the blood and the lymphatic systems. Metastasis through the lymphatic system is a major route of tumor cells spread in breast cancer. The presence of tumor cells in patients' regional or sentinel lymph nodes is associated with disease progression, poor prognosis, and determines the choice of therapies ^{62,215,216}. Although tumor cells metastasis via the bloodstream is well studied, little knowledge available about the lymphatic metastases and its association with distant metastasis and cancer progression ^{62,124,217,218}.

Tumors do not have a formed and functional lymphatic circulation within the tumor mass⁵⁹. While this contributes to an increase in intra-tumor interstitial pressure, it does not offer a direct entry route for tumor cells into the lymphatic circulation. Tumor cells can only enter the lymphatic circulation at the interface between the invasive edge of the tumor and the adjacent host stroma that contains the lymphatic circulation. The existence of this distance barrier means that it would be unlikely for tumor cells to enter the lymph drainage passively. Instead, it is expected that active migration and chemotaxis might aid tumor cells to traverse the space between the tumor mass and the peripheral lymphatics. Following this logic, it is self-evident that the derived chemotactic factors and cellular motility mechanisms of the lymph are essential targets for arresting the entry of tumor cells into the lymphatic drainage⁹¹.

Toll-like receptor (TLR) pathway regulates the expression of cytokines and chemokines as a part of lymph node activation during the early stages of infection. Recent growing experimental evidence suggests that TLR signaling pathways may be involved in cancer progression and constitute a link between cytokines stimulation of cancer cell metastasis, innate immunity, and inflammation^{94-96,219-223}. Researchers characterized several endogenous ligands collectively named danger-associated molecular patterns (DAMP), which implies a role for these receptors in the inflammatory responses resulting from tissue damage even in the absence of infection, such as in transformed cells²²⁴. Activation of these receptors leads to induction of multiple inflammatory pathways, including nuclear factor-kappa B (NF- κ B) and interferon regulatory factors (IRF), which lead to the expression of the IRF and NF- κ B-inducible genes that play a critical role in the activation of innate immunity including expression of several inflammatory cytokines and chemokines⁹⁹. Most Toll-like receptors (TLRs), except TLR3, interact and recruit the TLR adaptor protein, myeloid differentiation primary response 88 (MyD88), for their signaling pathway. TLR3, however, signals through the MyD88-independent pathway and activates IRF3, thereby inducing type 1 interferons (IFN) and IFN-inducible genes through the TLR adaptor protein, TIR domain-containing adaptor-inducing IFN- β (TRIF).

In humans, TLR3 expresses not only in immune cells but also in many different types of malignant cells, such as breast cells. In a study of patients with breast cancer, tumors with strong TLR3 expression had a higher probability of metastasis. Similarly, TLR3 is overexpressed in oral squamous cell carcinoma and associated with high-risk tumor histopathological features such as poor differentiation and perineural invasion^{97,225}. However, many studies reported on the

conflicting results concerning tumor formation and progression in response to TLR3 stimulation, with some studies reported the TLR3 anti-tumor effect^{226,227}. Therefore, here, we examined the role of TLR3 and its associated pathway in the lymphatic and blood metastasis. We report in this study that TLR3 upregulation in the lymph-circulating tumor cells (LCTCs) triggered NF- κ B and IRF3 nuclear translocation and induction of chemokine CXCL10 and its receptor, CXCR3, leading to tumor cell migration and metastasis *in vitro* and *in vivo*. TLR3 activation decreased the blood circulating tumor cells (BCTCs) growth and has no effect on their migration and metastasis *in vitro* and *in vivo*. Our data suggest that the activation of TLR3 resulting in the induction of chemokines CXCL10 contributes to tumor cell migration and metastasis through the lymphatic system and not via the blood circulation. We concluded that the role of TLR3 in inducing pro-tumor or anti-tumor effects is dependent on the route of cells dissemination.

4.2 Materials and methods

4.2.1 Cell lines and cell culture conditions

All cell lines are of mammary adenocarcinoma origin from rat, varying in metastatic properties. MTC and MTLN3 provided by Segall (Albert Einstein College of Medicine, Bronx, NY, USA). MTLn3 cell line clonally derived from a lung metastasis of the 13762NF rat mammary adenocarcinoma. LCTCs and BCTCs were established in our laboratory from the lymph or the blood, respectively, from rats with metastatic tumors. All cell lines were cultivated in Minimal Essential Medium (MEM) Alpha (Gibco, Waltham, Massachusetts, USA), containing GlutaMAX, and supplemented with 5% fetal bovine serum (FBS; Manassas, Virginia, USA). All cells were cultured at 37°C in a humidified CO₂ incubator.

4.2.2 Animal model and tumor assay

We carried the rat experiments following the National Institutes of Health (NIH) regulation on the care and use of experimental animals. Purdue University Animal Use and Care Committee approved the study protocol. The rats housed in the Purdue animal housing facility and fed standard rodent chow and water ad libitum and kept at a 12-hour light-dark cycle. We purchased the immunocompetent syngeneic female rats from Harlan Laboratories (Indianapolis, USA). We grew MTLn3, MTC, BCTCs, LCTCs, and LCTC-shTLR3 cells to 70-80% confluence and implanted

1x10⁶ cells in 0.1 ml PBS into the two left caudal- and rostral-most mammary fat pads. Animal weight and tumor size were measured every other day. We calculated the tumor size according to the formula: $V \text{ (volume)} = (LW^2)/2$, where "L" represents the length, and "W" represents the width. Metastasis to the lymph node and lung usually occurs after 14-21 days (determined previously) ²²⁸. Then, we anesthetized the rats and collected the lymph, the blood, and the primary tissues and metastasis (lymph nodes and lungs) lesions. Metastatic foci in lymph node and lung were evaluated and counted grossly as well histopathological using H&E stained sections.

4.2.3 Real-Time Quantitative PCR

We extracted total RNA from Poly(I:C)-stimulated or not stimulated cells using TRIzol RNA isolation reagents as per manufacturer's instructions (Invitrogen, Carlsbad, CA, USA). RNA purity and concentration were determined using NanoDrop (Thermo Fischer Scientific, Waltham, MA). We performed the reverse transcription of RNA to cDNA using Transcriptor First Strand cDNA Synthesis Kit from Roche (Basilea, Suiza), according to the manufacturer's instructions. Real-time thermal cycling was performed using Fast SYBR Green Master Mix from Applied Biosystems (Thermo Fisher Scientific, Waltham, MA, USA). TLR1-9, IL2, IL4, IL6, IL12a, IL12b, TNF, IFN γ , CXCL10, and CXCL12 were designed using Primer3 (<http://bioinfo.ut.ee/primer3-0.4.0/>) and ordered through Integrated DNA Technologies webpage (<https://www.idtdna.com/site>). We normalized gene expression to the expression of GAPDH.

4.2.4 Cell viability assay

LCTCs, BCTCs, MTLn3 and MTC cells were cultured with different concentrations (5, 10, 25, and 50 ug/ml) of Poly (I:C) (Ellisville, MO, USA) for 0-72 h. Cell viability was determined using Cell Titer-Glo luminescent cell viability assay according to manufacturer's instructions (Promega Corp., Madison, WI) and measured using SpectraMax i3x Multi-Mode Microplate Reader (Molecular Devices, San Jose, CA).

4.2.5 Western Blot

Cells were cultured to 75-85% confluence with and without poly(I:C) stimulation and lysed using RIPA lysis buffer (10mM Tris HCL (pH 7.6), 150mM NaCl, 5 mM EDTA, 1mM MPMSF,

2 mM Na₃VO₄, and protease inhibitor cocktail (Promega, Maddison, WI). Protein concentration for each sample was determined using the bicinchoninic acid (BCA protein assay; Pierce). Proteins (5-10 µg) were separated by 10% SDS-PAGE and transferred to nitrocellulose membranes. Detection was performed using the following primary antibodies TLR3 at dilution 1:500 (Novus Biological, Centennial, CO), and secondary rabbit antibody-conjugated with horseradish peroxidase at 1:20,000 dilution. Bound complexes were then detected using SuperSignal West Pico PLUS Chemiluminescent Substrate (Thermo Fisher Scientific, Waltham, MA). Equal loading was confirmed using β-actin (1:20,000; Sigma-Aldrich Co., San Luis, MO).

4.2.6 Immunofluorescence and confocal imaging

To visualize NF-κB and IRF3 nuclear translocation cells were cultured on coverslips and fixed with 4% paraformaldehyde in PBS for 30 mins at room temperature. Permeabilization was performed with 0.4% Triton X-100 (Sigma, San Luis, MO) in PBS for 10 min. Cells were then incubated in blocking buffer (5% fetal bovine serum in PBS) for 1 h and then incubated with primary antibodies diluted in incubation buffer at room temperature overnight. The following primary antibodies were used: Phospho-NF-κB (1:100; Cell Signaling, Danvers, MA) and IRF3 (1:100; Cell Signaling, Danvers, MA). Cells were washed and incubated with fluorescent-labeled secondary antibodies-conjugated to Alexa Fluor 488 (1:500, Cell Signaling, Danvers, MA) for 1 h. We detected Actin filaments with Alexa Fluor 555 Phalloidin (1:20; Cell Signaling, Danvers, MA). Then finally, samples were mounted in Prolong® Gold AntiFade with DAPI (Cell Signaling, Danvers, MA) and visualized using a confocal microscope Zeiss AXIO (Oberkochen, Germany).

4.2.7 Flow Cytometry

For analysis of intranuclear activation of NF-κB p65, cells were cultured until 70-80% confluency and then fixed with 4% paraformaldehyde in PBS for 15 mins at room temperature. Permeabilization was performed with ice-cold methanol (Sigma, San Luis, MO) in PBS for 30 min. Then, we incubated the cells with primary antibody Phospho-NF-κB (1:600; Cell Signaling, Danvers, MA) diluted in incubation buffer (0.5g BSA) at room temperature for 1 h. Cells were washed and incubated with Anti-rabbit IgG (H+L), F(ab')₂ Fragment (Alexa Flour 488 Conjugate; 1:1000; Cell Signaling, Danvers, MA) for 30 minutes at room temperature. Cells were then

counted and analyzed using BD Accuri C6 Plus personal flow cytometer and BD Accuri C6 Software (Franklin Lakes, NJ).

4.2.8 RNA interference

Lentiviral-based shRNA vectors designed to contain green fluorescent protein and an antibiotic-resistant puromycin gene were purchased from TransOMIC (Huntsville, AL). Three shRNAs with the different target sequences in the TLR3 coding sequence were prepared. Also, a non-targeting or scrambled shRNA as a negative control was prepared as well. These shRNAs were labeled as TLR3-shRNA-1, 2, 3, and scrambled shRNA or control. Stable knockdown of TLR3 in LCTCs was performed by shRNA transfection using polybrene (EMD Millipore, Burlington, MA). TLR3 knockdown was confirmed by detecting the green fluorescent protein under fluorescent microscope Zeiss AXIO in 293TN cells. The efficiency of TLR3 knockdown for each shRNA was evaluated by measuring RNA and protein expressions by RT-qPCR and western blot analysis, respectively.

4.2.9 Migration Assay

Cells were seeded under different conditions into a Transwell polycarbonate membrane inserts (Corning, Corning, NY) plate and grown overnight. We used a sterile cotton swab to scrape off the cells that did not migrate through the membrane. Transwell inserts were removed, and cells inside the insert were fixed using formaldehyde for 10 min and permeabilized using methanol for 20 min. DAPI solution was mixed with Triton X-100 into a final 1% solution and added to the transwell insert. Zeiss AXIO fluorescent microscope was used to observe DAPI expression of cells inside the transwell insert.

4.2.10 NF- κ B Transcription Factor Assay

The nuclear factor (NF- κ B) activity was measured by TransAM NF- κ B p65 Activation Assay, according to the manufacturer instructions (Active Motif, Carlsbad, CA).

4.2.11 Immunohistochemistry

All specimens were fixed in formalin and cut into paraffin slides for further testing. We performed the immunohistochemistry using products and reagents from Biocare Medical (Pacheco, CA) as follows: Tissue sections were deparaffinized in xylene and then rehydrated in graded concentrations of ethyl alcohol (100%, 96%, 80% 70% and water). Tissue slides were treated with 1% of Diva Decloaker at 95°C for 30 min using the Decloaking Chamber (Biocare Medical, Pacheco, CA) to enhance antigen retrieval. Endogenous peroxidase activity was blocked using PeroxAbolish for 5 min. We incubated tissues with CXCR3 antibody Novus (St. Charles, MO) for 1 h. MACH 4 Universal HRP-Polymer was used as a polymer, and tissues were incubated for 30 min. DAB Chromogen was used as the staining detection system incubating tissue slides for 5 min. Sections were counterstained with hematoxylin (Thermo Scientific, Waltham, MA), dehydrated with ethanol, and permanently coverslip using Clearmount (Zymed, San Francisco, CA).

4.2.12 Statistical analysis

We performed the statistical analysis with Microsoft Excel analysis tools. Two-tailed student t-test used to determine the differences between the groups. P-values of <0.05 were considered statistically significant

4.3 Results

4.3.1 Mapping of lymphatic vessels and the collection of lymph and LCTCs before reaching the regional lymph nodes in a breast cancer model.

The study used metastatic rat tumor cells, MTLn3, which form primary tumors and metastases in the lymph nodes and the lungs, and non-metastatic cells, MTC, which form primary tumors only when they are transplanted orthotopically in the mammary fat pad of immunocompetent female rats. Collection of tumor-draining lymph and tumor cells therein, LCTCs, and isolation of BCTCs from the blood and their growth are described previously⁸⁸.

4.3.2 Lymph circulating tumor cells (LCTCs) express TLR3.

To investigate differences in TLRs expression levels and signaling responses they mediate, we quantified TLR 1-9 mRNA expression levels in LCTCs, BCTCs, the metastatic tumor cell line, MTLn3, and the non-metastatic tumor cell line, MTC, in the absence of any TLRs ligands. At baseline without TLR stimulation, all cells examined showed comparable expression levels of TLR3 and TLR6, without significant changes in expression levels of TLR1, 2, 4, 5, 7, 8, 9 (Fig. 1A). To determine whether TLR3 expression changes in response to a TLR3 ligand, we quantified the TLR3 expression in LCTC, BCTC, and MTLn3 in the presence of polyinosinic-polycytidylic acid [Poly(I:C)], a synthetic analog of double-stranded RNA (dsRNA) that functions as a synthetic ligand for TLR3 activation. We showed that 5 µg Poly(I:C) upregulated TLR3 expression in LCTCs (2 folds) in comparison to BCTCs and MTLn3 (Fig. 1B). To examine whether the Poly (I:C) affects the viability of the cells, we examined the cell viability by Cell Titer-Glo Luminescent cell viability assay. We found that 5µg Poly(I:C) (the concentration used for the above experiments) had not affected the cell viability of LCTCs and MTLN3 but affected BCTCs growth after 72 h incubation (Fig. 1C). TLR3 stimulation increased the proliferation of LCTCs and MTLn3. Collectively, these findings demonstrate that LCTCs, BCTCs, MTLn3, and MTC cells did not upregulate TLR1-9 expression except for TLR3 and TLR6 and that Poly(I:C) stimulate TLR3 expression in LCTCs and not in BCTCs. To confirm the expression of TLR3 at the transcriptional and translational levels in LCTCs, we determined the mRNA and protein expression at the same time using RT-PCR and western blot analysis. We found that Poly(I:C)-stimulated LCTCs expressed a higher levels of TLR3 mRNA (Fig. 2A) or protein compared to unstimulated LCTCs (Fig. 2B).

4.3.3 TLR3 activation increases LCTCs, not BCTCs, migration and invasion in vitro and in vivo.

High expression of TLR3 is associated with a high probability of metastasis²²⁹. Activation of TLR3 in cancer cells release cytokines and chemokines that, in turn, may recruit immune cells for cancer cell metastasis and immune tolerance, and cancer progression²³⁰. Therefore, we examined TLR3 expression and its associated signaling pathways in LCTCs and BCTCs to determine its role in metastasis. To do so, we treated LCTCs with TLR3 ligand Poly(I:C) to stimulate TLR3 function, and we have knockdown TLR3 expression in LCTCs to suppress its

function. We then examined the effect of these treatments on the cells' ability to migrate and metastasize in vitro and in vivo. We performed the knockdown of TLR3 in LCTCs by using TLR3-specific shRNAs. We used three different shRNAs to eliminate any off-target effects. We constructed lentivirus shRNA vectors using three different shRNA sequences against TLR3 in addition to a scrambled shRNA control. We used the three lentiviral vectors expressing shRNA against TLR3 to transduce LCTCs, and we have selected the stably transfected cells in the presence of puromycin. Then, we determined the levels of TLR3 knockdown at the protein (Fig. 3A and B). Then, we examined the ability of LCTC-shTLR3 to migrate in vitro and to form tumor and metastasis in vivo. The migration rate of Poly(I:C) stimulated LCTC-shTLR3 significantly reduced in comparison to Poly(I:C) stimulated LCTCs. Activation of TLR3 by Poly(I:C) in BCTCs and MTC had not affected the cells' migratory aptitude (Fig. 3C). For the in vivo experiment, we implanted the Poly(I:C) stimulated cells, LCTC-shTLR3, LCTCs, BCTCs, MTLn3, and MTC into the mammary fat pad of syngeneic rats for potential tumor formation and metastasis. LCTCs and MTLn3 implanted rat showed a significant increase in tumor size compared to rat implanted with BCTCs, while LCTC-shTLR3 cells showed no tumor growth (Fig. 3d). Growth and microscopic examination of lymph nodes and lungs showed metastatic foci in lung of LCTCs- and MTLn3-implanted rats only (Fig. 3E). The results suggest that TLR3-stimulated LCTCs developed large tumors and lymph node and lung metastases, whereas TLR3-depleted LCTCs or BCTCs formed small or no tumors and metastases (node-negative). Thus, we inferred from this study that TLR3 increases cell proliferation and tumor growth and facilitates cell metastasis of LCTCs but not of BCTCs.

4.3.4 Upregulation of TLR3 in LCTCs leads to NF- κ B and IRF3 nuclear translocation.

Stimulation of TLR3 by its ligand, Poly(I:C), leads to IRF3 and NF- κ B signaling activation resulting in the upregulation of genes involved in inflammatory responses, cell proliferation, and invasion²³¹. IRF3 is located in the cytoplasm and must undergo phosphorylation to form dimers, translocate to the nucleolus, and bind to the specific gene promoters. Similarly, in a majority of cells, NF- κ B exists in an inactive form in the cytoplasm bound to the inhibitory protein I κ B α in the classical NF- κ B pathway. Treatment of cells with various inducers results in degradation of I κ B α protein releasing the bound NF- κ B, which translocate to the nucleus and binds NF- κ B sites in the promoter of target genes such as chemokines and their receptors, which lead to their

transcription^{232 232}. These chemokines act on autocrine and paracrine loops among tumor cells and cross signaling between tumor cells and the stroma²³³. Therefore, we tested whether treatment of LCTCs with Poly(I:C) causes IRF3 and NF- κ B translocation to the nucleus. We observed a significant increase in the nuclear translocation of NF- κ B in LCTCs compared with other cells (BCTC, MTLn3, and MTC) after Poly(I:C) treatment by flow cytometry (Fig. 4A and B). Also, there was a significant increase in NF- κ B and IRF3 translocation to the nucleus in Poly (I:C)-stimulated LCTCs compared to LCTC-shTLR3 (Fig. 4C and D).

4.3.5 Activation of NF- κ B and IRF3 result in the induction of CXCL10 in LCTCs.

NF- κ B nuclear translocation induces expression of pro-inflammatory cytokine genes, such as TNF α , IL-6, and IL-12, crucial for the generation of the acute phase response, and the differentiation of neutrophils and natural killer cells, while IRF3 is crucial modulators of production of type 1 IFNs²³⁴ and upregulation of genes essential for attracting immune cells such as chemokine CXCL10. Therefore, we examined the levels of two products of TLR3 signaling, INF- β and CXCL10 as well as others. Our results showed that Poly(I:C)-stimulated LCTCs expressed high levels of INF- β and CXCL10 and its receptor, CXCR3, while no increases in IL-6, IL-12, and TNF- α (Fig. 5A). Examination of growth medium for CXCL10, showed that stimulated LCTCs expressed higher level of CXCL10 compared to MTLn3, while BCTCs did not express detectable levels of CXCL10 (Fig 5B).

4.4 Discussion

In this study, we report differences in the TLRs expression in LCTCs and BCTCs in the breast cancer metastasis. Our investigation identified that all the cells examined, LCTCs, BCTCs, metastatic MTLn3, and non-metastatic MTC, showed expression of only TLR3 and TLR6 without any TLR ligands stimulation. Specifically, we report significant differences in TLR3 expression and responsiveness between LCTCs and BCTCs. Interestingly LCTCs expressed a high level of TLR3 at the transcription and translation levels upon TLR3 stimulation with its ligand Poly(I:C), and activation of TLR3-induced expression of CXCL10 in these cells. In contrast, its counterpart BCTCs showed no significant increase in TLR3 expression at the mRNA or protein levels in response to Poly(I:C) activation. Worth noting here, that MTLn3 and MTC were isolated from the

same parent tumor, 13762NF mammary adenocarcinoma, but differed in their ability to metastasize. LCTCs and BCTCs were originated from MTLn3 but metastasized via two different routes; therefore, we have ruled out any genetic bias that may have contributed to these differences in TLR expression and TLR3 activation. Also, we determined whether these differences could be explained by the effect of Poly(I:C) on cell viability, although our data was normalized to housekeeping gene GAPDH or β -actin, we observed that 5 μ g of Poly(I:C) has reduced BCTC growth. Our results demonstrate that LCTCs exhibit increased TLR3 expression and TLR3-mediated CXCL10 induction, while BCTCs show no TLR3 or CXCL10 expression. These attributes seem to be a route of dissemination specific and tumor microenvironment influenced.

Also, our work showed that TLR3 activation with its ligand could augment tumor migration and tumor formation ability of only LCTCs. However, research scrutinized the role of TLR3 in cancer progression culminated results with mixed outcomes. In some studies, TLR3 suggested to promoting tumor development through effects on cell proliferation and survival²³⁵, while in other studies TLR3 is proposed as a target for anti-tumor therapy by some investigators²³⁶

Studies in melanoma²³⁶, breast²²⁰, liver²³⁷ and prostate cancers²³⁸ reported that TLR3 protein expression in tumor cells could deliver pro-apoptotic and anti-proliferative signaling and TLR3 deficiency results in the development of acute lymphoblastic T cell leukemia after infection with endogenous retrovirus²³⁹. Furthermore, treatment with Poly(I:C) inhibited tumor growth in prostate cancer model overexpressing TRAMP transgene²³⁸. The pro-apoptotic and anti-proliferative effects of activated TLR3 were attributed to the induction of type 1 INF β - and effector cells^{238,240}. The effect of Type I IFN on cancer proliferation has been extensively studied in a variety of cancers, including breast cancer, and suggests the use of TLR3 agonists for cancer immune-based therapies to convert the often-tolerant immune response towards anti-tumor responses^{241,242}. Currently, several preclinical and clinical studies are ongoing to investigate the immunotherapeutic potency of TLRs against prostate and other cancers using TLR3 agonists as a potential anti-tumor therapeutic agent (Hilton and AmpligenTM derivative of Poly (I:C) for use in humans)^{243,244}.

However, other studies reported that TLR3 contributed to cell proliferation and promotion of tumor survival and metastasis in many cancers such as esophageal cancer²⁴⁵, breast cancer²⁴⁶ and intestinal cancer²⁴⁰, and attributed to the induction of chemokines such as CXCL10 and CXCL8. These chemokines are chemoattractant and implicated in cancer migration and

progression. CXCL10 is a member of the CXC chemokine family that bind to the CXCR3 receptor and involved in chemotaxis, induction of apoptosis, regulation of cell growth, and angiogenesis. These cytokines and their receptors are well known in breast cancer metastasis to perform a homing function by attracting CXCR3 cells to metastasis regions ²⁴⁷ and regulate adhesion and migration of tumor cells to site-specific metastasis ²⁴⁸. High expression of CXCR3 is highly predictive of poor survival in women without positive nodes at diagnosis ²⁴⁹. In this study, we saw a high secretion and expression of CXCL10 and its receptor, CXCR3, in metastatic cells in the lymph node and lung tissues. CXCL10 may be produced by other cells in the lymph microenvironment and act in a paracrine fashion to guide LCTCs migration to the lymph node or possibly in an autocrine circuit since CXCL10 and CXCR3 are found in the same cell. Also, in our previous study, we have seen an elevated level of CXCL10 in the lymph from metastatic tumor-bearing animals and not in the lymph from non-metastatic tumor-bearing animals ⁸⁸. Therefore, our data suggest that the CXCL10/CXCR3 axis plays a role in lymph node metastasis. Induction of CXCL10 upon activation of TLR3 in LCTCs may drive migration and invasiveness, and metastasis formation as seen with our data as well as data reported previously in intestinal cell cancer ²⁴⁰.

In conclusion, our study report differences in TLR3 expression in LCTCs and BTCs. Stimulation of TLR3 with its ligand Poly(I:C) argument tumor proliferation and migration of LCTCs. Our findings propose that TLR3 activation plays a role in tumor growth and metastasis depending on the tumor environment and the route of dissemination. More research is needed using human samples to elucidate the role of TLR3 activation in tumor cell dissemination and metastasis.

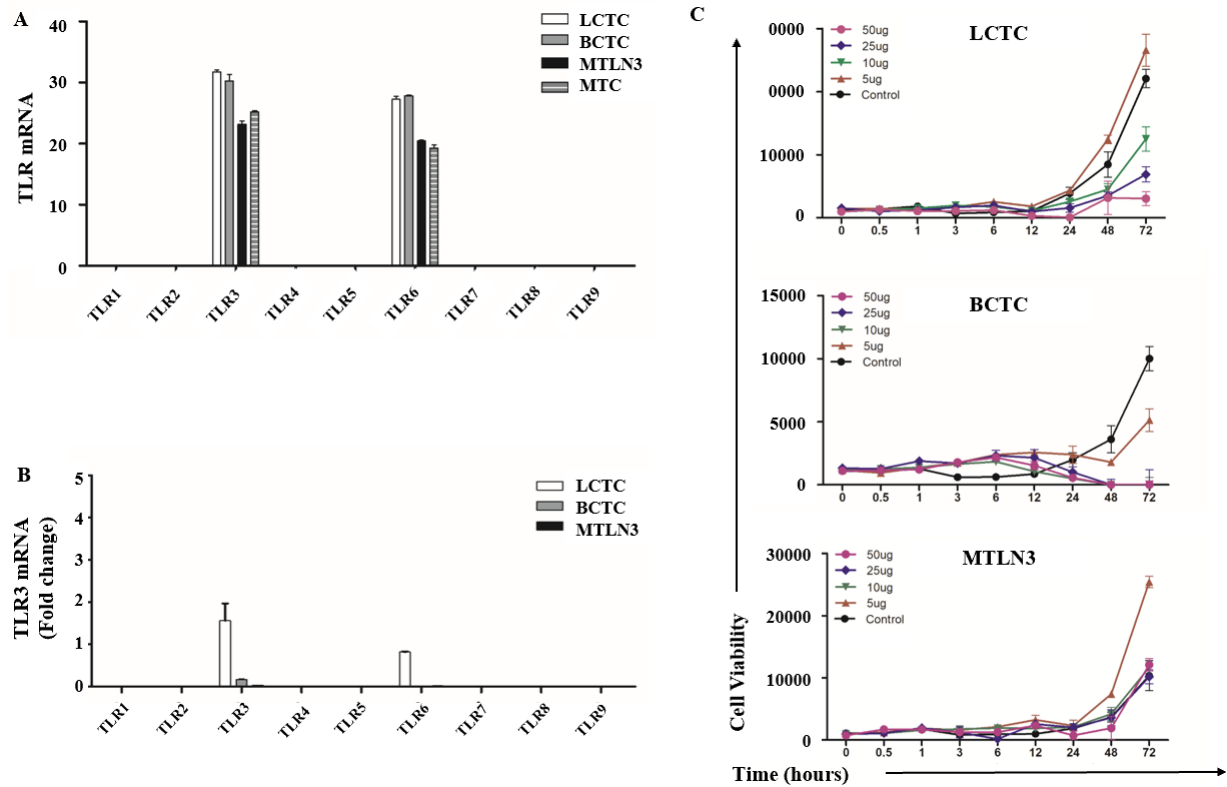


Figure 4.1: TLRs expression and effect of Poly(I:C) on cell viability.

A) mRNA expression of TLR 1-9 in LCTCs, BCTCs, MTLN3, and MTCs cells at baseline without stimulation. B) mRNA expression of TLR 1-9 in LCTCs, BCTCs, MTLN3, and MTC with Poly (I:C) stimulation. C) Viability of LCTCs, BCTCs, and MTLN3s stimulated with different concentrations of Poly (I:C) (0, 1, 5, 10, 25, and 50 ug/ml) for 72 h. Results show mean \pm S.D. of triplicates and are representatives of a minimum of two experiments.

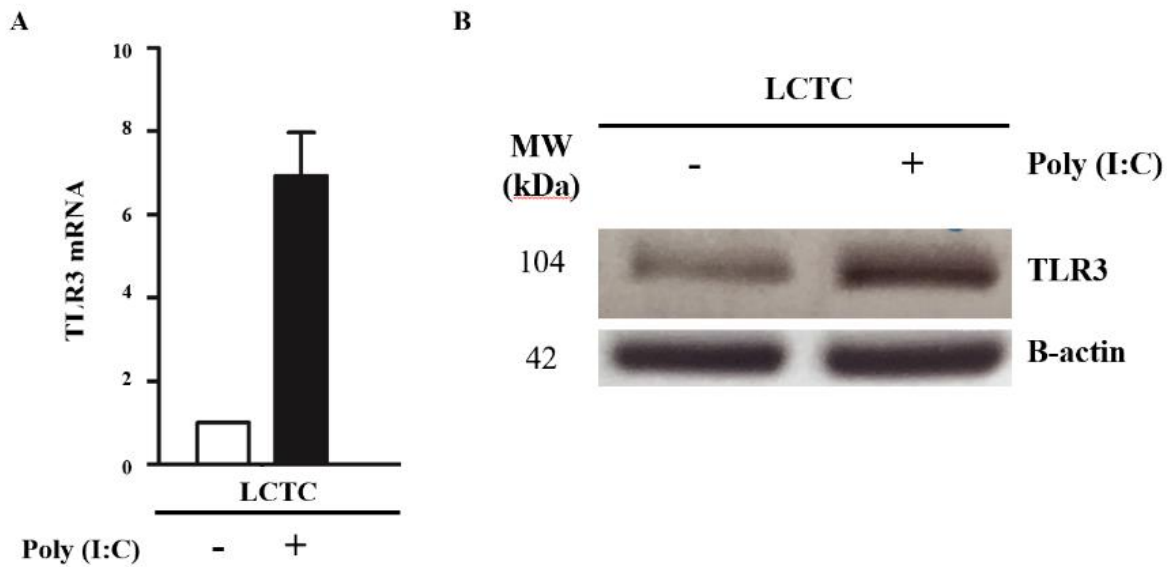


Figure 4.2: LCTCs highly express TLR3 when stimulated with Poly (I:C).

A) TLR3 mRNA expression level in unstimulated and stimulated LCTCs with Poly (I:C). The results are presented as mean \pm S.D. of triplicates and are representatives of a minimum of three experiments. * $p < 0.05$. B) Western blot of LCTCs unstimulated (-) and stimulated with 5ug Poly (I:C) (+), shows TLR3 protein expression level (104kDa) and β -actin (42kDa) as a loading control. MW, Molecular Weight.

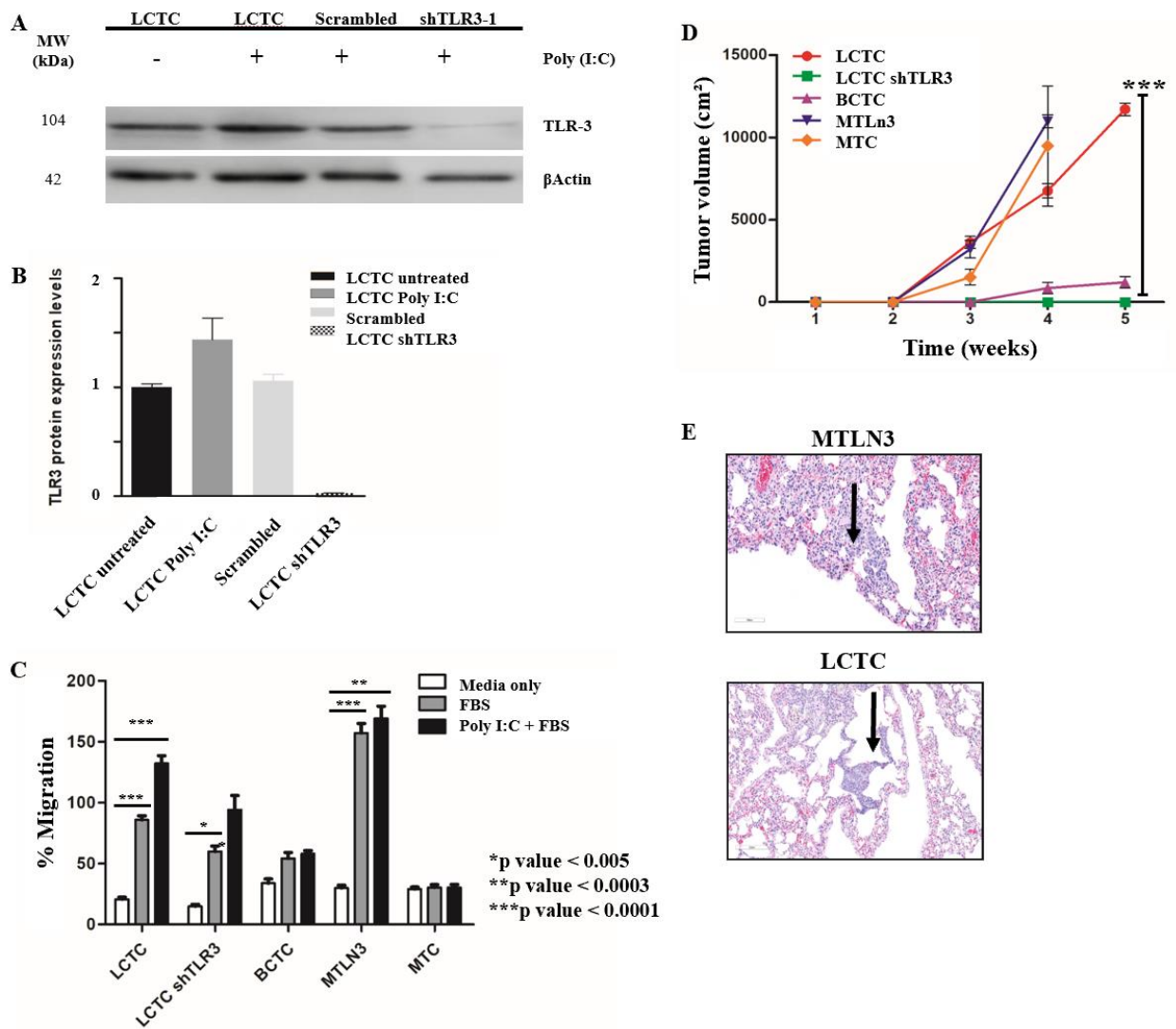


Figure 4.3: Knockdown of TLR3 in LCTCs decreased their migration and invasion in vitro and in vivo.

A&B) Western blot of LCTCs unstimulated (-) and stimulated with 5ug Poly (I:C) (+), scrambled shRNA, and LCTC-shTLR3-1. β -actin (42kDa) serves as a loading control. C) LCTCs, LCTC-shTLR3, BCTCs, MTLN3, and MTC percent of migration in vitro. D) Tumor sizes in rats for 6 weeks in different experimental groups. E) Metastatic cells in lung of MTLN3- and LCTC-tumor-bearing animals. B-D Data are presented as the mean \pm S.D. of the mean of three independent experiments and are representatives of a minimum of two experiments. * $p < 0.005$, ** $p < 0.0003$, *** $p < 0.0001$. MW, Molecular Weight.

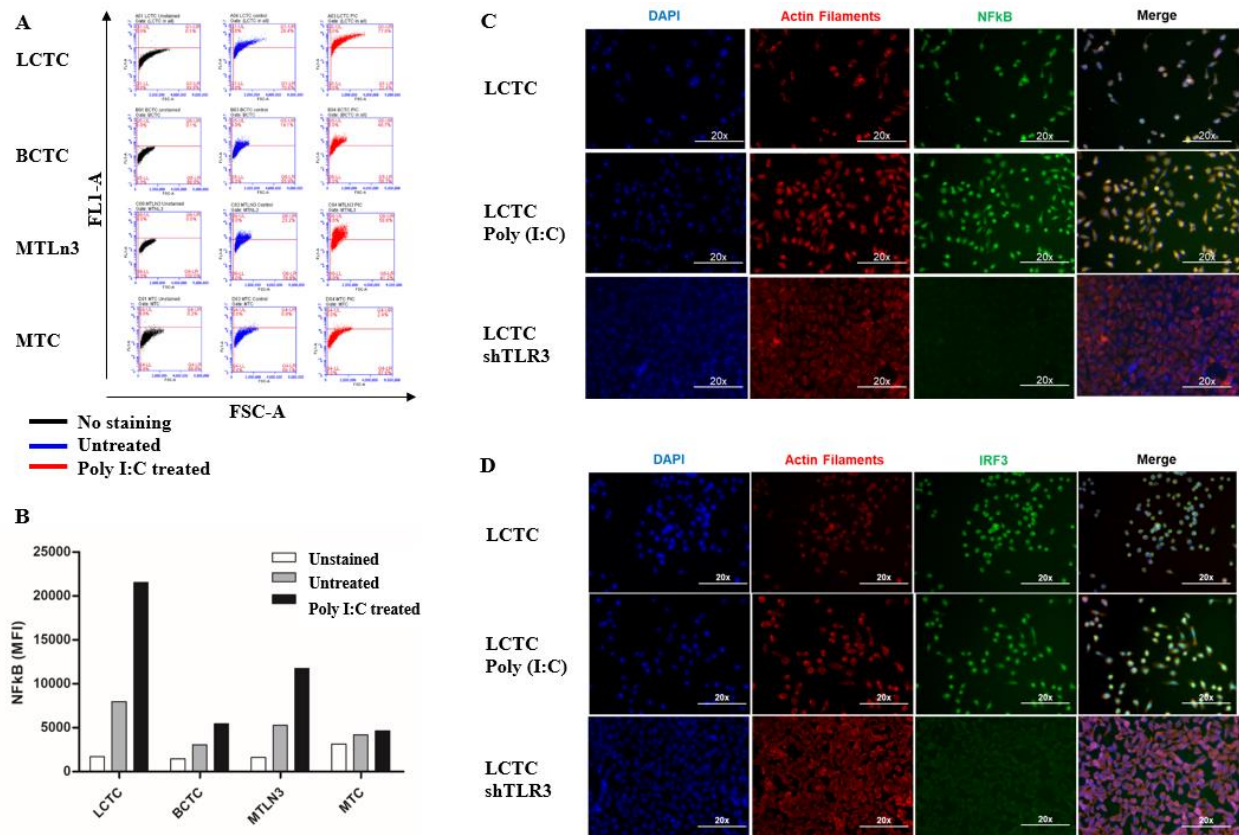


Figure 4.4: Stimulation of Poly (I:C) in LCTCs leads to NF-kB and IRF3 nuclear translocation.

A&B) Analysis of NF-kB intranuclear activation by flow cytometry of unstained (without antibodies; black), untreated (no Poly (I:C); blue) stimulation) and stimulated [with 5ug Poly (I:C); red] LCTCs, BCTCs, MTLn3s, and MTCs. MFI = Mean fluorescence intensity. C) Confocal images of Phospho NF-kB p65 (green) and D) IRF3 (green) in LCTCs, LCTCs (5ug/ml) Poly (I:C) and LCTC-shTLR3. As a positive control, images show AntiFade DAPI (blue), Actin filaments in Alexa Fluor 555 (red), and a merged column of all channels. The results are in a microscopic magnification of 20x and are representatives of a minimum of two experiments.

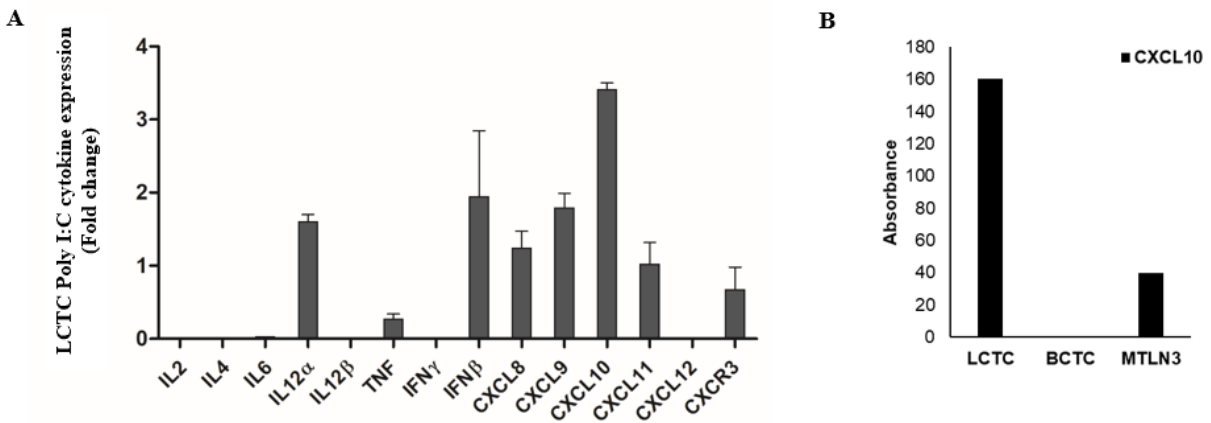


Figure 4.5: CXCL10 and its receptor, CXCR3, are highly expressed in LCTCs.

A) mRNA expression of cytokines (IFN β , CXCL10, CXCR3) in Poly(I:C)-stimulated LCTCs. The results are presented as the mean \pm S.D. of triplicates. B) CXCL10 expression in media of Poly(I:C)-stimulated LCTCs, BCTCs, and MTLn3.

CHAPTER 5. LXR/RXR PATHWAY SIGNALING ASSOCIATED WITH TRIPLE-NEGATIVE BREAST CANCER IN AFRICAN AMERICAN WOMEN.

THIS IS A PUBLISHED JOURNAL ARTICLE. Reprinted with permission from: Dove Med Press. **LXR/RXR pathway signaling associated with triple-negative breast cancer in African American women.** Breast Cancer (Dove Med Press). Torres-Luquis O, Madden K, N'dri NM, Berg R, Olopade OF, Ngwa W, Abuidris D, Mittal S, Lyn-Cook B, Mohammed SI. 2018 Dec 20;11:1-12. doi: 10.2147/BCTT.S185960. eCollection 2019. PMID: 30588086.

Abstract

Triple-negative breast cancer (TNBC) is more prevalent in African and African American (AA) women compared to European American (EA) women. African and AA women diagnosed with TNBC experience high frequencies of metastases and less favorable outcomes. Emerging evidence indicates that this disparity may in fact be the result of the uniquely aggressive biology of African and AA disease. To understand the reasons for TNBC in AA aggressive biology, we designed the present study to examine the proteomic profiles of TNBC and luminal A (LA) breast cancer within and across patients' racial demographic groups in order to identify proteins or molecular pathways altered in TNBC that offer some explanation for its aggressiveness and potential targets for treatment. Proteomic profiles of TNBC, LA tumors, and their adjacent normal tissues from AA and EA women were obtained using 2-dimensional gel electrophoresis and bioinformatics, and differentially expressed proteins were validated by Western blot and immunohistochemistry. Our data showed that a number of proteins have significantly altered in expression in LA tumors compared to TNBC, both within and across patients' racial demographic groups. The differentially overexpressed proteins in TNBC (compared to LA) of AA samples were distinct from those in TNBC (compared to LA) of EA women samples. Among the signaling pathways altered in AA TNBC compared to EA TNBC are innate immune signaling, calpain protease, and pyrimidine de novo synthesis pathways. Furthermore, liver LXR/RXR signaling pathway was altered between LA and TNBC in AA women and may be due to the deficiency of the CYP7B1 enzyme responsible for cholesterol degradation. These findings suggest that TNBC in AA women enriched in signaling pathways that are different from TNBC in EA women. Our

study draws a link between LXR/RXR expression, cholesterol, obesity, and the TNBC in AA women.

5.1 Introduction

Triple-negative breast cancer (TNBC) is a breast cancer subtype that does not express estrogen receptors (ER) and progesterone receptors (PR) and lacks human EGF receptor-2 (HER-2) amplification²⁵⁰. Although TNBC constitutes small percentage (10–20%) of all invasive breast cancers in women living in USA²⁵¹, it has very aggressive characteristics and distinct metastatic pattern and lacks targeted therapies²⁵². Epidemiological evidence showed that TNBC is more prevalent in young African and African American (AA) women compared to European American (EA) women and disproportionally lead to their death²⁵³. Previous research attributed this disparity in death rates to a various socioeconomic factors including income, co-morbid disease, and limited access to health care and medical treatment²⁵⁴. However, emerging evidence indicates that these disparities may in fact be due to the uniquely aggressive biology of the disease in African and AA. Results of studies comparing the biological differences between TNBC in AA and EA women were conflicted. Additional research has suggested that the interaction between the disparities and signaling pathways may promote TNBC's aggressive biology and genomic instability^{255,256}. Pathways that included cytoskeletal remodeling, cell adhesion, epithelial mesenchymal transition, and Wnt/ β -catenin were shown to be overrepresented in TNBC in AA and East African women. Activation of Wnt/ β -catenin pathway was suggested as the pathway that may contribute to the more aggressive TNBC phenotype in women of African origin²⁵⁷.

Despite the knowledge gained from previous studies, these comparative investigations have not yet examined the gene or protein expression of TNBC and LA tumor within patient's racial demographic to identify the differences that may have contributed to TNBC's aggressiveness. Compared to TNBC, LA tumors represent the commonest breast cancer subtype as it forms about 50–60% of all breast cancer and is characterized by ER and PR expression and negative HER-2 amplification.⁴ LA tumors are characterized by lower level of proliferation-related genes as well as low histological grade, low degree of nuclear pleomorphism, and low mitotic activity²⁵⁸. Unlike TNBC, patients with LA breast cancer have good prognoses, significantly lower relapse rates, and hormonal therapy treatment options²⁵⁹.

We designed the present study to examine the proteomic profiles of TNBC and LA breast cancer within patients' racial demographic groups (AA women) and across patients' racial demographics (AA vs EA). The goal is to identify proteins or molecular pathways altered in TNBC that offer explanation for its aggressiveness as well as potential targets for the treatment in African and AA women.

5.2 Materials and Methods

5.2.1 Chemicals and reagents.

The following reagents were purchased from Sigma-Aldrich Co. (St Louis, MO, USA): Coomassie Brilliant Blue R-250, dithiothreitol (DTT), urea, trypsin, glycerol, glacial acetic acid, alpha-cyano-4-hydroxycinnamic acid, acetonitrile, sodium carbonate, H₂AuCl₄, casein, and Ponceau S. We have purchased ReadyStrip (IPG strip pH 4–7) from Bio-Rad Laboratories Inc. (Hercules, CA, USA). Primary mouse monoclonal antibody or rabbit polyclonal antibodies against gelsolin, calpain, peroxire-doxin-2 (Abcam, Cambridge, UK), PEBP, LDH-B, crystalline (Abgent, San Diego, CA, USA), anexin-2 and LXR α and CRY7B1 (Novus, Littleton, CA, USA), and clusterin (R&D systems, Inc., Minneapolis, MN, USA) were used. We have purchased Mayer hematoxylin from Richard-Allan Scientific (Thermo Fisher Scientific, Waltham, MA, USA) and immunohistochemistry (IHC) reagents from Biocare Medical (Concord, CA, USA). All cell lines were purchased from the American Type Culture Collection (ATCC) (Manassas, VA, USA).

5.2.2 Breast cancer tissue preparation.

Treatment-naive fresh or frozen invasive tumor and matched adjacent normal tissue samples (Table 1) were obtained from patients diagnosed with and undergone surgical removal of their invasive breast cancer at Indiana Health Hospital at Lafayette or from Indiana University Cancer Center Tissue Procurement and Distribution Core. Furthermore, additional breast cancer samples from AA were obtained from the University of Chicago. The Institutional Board Review Committee of Indiana Health and Purdue University and University of Chicago approved the use of these samples. All patients whose tissue samples were used in this research had provided written informed consent, and this was in accordance with the Declaration of Helsinki. The obtained samples were age-matched from self-identified AA and EA women for a total of 153 invasive

cancer and normal samples. Pathological features and hormone and HER-2 amplification statuses were obtained from the pathology report. Tissue blocks/slides from invasive breast cancer that were formalin-fixed paraffin embedded (FFPE) from AA women and women from Sudan were obtained from Indiana University Cancer Center Tissue Procurement and Distribution Core (n=40; 20 each of LA and TNBC) and from National Cancer Institute, University of Gezira, Sudan (n=100), respectively, for biomarkers' validation by IHC.

5.2.3 Breast cancer tissues' protein extraction.

Approximately, 500 mg of each breast tissue was quickly thawed. To remove residual blood, the tissues were washed in ice-cold "salt-free" phosphate buffer (8 mM Na₂HPO₄, 2 mM KH₂PO₄). The samples were then homogenized in lysis buffer ("salt free" phosphate buffer pH 7.5, 0.5% Triton X-100, 1 mM phenylmethylsulfonyl fluoride (Sigma-Aldrich Co., St Louis, MO, USA), 15 µg/mL aprotinin, 10 µg/mL leupeptin, 10 µg/mL pepstatin, 100 µg/mL DNase 1, 25 µg/mL RNase A, 5 mM MgCl₂) and centrifuged at 20,000× g for 15 minutes at 4°C. Amersham 2-D Quant Kit was used to determine the concentration of proteins. The proteins were precipitated using the trichloroacetic acid (Sigma-Aldrich Co., St Louis, MO, USA) /acetone precipitation method, and pellets were suspended in urea solution (9 M urea, 4% Igepal, 1% DTT, and 2% carrier ampholytes).

5.2.4 2-Dimensional gel electrophoresis.

We performed 2-dimensional gel electrophoresis according to Li et al.²⁶⁰ Three gels per sample were prepared. Briefly, about 200 µg of protein of each sample was concentrated on isoelectric focusing tube gels (3.3% acrylamide, 9 M urea, 2% Igepal, 2% carrier ampholytes, pH 4–8) using the predetermined voltage program (500 V for 1 hour, 750 V for 1 hour, 1,000 V for 1 hour, and 1,400 V for 18.75 hours for a total of 28,500 V/hour). After that, tubes were loaded onto slab gels (linear gradient from 11 to 19%) in a Protean plus Dodeca Cell (Bio-Rad Laboratories Inc.) and the machine was switched to 160 V for 18 hours at 80°C. The gels were then fixed in a fixing solution (50% ethanol/2% phosphoric acid) overnight and then washed and stained by the Coomassie solution (methanol/17% ammonium sulfate/3% phosphoric acid and Coomassie Blue G-250). The gels were then washed and imaged using the GS-800 Calibrated Imaging

Densitometer (Bio-Rad Laboratories Inc.). PDQuest software (Bio-Rad Laboratories Inc.) was used for image analysis. Individual protein abundances were determined by Student's *t*-test using the PDQuest software.

5.2.5 Mass spectrophotometry analyses.

For mass spectrophotometry analysis, significantly expressed protein determined by PDQuest analysis as described earlier was cut from the gel, destained with 50 mM ammonium bicarbonate first and followed by 50% acetonitrile and 100% acetonitrile, then, reduced with 10 mM DTT, alkylated with 55 mM iodoacetamide, and washed with 50 mM ammonium bicarbonate and 100% acetonitrile. The samples were digested with trypsin overnight at 37°C, and the peptides were then extracted and analyzed by matrix assisted laser desorption/ionisation - time of flight mass spectrometry (MALDI-TOF-MS) using a MicroMass M@LDI System (MicroMass) after being calibrated using peptide standards. ProteinLynx (MicroMass) was used to generate the mass list, which then submitted to Profound for database searches. A *z* score of 1.65 was obtained, which corresponds to the 95th percentile. The score was used as a threshold for positive identification of selected proteins.

5.2.6 IHC.

IHC was performed according to Li et al. Approximately 5 µm of breast tissue sections were cut from FFPE tissues and mounted on positively charged SuperFrost slides (Thermo Fisher Scientific, Waltham, MA, USA). The tissue sections were then processed and stained with primary mouse monoclonal antibody or rabbit polyclonal antibodies PRDX2 (1:500), calpain (1:100), CYP7B1 (1:500), and LXRα (1:100) and visualized according to the manufacturer's protocol (Biocare Medical). The antibodies used are CYP7B1. The grading scale of 0–3 (0, no staining; 1, equivocal staining; 2, moderate-to-intense staining; 3, highest intensity staining) was used to determine the intensity of each protein.

5.2.7 Western blot analysis.

Western blot analysis was performed according to Mohammed et al.²⁶¹ To extract protein from cell lines, lysis buffer was added to cultured cells at 75% confluence and protein was

transferred to tubes and centrifuged. The protein concentration for each sample was determined using the Pierce bicinchoninic acid (BCA) Protein Assay Kit (Thermo Fisher Scientific). Proteins were separated by 10% SDS-PAGE and transferred onto nitrocellulose membrane. Detection was performed with primary anti-antibodies gelsolin, calpain, PRDX2, CRYAB, LDH-B, and PEBP2 at dilution at 1:1,000 and secondary antibody mouse or rabbit conjugated with horseradish peroxidase at 1:20,000 dilution. Bound complexes were then detected using the enhanced chemiluminescent system (Thermo Fisher Scientific). Equal loading was confirmed using β -actin (1:2,000) (Sigma-Aldrich Co.).

5.2.8 Ingenuity pathway analysis (IPA).

To determine the most relevant biological mechanisms, interaction networks, and functions of the differentially expressed proteins, proteins altered in expression between each category, hormonal and race status, or together list were submitted to Ingenuity Pathway Knowledge Base (Ingenuity System, Mountain View, CA, USA) and analyzed.

5.2.9 Statistical analysis.

Statistical analysis was performed according to Li et al. ²⁶⁰. Briefly, two-sample paired *t*-test was used to compare each group set using the log of the spot intensity. Zero was used to signify the lack of intensity if no spot was seen. We have used Bonferroni correction to adjust for multiple comparisons at the *P*-value of 0.05.

5.3 Results

5.3.1 The proteome landscape of LA tumors and TNBC in AA and EA women shows some similarity.

The concentration of the protein extracted from AA and EA women TNBC and LA tissues and their normal counter parts was determined so as quantitatively analyze these samples using proteomic analysis. For all samples, we used only 200 mg of protein to balance the sensitivity concerns regarding gel staining and mass spectrometry analysis. During the analysis, we used the images to compare paired samples by hormonal and race status or both. Doing so, we were able to match (79%) all spots and found many to be differentially expressed with the Student's *t*-test using

the PDQuest software. We considered the protein to be significantly differentially overexpressed or down expressed at a fold change of 1.5 and a *P*-value of <0.05. Representative gels showing the proteome expression landscapes of breast cancer compared by hormone and race status are shown in Figure 1, and some selected differentially expressed spots between AA and EA women regardless of hormonal status are shown in Figure 2. In this study, to eliminate possible false positives and give a more stringent *P*-value, Bonferroni correction ($P = 0.005$) was used. We used MALDI-TOF-MS to identify significantly differently expressed proteins between TNBC and LA in AA and EA women.

5.3.2 Differentially expressed proteins in LA vs TNBC in AA and EA women are different.

We found that 16 proteins were differentially expressed between TNBC and LA tissues from AA women (Figure 3A), while 11 proteins were differentially expressed between the two breast cancer subtypes in EA women (Figure 3B). However, only nine proteins were differentially expressed in TNBC in AA women compared to EA women. Vimentin, clusterin, HNRNP A2/B1, PRDX2, and crystalline were most overexpressed proteins between TNBC and LA in AA women. The protein differentially expressed between TNBC and LA tissues in AA women was different from that altered in expression between TNBC and LA tissues in EA women. Proteins that were differentially altered in TNBC and LA in EA women were HSP70, HNRNP C1/C2, HNRNP A2, and ELF-1B. However, HSP71 and HNRNP A2/B1 were the most altered proteins in expression when TNBC in AA women compared with that in EA women (Figure 3C). We show that TNBC from AA women characterized with high expression of vimentin while TNBC from EA women associated with high expression of myosin. These data suggested that TNBC in AA and EA women in our study belongs to the claudin-low subtype, however, expressing different proteins. These data also suggested that the landscape of TNBC in AA women is different from TNBC in EA women; however, not many proteins were altered in expression between AA and EA women TNBC.

5.3.3 Molecular pathway analysis of LA and TNBC proteins of AA women demonstrates upregulation of key nuclear receptors' signaling and immunomodulation networks.

We then submitted the identified overexpressed proteins gene identification to IPA to identify how these proteins are related to each other. We found that the top pathways altered

between LA and TNBC in AA women included LXR/RXR, SUMO, IL-12, pyruvate fermentation to lactate, and RhoGDI signaling (Figure 4A). While the top pathways altered between TNBC and LA in EA women included acute phase response signaling, pentose phosphate pathway, complement system, and regulation of actin-based motility by Rho (Figure 4B). The top altered pathways in TNBC in EA and AA women are acute phase response signaling, integrin signaling, telomere extension, complement system, calpain protease, and pyrimidine ribonucleotide de novo biosynthesis (Figure 4C). These findings suggest that TNBC in AA women enriched in signaling pathways is different from TNBC in EA women.

5.3.4 Validation of selected differentially expressed proteins.

We carried out a limited validation study in few of significantly differentially expressed proteins between TNBC and LA from AA tissue (Table 2) that included gelsolin, calpain, peroxiredoxin-2 (PRDX2), alpha-crystalline (CRYAB), lactate dehydrogenase β (LDH-B), and phosphatidylethanolamine binding protein-2 (PEBP2). For these validation studies, we have used both Western blot analysis and IHC. For Western blot analysis, we have used the following breast cancer cells: MDA468, a TNBC from a 51-year-old AA woman, HCC1500, a LA from a 31-year-old AA woman purchased from ATCC; and KTB 21 (normal). Gelsolin, calpain, PRDX2, and CRYAB were significantly (P -value <0.005) expressed in LA cells but not TNBC cells (Figure 5A and B). For IHC, we have used TNBC and LA tissues from AA women ($n=40$, 20 each) and African women ($n=100$). The IHC of PRDX2, calpain, CYP7B1, and LXR α was classified according to the score methods described in the “Materials and methods” section. PRDX2 had significantly ($P < 0.05$) strong immunoreactivity in 85–95% of tumor cells in both LA and TNBC and were predominantly concentrated in the cytoplasm around the nucleus as shown in 75% of samples (Figure 5C and D). Calpain and LXR α showed high nonsignificant ($P < 0.05$) expression in TNBC compared to LA tissues (Figure 5C and D). While CYP7B1 had strong immunoreactivity in tumor cells of LA and less expression in TNBC tissues (Figure 5C and D), CYP7B1 was significantly (P -value =0.005) expressed in LA relative TNBC cell lines (Figure 5E and F).

5.4 Discussion

In the era of personalized medicine, useful TNBC biomarkers and targeted therapeutic modalities do not exist. In this study, we have used proteomic analysis to identify proteins that account for the aggressive biology of TNBC in AA and African women. The precise knowledge of the proteome landscape of TNBC and LA in AA women compared to EA women may guide the development of new TNBC-targeted therapies. To our knowledge, the study described herein is the first to report on the differentially expressed proteins of TNBC and LA subtypes in AA and EA women using 2-dimensional gel electrophoresis coupled with protein identification via MALDI-TOF-MS and database analyses.

Our study defined the pattern of protein expression in TNBC and LA and their adjacent non-neoplastic tissues within and across racial demographics. We have identified a number of proteins that overexpressed in TNBC and LA in AA and EA patient samples. We did not identify a single protein that was significantly present in one subtype and missing in another; however, our work showed that certain proteins were increasingly upregulated in TNBC in AA patients than in EA patients. In addition, interestingly, the study showed that the differentially overexpressed proteins in the TNBC (compared to LA) of AA samples were distinct from the differentially expressed proteins in the TNBC (compared to LA) of EA samples. Our results agreed with recent transcriptomic analysis of data from white, black, and AA breast cancer patients' normal and cancerous tissues from The Cancer Genome Atlas data repository showing that TNBC in white and black produces different abundances of mRNA, which are controlled in different ways and different regulators in the white and black or AA triple-negative patients²⁶². Therefore, we believe that these differences in transcriptome as well as proteome in our study may manifest as racial disparity in TNBC and could provide the rationale for new diagnostics and targeted treatment for better overall survival rates in AA with TNBC.

A recently published study showed that the differentially expressed genes of age-matched TNBC in women of African descent and EA women were correlated with the Wnt- β -catenin pathway. This finding suggests that the activation of this pathway may contribute to the more aggressive TNBC phenotype of AA compared to the TNBC of EA women^{255,256}. However, our data showed increased representations of LXR/RXR, sumoylation, FXR/RXR, IL-12, and RhoGD1 signaling pathways in the LA (compared to TNBC) samples from AA women. Worth noting that, these LA and TNBC signaling pathways were not the same in the EA women samples.

LXR/RXR is a ligand-dependent transcriptional factor that is closely related to the nuclear receptors such as PPARs and FXR. The transcriptional activity of LXRs (two isoforms, LXR α and LXR β) is dependent on the formation of heterodimers with retinoid X receptors (RXRs) ^{263,264}. The LXR/RXR plays an important physiological role in stimulating genes that regulate cholesterol, glucose, and fatty acid metabolism ²⁶⁴.

Mice deficient in LXR α that were fed a high-cholesterol diet accumulated considerable amounts of cholesterol and lipid in their livers ²⁶⁵. Furthermore, mice deficient in LXR α receptors developed prostate hyperplasia lesions ²⁶⁶. LXR α deficiency caused prostate cancer cell line proliferation and survival in vitro and in vivo in animal models ^{267,268}. In our study, however, we found that LXR α was expressed in both the LA and TNBC tissues of AA women. Accordingly, LXR α may not contribute to the biological differences between the two breast cancer subtypes.

To elucidate, further, the role of LXR α in the LA and TNBC in AA women, we examined the signaling pathway downstream of the receptor. We demonstrated that CYP7B1 enzyme was expressed in LA cell lines from both EA women and AA women but not in TNBC cells. Reduced CYP7B1 expression, which breaks down 27-hydroxycholesterol (27HC), resulted in its increased levels in the extrahepatic tissues. LXR activation as a result of 27HC accumulation was reported to promote breast cancer ER-positive cell line proliferation in vitro and in vivo ²⁶⁹. Mammary glands and uteri of young female mice, that is CYP7B1 $-/-$, have the characteristics of tissues consistently exposed to estrogen and have showed advanced onset of puberty and early menarche, evidence of the premature fatigue of ovarian function in these mice ²⁶⁶. After adjusting for the effects of age, tumor size, nodal status, and perioperative therapy, multivariate Cox regression modeling demonstrated that low CYP7B1 expression was associated with poor breast cancer survival outcomes ²⁷⁰.

Increased 27HC accumulation was shown in postmenopausal, hypercholesterolemic, and obese women. Both increased cholesterol levels and obesity are associated with an increased risk of developing breast cancer and poor prognosis ^{271,272}; both factors were also suggested as potential drivers of aggressive TNBC in AA women ²⁷³. The National Health and Nutrition Examination Survey (NHANES III) reported that more than half of AA women aged over 40 years were obese and more than 80% were overweight ²⁷⁴. Numerous studies link the use of statins, cholesterol-lowering drugs, and improved breast cancer outcomes. Statin use by women with inflammatory breast cancer significantly improved progression-free survival rates ²⁷⁵. Generally speaking, cancer

patients who used statins were found to have a lower risk of dying from cancer compared to those cancer patients who are not on statins ²⁷⁶.

5.5 Acknowledgements

The authors thank Dr. Harikrishna Nakshatri for providing the African American Normal cells, KTB 21, and Dr. Frank Weizmann, Cellular and Integrative Physiology, Indiana University School of Medicine, for performing the MALDI– TOF analysis.

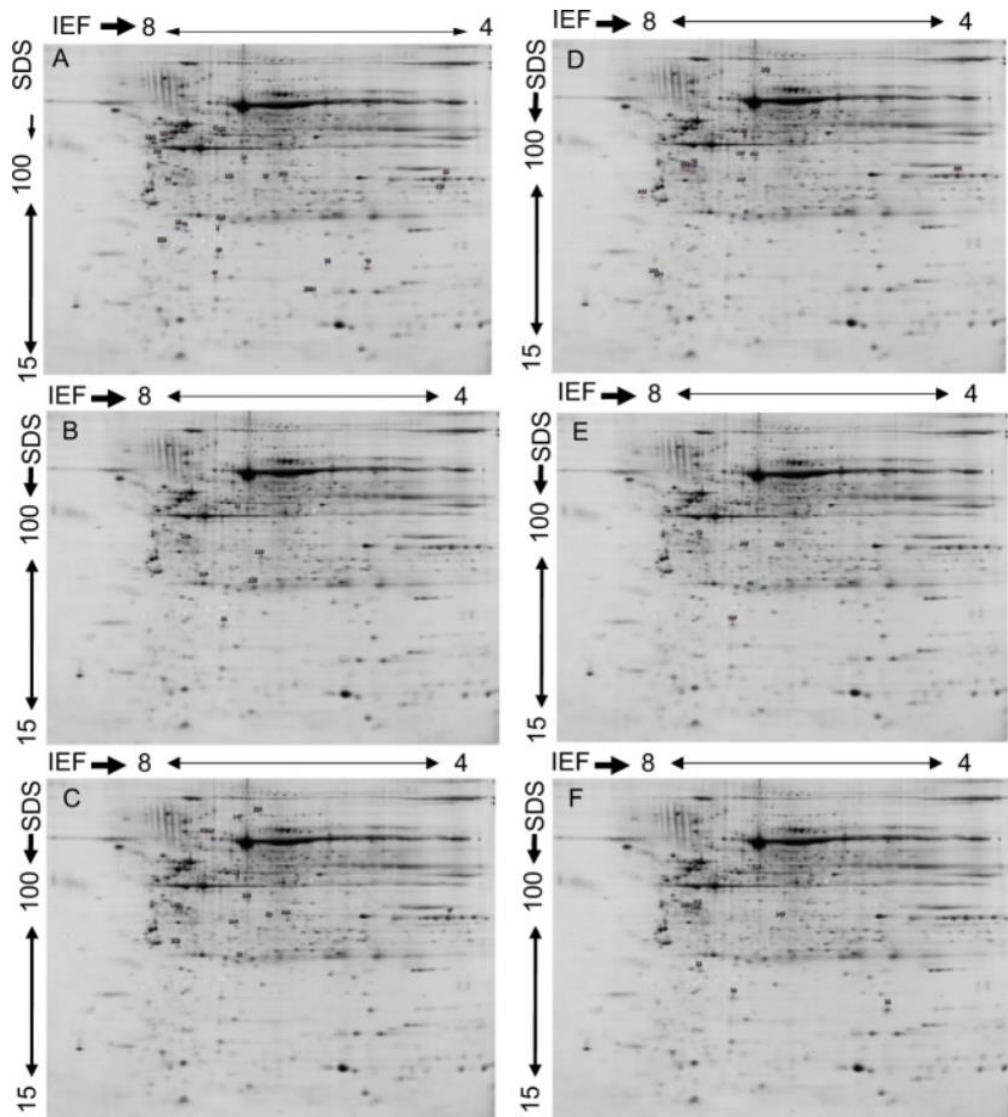


Figure 5.1: Representative 2-DE gel images of protein profiles of invasive breast carcinoma.

(A) TNBC vs LA in African American women, (B) African American vs European American women breast cancer samples, (C) TNBC in African American vs European American women, (D) TNBC vs LA in European American women, (E) TNBC vs LA regardless of race, and (F) LA in African American women vs LA in European American women. Proteins were separated by IEF as the first dimension, using 24 cm tube gels (pH 4–8), and linear gradient gel (11–19%) as the second dimension. The protein spots were cut from the gel, tryptically digested, and identified via MALDI–MS. Significantly expressed spots are posted in Table 2 along with their individual PDQuest spot number assignment and other data.

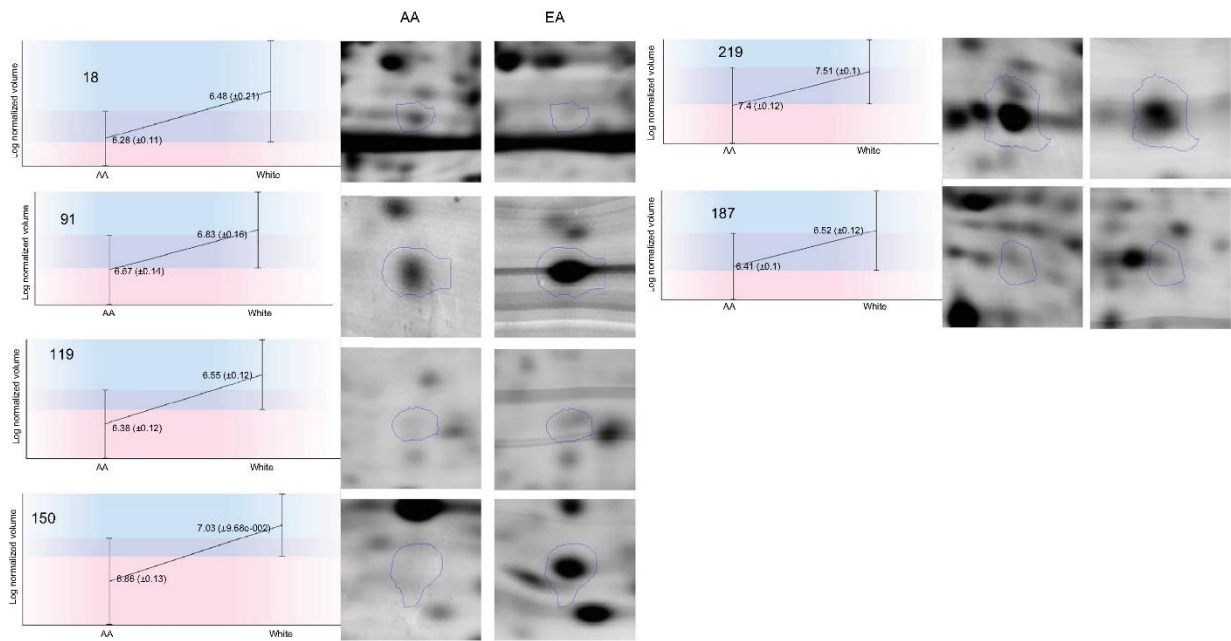


Figure 5.2: Differentially expressed proteins in breast cancer tissues from AA compared to European women regardless of hormonal status.

Selected area of the spots showing intensity differences between AA breast and Caucasian women breast tissues was amplified and is indicated by circles.

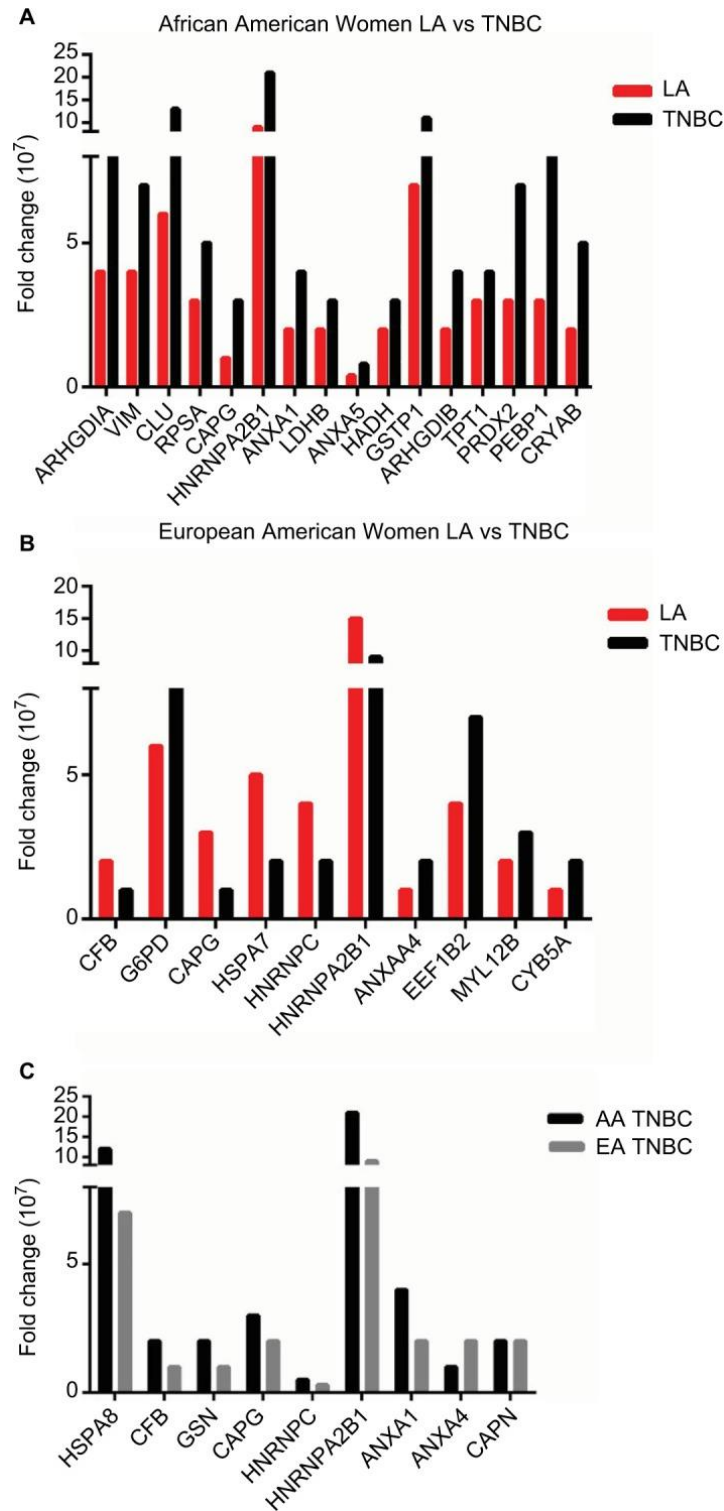


Figure 5.3: Differentially expressed proteins

Differentially expressed proteins in (A) Luminal A breast cancer vs TNBC in AA women, (B) LA vs TNBC in European American women, and (C) TNBC in AA women vs TNBC in European American women.

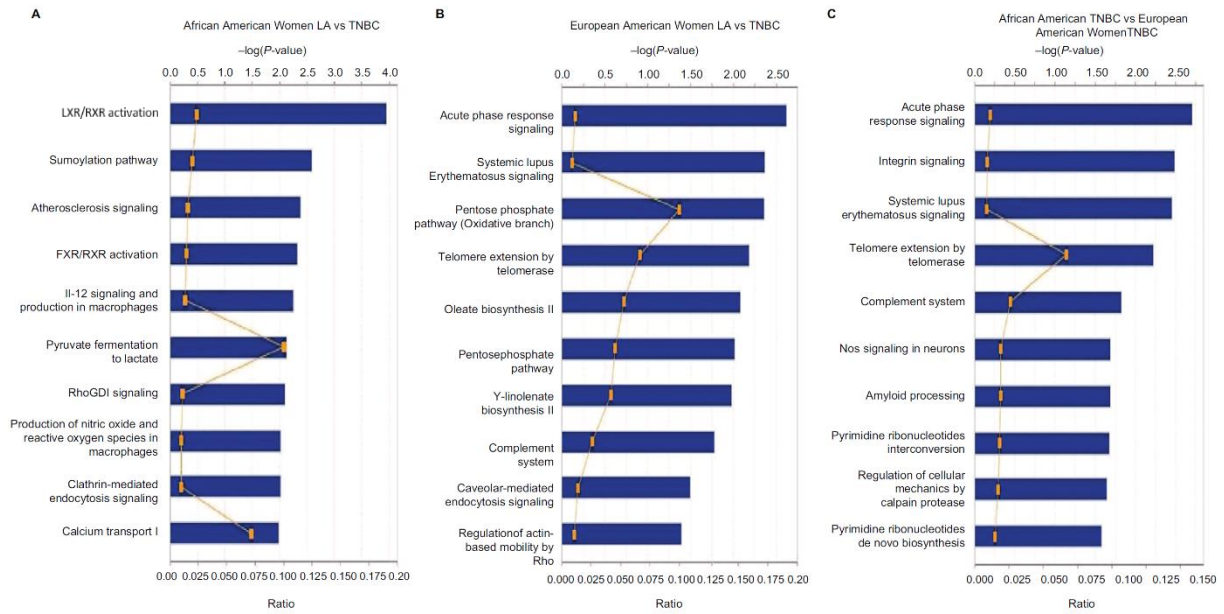


Figure 5.4: IPA of canonical pathways of differentially altered protein expressed in breast carcinoma.

(A) LA vs TNBC in African American women; (B) LA vs TNBC in European American women; (C) TNBC in African American women vs TNBC in European American women.

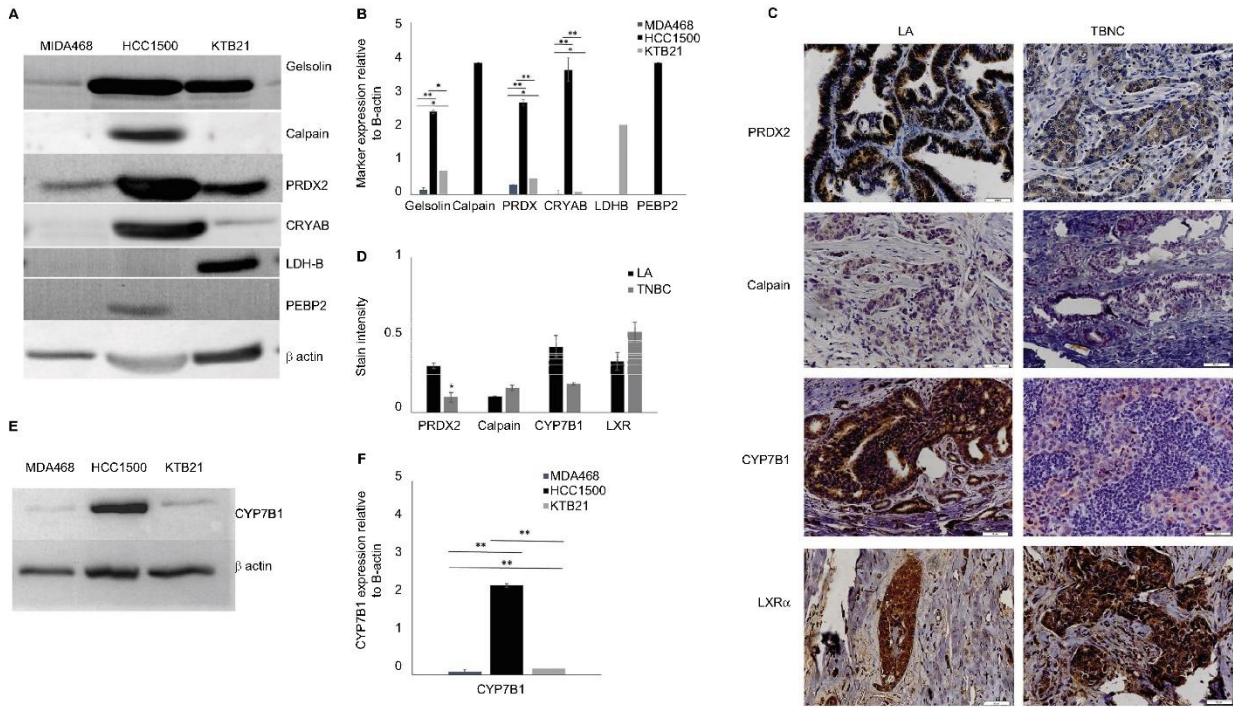


Figure 5.5: Western Blot, Immunohistochemistry and bar graphs of selected proteins.

Western blot (A and E) and immunohistochemistry (C) validation of selected shown proteins. Bar graph of the Western blotting assay of all proteins (B) and CYP7B1 (F). Stain intensity of IHC for each protein tested is shown in (D). Each bar represents the relative value of the protein relative to β -actin. For each data point, samples were tested in triplicate; the graph represents the mean \pm SD. Asterisks denote significance: *significant at 0.05 and **significant at <0.005 .

Table 5.1: Patient's characteristics

European American women				
Sample	Number	Ave range	Type	Grade
LA	20	31-91	Invasive	II-III
TNBC	37	43-86	Invasive	II-III
Normal	13	31-91	Normal adjacent	
African American women				
Sample	Number	Ave range	Type	Grade
LA	33	40-86	Invasive	II-III
TNBC	38	34-92	Invasive	II-III
Normal	12	34-92	Normal adjacent	
TOTAL	153			

Table 5.2: Proteins altered in expression between TNBC and LA in African American and European American women

Protein identification	ANOVA (<i>P</i> -value)	Fold change	LA	TNBC
European American women LA vs TNBC				
Complement factor B (fragment), isoform 1	4.40E-02	1.8	2,046,058.5	1,157,344.3
Glucose-6-phosphate 1-dehydrogenase, isoform 3	4.50E-02	1.4	5,759,682.4	8,164,992.4
Serum albumin, isoform 1	1.00E-03	3.7	2,169,303.8	8,035,969.1
Macrophage-capping protein	6.00E-03	1.7	2,102,541.9	1,212,872.7
Macrophage-capping protein	5.00E-03	2	3,480,462.1	1,712,235.2
Putative heat shock 70 kDa protein 7	7.12E-05	2.5	4,909,509.5	1,935,994.1
Heterogeneous nuclear ribonucleoproteins C1/C2, isoform C1	8.51E-04	2.3	3,911,698.0	1,730,063.3
Heterogeneous nuclear ribonucleoproteins C1/C2, isoform 4	4.20E-02	1.6	4,390,988.4	2,696,021.8
Heterogeneous nuclear ribonucleoproteins C1/C2, isoform C1	3.00E-03	2	2,093,614.4	1,030,843.5
Heterogeneous nuclear ribonucleoproteins A2/B1, isoform B1	4.00E-02	1.7	14,513,621.3	8,564,268.4
Annexin A4	3.20E-02	1.5	1,317,767.5	2,031,717.1
Elongation factor 1-beta	9.00E-03	1.6	4,319,469.9	6,703,359.1
Albumin (23 kDa protein)	1.00E-02	3	8,297,381.6	24,607,159.0
Myosin regulatory light chain 12B	1.60E-02	1.5	1,789,563.4	2,681,546.2
Cytochrome b5, isoform 2	3.20E-02	1.5	1,457,824.7	2,169,439.7
African American LA vs TNBC				
Rho GDP dissociation inhibitor 1	1.80E-02	2	3,696,323.6	7,548,529.8
Vimentin	2.00E-03	2	4,863,058.0	9,533,817.1
Vimentin	5.00E-03	2.1	1,083,399.3	2,310,550.5
Vimentin	7.00E-03	1.9	3,699,484.4	7,017,884.6
Clusterin, isoform 1	3.00E-03	2	6,257,017.2	12,576,387.9
Vimentin	2.00E-03	2	5,357,467.6	10,956,316.1
40S ribosomal protein SA	9.00E-03	1.7	2,819,557.5	4,855,438.4
Macrophage-capping protein	1.00E-03	2.5	1,335,309.8	3,313,789.7
Heterogeneous nuclear ribonucleoproteins A2/B1, isoform B1	1.10E-02	2.3	8,913,869.6	20,563,341.4
Annexin A1	1.00E-03	2	2,809,205.8	5,649,519.9
l-Lactate dehydrogenase B chain	7.00E-03	1.8	1,895,789.3	3,467,282.4
Annexin A1	6.11E-06	2.4	737,825.3	1,785,740.0
Annexin A5	1.86E-04	2.1	364,466.1	751,385.3
Hydroxyacyl-coenzyme A dehydrogenase, isoform 1, mitochondrial	7.00E-03	1.9	1,801,454.0	3,456,646.5
Glutathione S-transferase P	3.20E-02	1.5	7,276,096.9	10,706,067.6
Rho GDP-dissociation inhibitor 2	1.20E-02	2.2	1,973,725.2	4,253,762.8
Tumor protein, translationally controlled 1	9.00E-03	1.6	2,603,038.2	4,090,610.0
Peroxiredoxin-2	1.00E-03	2.1	3,370,194.4	7,130,840.9
Phosphatidylethanolamine-binding protein 1	8.94E-04	2.4	3,454,800.6	8,236,867.7
Alpha-crystalline B chain	3.00E-03	2.3	2,031,592.0	4,659,843.3
Serum albumin, 23 kDa protein	4.40E-02	2.3	1,735,763.4	4,064,164.5

Table 5.2: Continued

African American women TNBC vs European American women TNBC				
Heat shock cognate 71 kDa protein, isoform 1	6.00E-03	1.7	5,803,712.113	3,366,785.176
Heat shock cognate 71 kDa protein, isoform 1	6.00E-03	1.6	17,264,343.42	10,621,537.67
Complement factor B (fragment), isoform 1	3.10E-02	1.5	1,733,432.767	1,157,344.258
Gelsolin, isoform 1	1.40E-02	1.7	1,880,227.112	1,079,142.577
Serum albumin, isoform 1	4.74E-05	4.6	1,741,355.743	8,035,969.144
Macrophage-capping protein	2.30E-02	1.9	3,312,230.328	1,712,235.174
Heterogeneous nuclear ribonucleoproteins C1/C2, isoform C1	1.50E-02	1.9	3,205,599.536	1,730,063.323
Heterogeneous nuclear ribonucleoproteins C1/C2, isoform C1	4.20E-02	2	2,073,516.387	1,030,843.475
Heterogeneous nuclear ribonucleoproteins A2/B1, isoform B1	8.00E-03	2.4	20,556,239.64	8,564,268.363
Annexin A1	3.00E-02	1.5	5,647,227.515	3,774,625.185
Annexin A1	1.24E-05	2.2	1,784,813.078	804,426.105
Annexin A4	2.80E-02	1.5	1,331,668.803	2,031,717.093
Calpain small subunit 1	2.60E-02	1.4	1,580,163.351	2,135,369.651
Albumin (23 kDa protein)	2.00E-03	3.7	6,600,108.282	24,607,158.99
African American women LA vs European American women LA				
Pigment epithelium-derived factor	3.20E-02	1.4	5,965,922.416	8,276,562.023
Putative heat shock 70 kDa protein 7	5.00E-03	1.8	2,618,239.462	4,815,848.665
Heterogeneous nuclear ribonucleoproteins C1/C2, isoform C1	8.00E-03	1.7	2,368,834.55	3,930,357.94
Heterogeneous nuclear ribonucleoproteins C1/C2, isoform 4	1.80E-02	1.7	2,603,644.517	4,535,110.255
Annexin A1	2.90E-02	1.7	737,630.011	1,246,932.583
Rho GDP-dissociation inhibitor 2	2.00E-03	2.2	1,973,121.112	4,312,255.883
Peroxiredoxin-2	2.20E-02	1.9	3,368,711.034	6,450,370.117
Phosphatidylethanolamine-binding protein 1	3.00E-03	2.5	3,454,069.514	8,571,118.885
LA vs TNBC regardless of race				
Putative heat shock 70 kDa protein 7	4.36E-04	1.9	3,763,874.488	1,963,674.673
l-Lactate dehydrogenase B chain	7.00E-03	1.4	2,167,646.098	3,113,091.943
Annexin A1	4.10E-02	1.4	988,476.27	1,349,085.534
Albumin (23 kDa protein)	4.80E-02	2	7,373,421.569	14,603,241.93
Peroxiredoxin-2	3.00E-02	1.3	4,925,950.185	6,442,189.12
African American women vs European American women regardless of hormonal status				
Serum albumin, isoform 1	1.60E-02	2	2,129,360.3	4,199,926.2
Heterogeneous nuclear ribonucleoproteins C1/C2, isoform 4	4.20E-02	1.3	2,834,716.5	3,749,438.7
Complement factor B (fragment), isoform 1	4.00E-03	1.5	2,727,366.5	4,026,370.4
Apo lipoprotein A-I	4.70E-02	1.3	28,231,591.3	35,321,118.4
Heat shock protein beta-1	3.00E-03	1.4	8,331,898.7	11,658,860.3
Peroxiredoxin-2	2.40E-02	1.6	5,434,456.9	8,457,860.3

REFERENCES

1. Society, A. C. 2020 Breast Cancer Statistics. (2020).
2. Society, A. C. How Common is Breast Cancer? (2020).
3. Chaffer, C. L. & Weinberg, R. A. A perspective on cancer cell metastasis. *Science* (2011) doi:10.1126/science.1203543.
4. Chun, C. Metastatic Breast Cancer: Life Expectancy and Prognosis. (2017).
5. Farnsworth, R. H., Achen, M. G. & Stacker, S. A. The evolving role of lymphatics in cancer metastasis. *Current Opinion in Immunology* **53**, 64–73 (2018).
6. Lambert, A. W., Pattabiraman, D. R. & Weinberg, R. A. Emerging Biological Principles of Metastasis. *Cell* vol. 168 670–691 (2017).
7. Gonzalez, H., Robles, I. & Werb, Z. Innate and acquired immune surveillance in the postdissemination phase of metastasis. *FEBS Journal* vol. 285 654–664 (2018).
8. Stacker, S. A. *et al.* Lymphangiogenesis and lymphatic vessel remodelling in cancer. *Nature Reviews Cancer* vol. 14 159–172 (2014).
9. Karaman, S. & Detmar, M. Mechanisms of lymphatic metastasis. *Journal of Clinical Investigation* vol. 124 922–928 (2014).
10. Ran, S., Volk, L., Hall, K. & Flister, M. J. Lymphangiogenesis and Lymphatic Metastasis in Breast Cancer. doi:10.1016/j.pathophys.2009.11.003.
11. Choi, I., Lee, S. & Hong, Y. K. The new era of the lymphatic system: No longer secondary to the blood vascular system. *Cold Spring Harbor Perspectives in Medicine* **2**, 1–23 (2012).
12. Betterman, K. L. & Harvey, N. L. The lymphatic vasculature: Development and role in shaping immunity. *Immunological Reviews* **271**, 276–292 (2016).
13. Margaritis, K. N. & Black, R. a. Modelling the lymphatic system: challenges and opportunities. *J R Soc Interface* **9**, 601–612 (2012).
14. Kazenwadel, J. & Harvey, N. L. Morphogenesis of the lymphatic vasculature: A focus on new progenitors and cellular mechanisms important for constructing lymphatic vessels. *Developmental Dynamics* **245**, 209–219 (2016).
15. Padera, T. P., Meijer, E. F. J. & Munn, L. L. The Lymphatic System in Disease Processes and Cancer Progression. *Annual Review of Biomedical Engineering* **18**, 125–158 (2016).

16. Pan, W.-R., le Roux, C. M., Levy, S. M. & Briggs, C. A. The morphology of the human lymphatic vessels in the head and neck. *Clinical Anatomy* **23**, 654–661 (2010).
17. Scallan, J., Huxley, V. H. & Korthuis, R. J. *Capillary Fluid Exchange. Capillary Fluid Exchange: Regulation, Functions, and Pathology* (2010). doi:10.4199/C00006ED1V01Y201002ISP003.
18. Hong, Y. K., Shin, J. W. & Detmar, M. Development of the lymphatic vascular system: A mystery unravels. *Developmental Dynamics* **231**, 462–473 (2004).
19. Christiansen, A. & Detmar, M. Lymphangiogenesis and Cancer. *Genes & Cancer* **2**, 1146–1158 (2011).
20. Shayan, R., Achen, M. G. & Stacker, S. A. Lymphatic vessels in cancer metastasis: Bridging the gaps. *Carcinogenesis* **27**, 1729–1738 (2006).
21. Rahman, M. & Mohammed, S. Breast cancer metastasis and the lymphatic system. *Oncology letters* **10**, 1233–1239 (2015).
22. Willard-Mack, C. L. Normal structure, function, and histology of lymph nodes. *Toxicologic pathology* **34**, 409–24 (2006).
23. Datta, K., Muders, M., Zhang, H. & Tindall, D. J. Mechanism of lymph node metastasis in prostate cancer. doi:10.2217/fon.10.33.
24. Elmore, S. A. Enhanced histopathology of the lymph nodes. *Toxicologic pathology* **34**, 634–47 (2006).
25. Kesler, C. T., Liao, S., Munn, L. L. & Padera, T. P. Lymphatic vessels in health and disease. *NIH Public access* **5**, 111–124 (2014).
26. Cueni, L. N., Detmar, M., Sc, M. & Detmar, M. The lymphatic system in health and disease. *Lymphatic Research and Biology* **6**, 109–122 (2008).
27. Nathanson, S. D. *et al.* Breast cancer metastasis through the lympho-vascular system. *Clinical and Experimental Metastasis* (2018) doi:10.1007/s10585-018-9902-1.
28. Yasuoka, H. *et al.* Cytoplasmic CXCR4 expression in breast cancer: Induction by nitric oxide and correlation with lymph node metastasis and poor prognosis. *BMC Cancer* (2008) doi:10.1186/1471-2407-8-340.

29. Mohammed, R. A. A., Ellis, I. O., Elsheikh, S., Paish, E. C. & Martin, S. G. Lymphatic and angiogenic characteristics in breast cancer: Morphometric analysis and prognostic implications. *Breast Cancer Research and Treatment* (2009) doi:10.1007/s10549-008-9936-1.
30. Van Der Auwera, I. *et al.* Tumor lymphangiogenesis in inflammatory breast carcinoma: A histomorphometric study. *Clinical Cancer Research* **11**, 7637–7642 (2005).
31. Van Trappen, P. O. & Pepper, M. S. Lymphangiogenesis and lymph node microdissemination. *Gynecologic Oncology* vol. 82 1–3 (2001).
32. Alitalo, K. & Carmeliet, P. Molecular mechanisms of lymphangiogenesis in health and disease. *Cancer Cell* vol. 1 219–227 (2002).
33. Kaipainen, A. *et al.* Expression of the fms-like tyrosine kinase 4 gene becomes restricted to lymphatic endothelium during development. *Proceedings of the National Academy of Sciences of the United States of America* **92**, 3566–3570 (1995).
34. Nakamura, Y. *et al.* Flt-4-positive vessel density correlates with vascular endothelial growth factor-d expression, nodal status, and prognosis in breast cancer. *Clin Cancer Res* **9**, 5313–7 (2003).
35. He, Y. *et al.* Suppression of tumor lymphangiogenesis and lymph node metastasis by blocking vascular endothelial growth factor receptor 3 signaling. *Journal of the National Cancer Institute* **94**, 819–825 (2002).
36. Wigle, J. T. *et al.* An essential role for Prox1 in the induction of the lymphatic endothelial cell phenotype. *EMBO Journal* **21**, 1505–1513 (2002).
37. Wang, M. *et al.* Role of tumor microenvironment in tumorigenesis. *Journal of Cancer* vol. 8 761–773 (2017).
38. Folgueira, M. A. A. K. *et al.* Markers of breast cancer stromal fibroblasts in the primary tumour site associated with lymph node metastasis: A systematic review including our case series. *Bioscience Reports* **33**, (2013).
39. Roy, D. M. & Walsh, L. A. Candidate prognostic markers in breast cancer: Focus on extracellular proteases and their inhibitors. *Breast Cancer: Targets and Therapy* vol. 6 81–91 (2014).
40. Lu, P., Weaver, V. M. & Werb, Z. The extracellular matrix: A dynamic niche in cancer progression. *Journal of Cell Biology* vol. 196 395–406 (2012).

41. Levental, K. R. *et al.* Matrix Crosslinking Forces Tumor Progression by Enhancing Integrin Signaling. *Cell* **139**, 891–906 (2009).
42. Da Cunha, A., Michelin, M. A. & Murta, E. F. C. Pattern response of dendritic cells in the tumor microenvironment and breast cancer. *World Journal of Clinical Oncology* vol. 5 495–502 (2014).
43. Fainaru, O. *et al.* Tumor growth and angiogenesis are dependent on the presence of immature dendritic cells. *The FASEB Journal* **24**, 1411–1418 (2010).
44. Korkaya, H., Liu, S. & Wicha, M. S. Breast cancer stem cells, cytokine networks, and the tumor microenvironment. *Journal of Clinical Investigation* vol. 121 3804–3809 (2011).
45. Allen, M. & Jones, J. L. Jekyll and Hyde: The role of the microenvironment on the progression of cancer. *Journal of Pathology* vol. 223 163–177 (2011).
46. Mahmoud, S. M. A. *et al.* Tumor-infiltrating CD8+ lymphocytes predict clinical outcome in breast cancer. *Journal of Clinical Oncology* **29**, 1949–1955 (2011).
47. Jiang, X. & Shapiro, D. J. The immune system and inflammation in breast cancer. *Molecular and Cellular Endocrinology* **382**, 673–682 (2014).
48. Tan, W. *et al.* Tumour-infiltrating regulatory T cells stimulate mammary cancer metastasis through RANKL-RANK signalling. *Nature* **470**, 548–553 (2011).
49. Bohling, S. D. & Allison, K. H. Immunosuppressive regulatory T cells are associated with aggressive breast cancer phenotypes: A potential therapeutic target. *Modern Pathology* **21**, 1527–1532 (2008).
50. Ohara, M. *et al.* Possible involvement of regulatory T cells in tumor onset and progression in primary breast cancer. *Cancer Immunology, Immunotherapy* **58**, 441–447 (2009).
51. Whiteside, T. L. Immune suppression in cancer: Effects on immune cells, mechanisms and future therapeutic intervention. *Seminars in Cancer Biology* vol. 16 3–15 (2006).
52. Linehan, D. C. & Goedegebuure, P. S. CD25+CD4+ regulatory t-cells in cancer. *Immunologic Research* vol. 32 155–168 (2005).
53. Jiang, X. Harnessing the immune system for the treatment of breast cancer. *Journal of Zhejiang University: Science B* vol. 15 1–15 (2014).
54. Muenst, S., Soysal, S. D., Tzankov, A. & Hoeller, S. The PD-1/PD-L1 pathway: Biological background and clinical relevance of an emerging treatment target in immunotherapy. *Expert Opinion on Therapeutic Targets* vol. 19 201–211 (2015).

55. Pedoeem, A., Azoulay-Alfaguter, I., Strazza, M., Silverman, G. J. & Mor, A. Programmed death-1 pathway in cancer and autoimmunity. *Clinical Immunology* vol. 153 145–152 (2014).
56. Muenst, S. *et al.* Expression of programmed death ligand 1 (PD-L1) is associated with poor prognosis in human breast cancer. *Breast Cancer Research and Treatment* **146**, 15–24 (2014).
57. Muenst, S. *et al.* The presence of programmed death 1 (PD-1)-positive tumor-infiltrating lymphocytes is associated with poor prognosis in human breast cancer. *Breast Cancer Research and Treatment* **139**, 667–676 (2013).
58. Blank, C., Gajewski, T. F. & Mackensen, A. Interaction of PD-L1 on tumor cells with PD-1 on tumor-specific T cells as a mechanism of immune evasion: Implications for tumor immunotherapy. *Cancer Immunology, Immunotherapy* vol. 54 307–314 (2005).
59. Padera, T. P. *et al.* Lymphatic metastasis in the absence of functional intratumor lymphatics. *Science* **296**, 1883–1886 (2002).
60. Hoshida, T. *et al.* Imaging steps of lymphatic metastasis reveals that vascular endothelial growth factor-C increases metastasis by increasing delivery of cancer cells to lymph nodes: Therapeutic implications. *Cancer Research* **66**, 8065–8075 (2006).
61. Miller, M. C. & Mayo, K. H. Chemokines from a structural perspective. *International Journal of Molecular Sciences* vol. 18 (2017).
62. Pereira, E. R., Jones, D., Jung, K. & Padera, T. P. The lymph node microenvironment and its role in the progression of metastatic cancer. *Seminars in Cell and Developmental Biology* vol. 38 98–105 (2015).
63. Liu, L. *et al.* Combination Immunotherapy of MUC1 mRNA Nano-vaccine and CTLA-4 Blockade Effectively Inhibits Growth of Triple Negative Breast Cancer. *Molecular Therapy* **26**, 45–55 (2018).
64. Burke, D. L. *et al.* Sustained hypoxia promotes the development of a pulmonary artery-specific chronic inflammatory microenvironment. *American Journal of Physiology - Lung Cellular and Molecular Physiology* **297**, (2009).
65. Boudot, A. *et al.* Differential estrogen-regulation of CXCL12 chemokine receptors, CXCR4 and CXCR7, contributes to the growth effect of estrogens in breast cancer cells. *PLoS ONE* **6**, (2011).

66. Müller, A. *et al.* Involvement of chemokine receptors in breast cancer metastasis. *Nature* **410**, 50–56 (2001).
67. Tardáguila, M. *et al.* CX3CL1 promotes breast cancer via transactivation of the EGF pathway. *Cancer Research* **73**, 4461–4473 (2013).
68. Yao, M. *et al.* CCR2 chemokine receptors enhance growth and cell-cycle progression of breast cancer cells through SRC and PKC activation. *Molecular Cancer Research* **17**, 604–617 (2019).
69. Xu, K. *et al.* Hypoxia Induces Drug Resistance in Colorectal Cancer through the HIF-1 α /miR-338-5p/IL-6 Feedback Loop. *Molecular Therapy* **27**, 1810–1824 (2019).
70. Zhang, Y. *et al.* A novel role of hematopoietic CCL5 in promoting triple-negative mammary tumor progression by regulating generation of myeloid-derived suppressor cells. *Cell Research* **23**, 394–408 (2013).
71. Lin, S. *et al.* Chemokine C-C motif receptor 5 and C-C motif ligand 5 promote cancer cell migration under hypoxia. *Cancer Science* **103**, 904–912 (2012).
72. Nishida, N., Yano, H., Nishida, T., Kamura, T. & Kojiro, M. Angiogenesis in cancer. *Vascular Health and Risk Management* vol. 2 213–219 (2006).
73. Cai, Z., Gao, C., Zhang, Y. & Xing, K. Functional characterization of the ELR motif in piscine ELR +CXC-like chemokine. *Marine Biotechnology* **11**, 505–512 (2009).
74. Soria, G. & Ben-Baruch, A. The inflammatory chemokines CCL2 and CCL5 in breast cancer. *Cancer Letters* vol. 267 271–285 (2008).
75. Liekens, S., Schols, D. & Hatse, S. CXCL12-CXCR4 Axis in Angiogenesis, Metastasis and Stem Cell Mobilization. *Current Pharmaceutical Design* **16**, 3903–3920 (2011).
76. Griffith, J. W., Sokol, C. L. & Luster, A. D. Chemokines and Chemokine Receptors: Positioning Cells for Host Defense and Immunity. *Annual Review of Immunology* (2014) doi:10.1146/annurev-immunol-032713-120145.
77. Lin, L. *et al.* CCL18 from tumor-associated macrophages promotes angiogenesis in breast cancer. *Oncotarget* **6**, 34758–34773 (2015).
78. Lee, D. F. & Hung, M. C. All roads lead to mTOR: Integrating inflammation and tumor angiogenesis. *Cell Cycle* vol. 6 3011–3014 (2007).
79. Steiner, J. L. & Angela Murphy, E. Importance of chemokine (CC-motif) ligand 2 in breast cancer. *International Journal of Biological Markers* vol. 27 (2012).

80. Shellenberger, T. D. *et al.* BRAK/CXCL14 is a potent inhibitor of angiogenesis and a chemotactic factor for immature dendritic cells. *Cancer Research* **64**, 8262–8270 (2004).
81. Gu, X. L. *et al.* Expression of CXCL14 and its anticancer role in breast cancer. *Breast Cancer Research and Treatment* **135**, 725–735 (2012).
82. Steeg, P. S. Targeting metastasis. *Nature Reviews Cancer* vol. 16 201–218 (2016).
83. Homey, B. *et al.* CCL27-CCR10 interactions regulate T cell-mediated skin inflammation. *Nature Medicine* **8**, 157–165 (2002).
84. Müller, A. *et al.* Involvement of chemokine receptors in breast cancer metastasis. *Nature* **410**, 50–56 (2001).
85. Zhou, W. *et al.* Cancer-Secreted miR-105 destroys vascular endothelial barriers to promote metastasis. *Cancer Cell* (2014) doi:10.1016/j.ccr.2014.03.007.
86. Curtaz, C. J. *et al.* Serum-derived factors of breast cancer patients with brain metastases alter permeability of a human blood-brain barrier model. *Fluids and Barriers of the CNS* **17**, (2020).
87. Billottet, C., Quemener, C. & Bikfalvi, A. CXCR3, a double-edged sword in tumor progression and angiogenesis. *Biochimica et Biophysica Acta - Reviews on Cancer* (2013) doi:10.1016/j.bbcan.2013.08.002.
88. Mohammed, S., Torres-Luquis, O., Walls, E. & Lloyd, F. Lymph-circulating tumor cells show distinct properties to blood-circulating tumor cells and are efficient metastatic precursors. *Mol Oncol* **13**, 1400–1418 (2019).
89. Sharma, B., Singh, S., Varney, M. L. & Singh, R. K. Targeting CXCR1/CXCR2 receptor antagonism in malignant melanoma. *Expert Opinion on Therapeutic Targets* vol. 14 435–442 (2010).
90. Wu, J. *et al.* CC chemokine receptor 7 promotes triple-negative breast cancer growth and metastasis. *Acta Biochimica et Biophysica Sinica* **50**, 835–842 (2018).
91. Lund, A. W. & Swartz, M. A. Role of lymphatic vessels in tumor immunity: Passive conduits or active participants? *Journal of Mammary Gland Biology and Neoplasia* (2010) doi:10.1007/s10911-010-9193-x.
92. Sato, Y., Goto, Y., Narita, N. & Hoon, D. S. B. Cancer cells expressing toll-like receptors and the tumor microenvironment. in *Cancer Microenvironment* vol. 2 205 (Springer, 2009).

93. Zhou, M. *et al.* Toll-like receptor expression in normal ovary and ovarian tumors. *Cancer Immunology, Immunotherapy* **58**, 1375–1385 (2009).
94. Killeen, S. D., Wang, J. H., Andrews, E. J. & Redmond, H. P. Exploitation of the toll-like receptor system in cancer: A doubled-edged sword? *British Journal of Cancer* (2006) doi:10.1038/sj.bjc.6603275.
95. Lin, W. W. & Karin, M. A cytokine-mediated link between innate immunity, inflammation, and cancer. *Journal of Clinical Investigation* (2007) doi:10.1172/JCI31537.
96. Morikawa, T. *et al.* Identification of toll-like receptor 3 as a potential therapeutic target in clear cell renal cell carcinoma. *Clinical Cancer Research* (2007) doi:10.1158/1078-0432.CCR-07-0603.
97. Goto, Y. *et al.* Activation of toll-like receptors 2, 3, and 4 on human melanoma cells induces inflammatory factors. *Molecular Cancer Therapeutics* (2008) doi:10.1158/1535-7163.MCT-08-0582.
98. Ellerman, J. E. *et al.* Masquerader: High mobility group box-1 and cancer. *Clinical Cancer Research* vol. 13 2836–2848 (2007).
99. Bhatelia, K., Singh, K. & Singh, R. TLRs: Linking inflammation and breast cancer. *Cellular Signalling* (2014) doi:10.1016/j.cellsig.2014.07.035.
100. Xie, W. *et al.* Toll-like receptor 2 mediates invasion via activating NF- κ B in MDA-MB-231 breast cancer cells. *Biochemical and Biophysical Research Communications* **379**, 1027–1032 (2009).
101. Cailleau, R., Olivé, M. & Cruciger, Q. v. Long-term human breast carcinoma cell lines of metastatic origin: preliminary characterization. *In vitro* **14**, 911–5 (1978).
102. Amarante, M. K. *et al.* Toll-like receptor 3: implications for proinflammatory microenvironment in human breast cancer. *Molecular biology reports* **39**, 11087–11092 (2012).
103. Chakraborty, A. *et al.* Determinants of lymph node status in women with breast cancer: A hospital based study from eastern India. *Indian Journal of Medical Research, Supplement* **143**, 45–51 (2016).
104. Cox, C. E. *et al.* *Guidelines for Sentinel Node Biopsy and Lymphatic Mapping of Patients With Breast Cancer.* *ANNALS OF SURGERY* vol. 227 (1998).

105. Pulaski, B. A. & Ostrand-Rosenberg, S. Reduction of Established Spontaneous Mammary Carcinoma Metastases following Immunotherapy with Major Histocompatibility Complex Class II and B7.1 Cell-based Tumor Vaccines. *Cancer Research* **58**, (1998).
106. Albertini, J. *et al.* Lymphatic mapping and sentinel node biopsy in the patient with breast cancer. *JAMA* **276**, 1818–22 (1996).
107. Burak, W. E. *et al.* Sentinel lymph node biopsy results in less postoperative morbidity compared with axillary lymph node dissection for breast cancer. *American Journal of Surgery* **183**, 23–27 (2002).
108. Krag, D. N. *et al.* Sentinel-lymph-node resection compared with conventional axillary-lymph-node dissection in clinically node-negative patients with breast cancer: Overall survival findings from the NSABP B-32 randomised phase 3 trial. *The Lancet Oncology* **11**, 927–933 (2010).
109. Pilewskie, M. & Morrow, M. Axillary nodal management following neoadjuvant chemotherapy: A review. *JAMA Oncology* vol. 3 549–555 (2017).
110. Ullah, I. *et al.* Evolutionary history of metastatic breast cancer reveals minimal seeding from axillary lymph nodes. *Journal of Clinical Investigation* **128**, 1355–1370 (2018).
111. Reiter, J. G. *et al.* Lymph node metastases develop through a wider evolutionary bottleneck than distant metastases. *Nature Genetics* **52**, 692–700 (2020).
112. Jatoi, I., Hilsenbeck, S. G., Clark, G. M. & Kent Osborne, C. Significance of axillary lymph node metastasis in primary breast cancer. *Journal of Clinical Oncology* **17**, 2334–2340 (1999).
113. Cady, B. Regional lymph node metastases; a singular manifestation of the process of clinical metastases in cancer: contemporary animal research and clinical reports suggest unifying concepts. *Ann Surg Oncol* **14**, 1790–800 (2007).
114. Halsted, W. I. The Results of Radical Operations for the Cure of Carcinoma of the Breast. *Ann Surg* **46**, 1–19 (1907).
115. Abe, O. *et al.* Effects of radiotherapy and of differences in the extent of surgery for early breast cancer on local recurrence and 15-year survival: An overview of the randomised trials. *The Lancet* **366**, 2087–2106 (2005).

116. Giuliano, A. E. *et al.* Axillary dissection vs no axillary dissection in women with invasive breast cancer and sentinel node metastasis: A randomized clinical trial. *JAMA - Journal of the American Medical Association* **305**, 569–575 (2011).
117. Poortmans, P. M. *et al.* Internal Mammary and Medial Supraclavicular Irradiation in Breast Cancer. *New England Journal of Medicine* (2015) doi:10.1056/NEJMoa1415369.
118. Ly, B. H., Nguyen, N. P., Vinh-Hung, V., Rapiti, E. & Vlastos, G. Loco-regional treatment in metastatic breast cancer patients: Is there a survival benefit? *Breast Cancer Research and Treatment* vol. 119 537–545 (2010).
119. Crile, G., Isbister, W. & Deodhar, S. D. Demonstration that large metastases in lymph nodes disseminate cancer cells to blood and lungs. *Cancer* **28**, 657–657 (1971).
120. Kerjaschki, D. *et al.* Lipoxygenase mediates invasion of intrametastatic lymphatic vessels and propagates lymph node metastasis of human mammary carcinoma xenografts in mouse. *Journal of Clinical Investigation* **121**, 2000–2012 (2011).
121. Abe, O. *et al.* Effects of radiotherapy and of differences in the extent of surgery for early breast cancer on local recurrence and 15-year survival: An overview of the randomised trials. *The Lancet* **366**, 2087–2106 (2005).
122. Ragaz, J. *et al.* Adjuvant Radiotherapy and Chemotherapy in Node-Positive Premenopausal Women with Breast Cancer. *New England Journal of Medicine* **337**, 956–962 (1997).
123. Pereira, E. R. *et al.* Lymph node metastases can invade local blood vessels, exit the node, and colonize distant organs in mice. *Science* **359**, 1403–1407 (2018).
124. Brown, M. *et al.* Lymph node blood vessels provide exit routes for metastatic tumor cell dissemination in mice. *Science* **359**, 1408–1411 (2018).
125. Jemal, A. *et al.* Global cancer statistics. *CA: A Cancer Journal for Clinicians* (2011) doi:10.3322/caac.20107.
126. Wong, S. Y. & Hynes, R. O. Lymphatic or hematogenous dissemination: How does a metastatic tumor cell decide? *Cell Cycle* vol. 5 812–817 (2006).
127. Liotta, L., Kleinerman, J. & Saidel, G. M. Quantitative Relationships of Intravascular Tumor Cells, Tumor Vessels, and Pulmonary Metastases following Tumor Implantation. *Cancer Research* **34**, 997–1004 (1974).

128. Hansen, K. C., D'Alessandro, A., Clement, C. C. & Santambrogio, L. Lymph formation, composition and circulation: A proteomics perspective. *International Immunology* **27**, 219–227 (2015).
129. Paget, S. The Distribution of Secondary Growths in Cancer of the Breast. *The Lancet* **133**, 571–573 (1889).
130. Sleeman, J. P. Metastasis: Understanding is the beginning of order in chaos. *Seminars in Cancer Biology* vol. 22 173 (2012).
131. Chen, S. L., Iddings, D. M., Scheri, R. P. & Bilchik, A. J. Lymphatic Mapping and Sentinel Node Analysis: Current Concepts and Applications. *CA: A Cancer Journal for Clinicians* (2006) doi:10.3322/canjclin.56.5.292.
132. Wyckoff, J., Jones, J., Condeelis, J. & Segall, J. A critical step in metastasis: in vivo analysis of intravasation at the primary tumor. *Cancer Res* **60**, 2504–11 (2000).
133. Allard, W. J. *et al.* Tumor cells circulate in the peripheral blood of all major carcinomas but not in healthy subjects or patients with nonmalignant diseases. *Clinical Cancer Research* **10**, 6897–6904 (2004).
134. Brady, N., Chuntova, P., Bade, L. K. & Schwertfeger, K. L. The FGF/FGFR axis as a therapeutic target in breast cancer. *Expert review of endocrinology & metabolism* **8**, 391–402 (2013).
135. Danø, K. *et al.* Plasminogen Activators, Tissue Degradation, and Cancer. *Advances in Cancer Research* **44**, 139–266 (1985).
136. Li, J. *et al.* Downregulation of FBP1 promotes tumor metastasis and indicates poor prognosis in gastric cancer via regulating epithelial-mesenchymal transition. *PLoS ONE* **11**, (2016).
137. Hollier, B. G., Evans, K. & Mani, S. A. The epithelial-to-mesenchymal transition and cancer stem cells: a coalition against cancer therapies. *J Mammary Gland Biol Neoplasia* **14**, 29–43 (2009).
138. Thiery, J. P., Acloque, H., Huang, R. Y. J. & Nieto, M. A. Epithelial-Mesenchymal Transitions in Development and Disease. *Cell* vol. 139 871–890 (2009).
139. Sulaiman, A., Yao, Z. & Wang, L. Re-evaluating the role of epithelial-mesenchymal-transition in cancer progression. *J Biomed Res* (2017) doi:10.7555/JBR.31.20160124.

140. Jolly, M. K. Implications of the Hybrid Epithelial/Mesenchymal Phenotype in Metastasis. *Frontiers in Oncology* **5**, (2015).
141. Mani, S. A. *et al.* The Epithelial-Mesenchymal Transition Generates Cells with Properties of Stem Cells. *Cell* **133**, 704–715 (2008).
142. Al-Hajj, M., Wicha, M. S., Benito-Hernandez, A., Morrison, S. J. & Clarke, M. F. Prospective identification of tumorigenic breast cancer cells. *Proceedings of the National Academy of Sciences* **100**, 3983–3988 (2003).
143. Karsten, U. & Goletz, S. What makes cancer stem cell markers different? *SpringerPlus* **2**, 1–8 (2013).
144. Ouhtit, A., Abd Elmageed, Z. Y., Abdraboh, M. E., Lioe, T. F. & Raj, M. H. G. In vivo evidence for the role of CD44s in promoting breast cancer metastasis to the liver. *American Journal of Pathology* **171**, 2033–2039 (2007).
145. Shackleton, M. *et al.* Generation of a functional mammary gland from a single stem cell. *Nature* **439**, 84–88 (2006).
146. Ginestier, C. *et al.* ALDH1 Is a Marker of Normal and Malignant Human Mammary Stem Cells and a Predictor of Poor Clinical Outcome. *Cell Stem Cell* **1**, 555–567 (2007).
147. Dontu, G. In vitro propagation and transcriptional profiling of human mammary stem/progenitor cells. *Genes & Development* **17**, 1253–1270 (2003).
148. Grosse-Wilde, A. *et al.* Stemness of the hybrid epithelial/mesenchymal state in breast cancer and its association with poor survival. *PLoS ONE* **10**, (2015).
149. Balkwill, F. Tumour necrosis factor and cancer. *Nature Reviews Cancer* vol. 9 361–371 (2009).
150. Wajant, H. The role of TNF in cancer. *Results and Problems in Cell Differentiation* **49**, 1–15 (2009).
151. Egberts, J.-H. *et al.* Anti-tumor necrosis factor therapy inhibits pancreatic tumor growth and metastasis. *Cancer research* **68**, 1443–50 (2008).
152. Moriai, S. *et al.* Production of interferon- γ -inducible protein-10 and its role as an autocrine invasion factor in nasal natural killer/T-cell lymphoma cells. *Clinical Cancer Research* **15**, 6771–6779 (2009).
153. Ran, S., Volk, L., Hall, K. & Flister, M. J. Lymphangiogenesis and lymphatic metastasis in breast cancer. *Pathophysiology* vol. 17 229–251 (2010).

154. Wei, L. M., Cao, S., Yu, W. D., Liu, Y. L. & Wang, J. T. Overexpression of CX3CR1 is associated with cellular metastasis, proliferation and survival in gastric cancer. *Oncology Reports* **33**, 615–624 (2015).
155. Yang, Y. *et al.* Interleukin-18 enhances breast cancer cell migration via down-regulation of claudin-12 and induction of the p38 MAPK pathway. *Biochemical and Biophysical Research Communications* **459**, 379–386 (2015).
156. Goodsell, D. The molecular perspective: epidermal growth factor. *Stem Cells* **21**, 702–3 (2003).
157. Acharyya, S. *et al.* A CXCL1 paracrine network links cancer chemoresistance and metastasis. *Cell* **150**, 165–178 (2012).
158. Yan, H. H. *et al.* Gr-1+CD11b+ myeloid cells tip the balance of immune protection to tumor promotion in the premetastatic lung. *Cancer Research* **70**, 6139–6149 (2010).
159. Jakóbisiak, M., Lasek, W. & Gołąb, J. Natural mechanisms protecting against cancer. *Immunology Letters* vol. 90 103–122 (2003).
160. Lasek, W., Zagożdżon, R. & Jakobisiak, M. Interleukin 12: still a promising candidate for tumor immunotherapy? *Cancer immunology, immunotherapy : CII* **63**, 419–35 (2014).
161. Borsellino, N. *et al.* Blocking signaling through the Gp130 receptor chain by interleukin-6 and oncostatin M inhibits PC-3 cell growth and sensitizes the tumor cells to etoposide and cisplatin-mediated cytotoxicity. *Cancer* **85**, 134–144 (1999).
162. Lin, C. F. *et al.* Escape from IFN- γ -dependent immunosurveillance in tumorigenesis. *Journal of Biomedical Science* vol. 24 1–9 (2017).
163. Mego, M. *et al.* CXCR4-SDF-1 interaction potentially mediates trafficking of circulating tumor cells in primary breast cancer. *BMC Cancer* **16**, (2016).
164. Aceto, N. *et al.* Circulating tumor cell clusters are oligoclonal precursors of breast cancer metastasis. *Cell* **158**, 1110–1122 (2014).
165. Alix-Panabières, C. & Pantel, K. Challenges in circulating tumour cell research. *Nature Reviews Cancer* **14**, 623–631 (2014).
166. O’Flaherty, J. D. *et al.* Circulating tumour cells, their role in metastasis and their clinical utility in lung cancer. *Lung Cancer* vol. 76 19–25 (2012).
167. Kim, M. Y. *et al.* Tumor Self-Seeding by Circulating Cancer Cells. *Cell* **139**, 1315–1326 (2009).

168. Giampieri, S. *et al.* Localized and reversible TGF β signalling switches breast cancer cells from cohesive to single cell motility. *Nature Cell Biology* **11**, 1287–1296 (2009).
169. Fidler, I. J. The relationship of embolic homogeneity, number, size and viability to the incidence of experimental metastasis. *European Journal of Cancer (1965)* **9**, 223–227 (1973).
170. Hou, J. M. *et al.* Clinical significance and molecular characteristics of circulating tumor cells and circulating tumor microemboli in patients with small-cell lung cancer. *Journal of Clinical Oncology* **30**, 525–532 (2012).
171. Hong, B. & Zu, Y. Detecting circulating tumor cells: Current challenges and new trends. *Theranostics* vol. 3 377–394 (2013).
172. Babayan, A. *et al.* Heterogeneity of Estrogen Receptor Expression in Circulating Tumor Cells from Metastatic Breast Cancer Patients. *PLoS ONE* **8**, e75038 (2013).
173. Pestrin, M. *et al.* Correlation of HER2 status between primary tumors and corresponding circulating tumor cells in advanced breast cancer patients. *Breast Cancer Research and Treatment* **118**, 523–530 (2009).
174. Zhong, X. & Rescorla, F. J. Cell surface adhesion molecules and adhesion-initiated signaling: understanding of anoikis resistance mechanisms and therapeutic opportunities. *Cell Signal* **24**, 393–401 (2012).
175. Aktas, B. *et al.* Comparison of the HER2, estrogen and progesterone receptor expression profile of primary tumor, metastases and circulating tumor cells in metastatic breast cancer patients. *BMC Cancer* **16**, (2016).
176. Paoletti, C. *et al.* Heterogeneous estrogen receptor expression in circulating tumor cells suggests diverse mechanisms of fulvestrant resistance. *Molecular Oncology* **10**, 1078–1085 (2016).
177. Rossi, S. *et al.* Hormone Receptor Status and HER2 Expression in Primary Breast Cancer Compared with Synchronous Axillary Metastases or Recurrent Metastatic Disease. *Clinical Breast Cancer* vol. 15 307–312 (2015).
178. Ashwell, S. & Zabludoff, S. DNA damage detection and repair pathways-recent advances with inhibitors of checkpoint kinases in cancer therapy. *Clinical Cancer Research* **14**, 4032–4037 (2008).

179. Gong, C. *et al.* Potentiated DNA Damage Response in Circulating Breast Tumor Cells Confers Resistance to Chemotherapy. *The Journal of biological chemistry* **290**, 14811–25 (2015).
180. Yu, M. *et al.* Circulating breast tumor cells exhibit dynamic changes in epithelial and mesenchymal composition. *Science (New York, N.Y.)* **339**, 580–4 (2013).
181. Fair, R. Incidence of glaucoma in optometric practice--an eight year evaluation of 6,580 tonograms. *Am J Optom Arch Am Acad Optom* **49**, 754–61 (1972).
182. Bulfoni, M. *et al.* In patients with metastatic breast cancer the identification of circulating tumor cells in epithelial-to-mesenchymal transition is associated with a poor prognosis. *Breast cancer research : BCR* **18**, 30 (2016).
183. Fillmore, C. M. & Kuperwasser, C. Human breast cancer cell lines contain stem-like cells that self-renew, give rise to phenotypically diverse progeny and survive chemotherapy. *Breast Cancer Research* **10**, (2008).
184. Kim, R. Cancer Immunoediting: From Immune Surveillance to Immune Escape. in *Cancer Immunotherapy* 9–27 (2007). doi:10.1016/B978-012372551-6/50066-3.
185. Vesely, M. D. & Schreiber, R. D. Cancer immunoediting: Antigens, mechanisms, and implications to cancer immunotherapy. *Annals of the New York Academy of Sciences* **1284**, 1–5 (2013).
186. Rosen, E. M. & Goldberg, I. D. Protein factors which regulate cell motility. *In vitro cellular & developmental biology : journal of the Tissue Culture Association* **25**, 1079–1087 (1989).
187. Wells, A. Tumor invasion: role of growth factor-induced cell motility. *Advances in cancer research* **78**, 31–101 (2000).
188. Odenthal, J., Takes, R. & Friedl, P. Plasticity of tumor cell invasion: Governance by growth factors and cytokines. *Carcinogenesis* vol. 37 1117–1128 (2016).
189. Andre, F. *et al.* Expression of chemokine receptors predicts the site of metastatic relapse in patients with axillary node positive primary breast cancer. *Annals of Oncology* **17**, 945–951 (2006).
190. Li, K. *et al.* Impact of chemokine receptor CXCR3 on tumor-infiltrating lymphocyte recruitment associated with favorable prognosis in advanced gastric cancer. *Int J Clin Exp Pathol* **8**, 14725–14732 (2015).

191. Karpanen, T. & Alitalo, K. Lymphatic vessels as targets of tumor therapy? *J Exp Med* **194**, F37-42 (2001).
192. Popova, T. G. *et al.* Whole proteome analysis of mouse lymph nodes in cutaneous anthrax. *PLoS ONE* **9**, (2014).
193. Swartz, M. A. & Lund, A. W. Lymphatic and interstitial flow in the tumour microenvironment: linking mechanobiology with immunity. *Nature Reviews Cancer* **12**, 210–219 (2012).
194. Sleeman, J. P. The metastatic niche and stromal progression. *Cancer and Metastasis Reviews* **31**, 429–440 (2012).
195. Neri, A., Welch, D., Kawaguchi, T. & Nicolson, G. Development and biologic properties of malignant cell sublines and clones of a spontaneously metastasizing rat mammary adenocarcinoma. *J Natl Cancer Inst.* **68**, 507–17 (1982).
196. Zhou, W. *et al.* Mass spectrometry analysis of the post-translational modifications of renolase from pancreatic ductal adenocarcinoma cells. *Journal of Proteome Research* **9**, 2929–2936 (2010).
197. Gkoutela, S., Szczerba, B., Donato, C. & Aceto, N. Recent advances in the biology of human circulating tumour cells and metastasis. *ESMO Open* **1**, (2016).
198. Dennis, G. *et al.* DAVID: Database for Annotation, Visualization, and Integrated Discovery. *Genome biology* (2003).
199. Kaimal, V., Bardes, E. E., Tabar, S. C., Jegga, A. G. & Aronow, B. J. ToppCluster: A multiple gene list feature analyzer for comparative enrichment clustering and networkbased dissection of biological systems. *Nucleic Acids Research* **38**, (2010).
200. Zhou, W. *et al.* Proteomic analysis of pancreatic ductal adenocarcinoma cells reveals metabolic alterations. *Journal of Proteome Research* **10**, 1944–1952 (2011).
201. Xu, J. *et al.* Overexpression of the Kininogen-1 inhibits proliferation and induces apoptosis of glioma cells. *Journal of Experimental and Clinical Cancer Research* (2018) doi:10.1186/s13046-018-0833-0.
202. Interewicz, B., Olszewski, W. L., Leak, L. V, Petricoin, E. F. & Liotta, L. A. Profiling of normal human leg lymph proteins using the 2-D electrophoresis and SELDI-TOF mass spectrophotometry approach. *Lymphology* **37**, 65–72 (2004).

203. Leak, L. V. *et al.* Proteomic analysis of lymph. *Proteomics* (2004) doi:10.1002/pmic.200300573.
204. Nanjee, M. N., Cooke, C. J., Olszewski, W. L. & Miller, N. E. Lipid and apolipoprotein concentrations in prenodal leg lymph of fasted humans. Associations with plasma concentrations in normal subjects, lipoprotein lipase deficiency, and LCAT deficiency. *Journal of lipid research* **41**, 1317–1327 (2000).
205. Olszewski, W. L. *et al.* Lymph draining from foot joints in rheumatoid arthritis provides insight into local cytokine and chemokine production and transport to lymph nodes. *Arthritis and Rheumatism* **44**, 541–549 (2001).
206. Ogundiran, T. O. *et al.* Case-control study of body size and breast cancer risk in Nigerian women. *American Journal of Epidemiology* (2010) doi:10.1093/aje/kwq180.
207. Broggi, M. A. S. *et al.* Tumor-associated factors are enriched in lymphatic exudate compared to plasma in metastatic melanoma patients. *Journal of Experimental Medicine* (2019) doi:10.1084/jem.20181618.
208. Yang, K. M. *et al.* Co-chaperone BAG2 Determines the Pro-oncogenic Role of Cathepsin B in Triple-Negative Breast Cancer Cells. *Cell Reports* (2017) doi:10.1016/j.celrep.2017.11.026.
209. Yue, X. *et al.* BAG2 promotes tumorigenesis through enhancing mutant p53 protein levels and function. *eLife* (2015) doi:10.7554/eLife.08401.
210. García-Silva, S. *et al.* Use of extracellular vesicles from lymphatic drainage as surrogate markers of melanoma progression and BRAF V600E mutation. *The Journal of Experimental Medicine* (2019) doi:10.1084/jem.20181522.
211. Becker, B. *et al.* Induction of Hsp90 protein expression in malignant melanomas and melanoma metastases. *Experimental Dermatology* **13**, 27–32 (2004).
212. Capello, M., Ferri-Borgogno, S., Cappello, P. & Novelli, F. α -enolase: A promising therapeutic and diagnostic tumor target. *FEBS Journal* vol. 278 1064–1074 (2011).
213. Gibbs, P. E. M., Miralem, T. & Maines, M. D. Biliverdin reductase: a target for cancer therapy? *Frontiers in Pharmacology* **6**, 119 (2015).
214. Colman, R. W. Role of the light chain of high molecular weight kininogen in adhesion, cell-associated proteolysis and angiogenesis. *Biological Chemistry* vol. 382 65–70 (2001).

215. Harris, E. E. R., Hwang, W. T., Seyednejad, F. & Solin, L. J. Prognosis after Regional Lymph Node Recurrence in Patients with Stage I-II Breast Carcinoma Treated with Breast Conservation Therapy. *Cancer* (2003) doi:10.1002/cncr.11767.
216. Behranwala, K. A., A'Hern, R., Omar, A. M. & Thomas, J. M. Prognosis of lymph node metastasis in soft tissue sarcoma. *Annals of Surgical Oncology* (2004) doi:10.1245/ASO.2004.04.027.
217. Podgrabinska, S. & Skobe, M. Role of lymphatic vasculature in regional and distant metastases. *Microvascular Research* vol. 95 46–52 (2014).
218. Wong, S. Y. & Hynes, R. O. Lymphatic or Hematogenous Dissemination: How Does a Metastatic Tumor Cell Decide?
219. Shojaei, H. *et al.* Toll-like receptors 3 and 7 agonists enhance tumor cell lysis by human $\gamma\sigma$ T cells. *Cancer Research* (2009) doi:10.1158/0008-5472.CAN-09-1602.
220. Salaun, B., Coste, I., Rissoan, M.-C., Lebecque, S. J. & Renno, T. TLR3 Can Directly Trigger Apoptosis in Human Cancer Cells. *The Journal of Immunology* (2006) doi:10.4049/jimmunol.176.8.4894.
221. Umemura, N. *et al.* Defective NF- κ B signaling in metastatic head and neck cancer cells leads to enhanced apoptosis by double-stranded RNA. *Cancer Research* (2012) doi:10.1158/0008-5472.CAN-11-1484.
222. O'Neill, L. A. J., Hennessy, E. J. & Parker, A. E. Targeting Toll-like receptors: Emerging therapeutics? *Nature Reviews Drug Discovery* (2010) doi:10.1038/nrd3203.
223. Salaun, B. *et al.* TLR3 as a biomarker for the therapeutic efficacy of double-stranded RNA in breast cancer. *Cancer Research* (2011) doi:10.1158/0008-5472.CAN-10-3490.
224. Rakoff-Nahoum, S. & Medzhitov, R. Toll-like receptors and cancer. *Nature Reviews Cancer* (2009) doi:10.1038/nrc2541.
225. Chuang, H. C., Huang, C. C., Chien, C. Y. & Chuang, J. H. Toll-like receptor 3-mediated tumor invasion in head and neck cancer. *Oral Oncology* (2012) doi:10.1016/j.oraloncology.2011.10.008.
226. Zhang, Y. *et al.* TLR3 activation inhibits nasopharyngeal carcinoma metastasis via downregulation of chemokine receptor CXCR4. *Cancer Biology and Therapy* (2009) doi:10.4161/cbt.8.19.9437.

227. Panter, G., Kužnik, A. & Jerala, R. Therapeutic applications of nucleic acids as ligands for toll-like receptors. *Current Opinion in Molecular Therapeutics* (2009).
228. Mohammed, S. I., Torres-Luquis, O., Walls, E. & Lloyd, F. Lymph-circulating tumor cells show distinct properties to blood-circulating tumor cells and are efficient metastatic precursors. *Molecular Oncology* (2019) doi:10.1002/1878-0261.12494.
229. Galardi, S., Mercatelli, N., Farace, M. G. & Ciafrè, S. A. NF- κ B and c-Jun induce the expression of the oncogenic miR-221 and miR-222 in prostate carcinoma and glioblastoma cells. *Nucleic Acids Research* (2011) doi:10.1093/nar/gkr006.
230. Stowell, N. C. *et al.* Long-term activation of TLR3 by Poly(I:C) induces inflammation and impairs lung function in mice. *Respiratory Research* (2009) doi:10.1186/1465-9921-10-43.
231. Riris, S., Webster, P. & Homer, H. Digital multiplexed mRNA analysis of functionally important genes in single human oocytes and correlation of changes in transcript levels with oocyte protein expression. *Fertility and Sterility* (2014) doi:10.1016/j.fertnstert.2013.11.125.
232. Baeuerle, P. A. & Baltimore, D. NF-kappa B: ten years after. *Cell* (1996).
233. Geismann, C. *et al.* Nf-kb dependent chemokine signaling in pancreatic cancer. *Cancers* (2019) doi:10.3390/cancers11101445.
234. Doherty, M. R. *et al.* In1. Doherty MR, Cheon HJ, Junk DJ, Vinayak S, Varadan V, Telli ML, et al. Interferon-beta represses cancer stem cell properties in triple-negative breast cancer. Proc. Natl. Acad. Sci. U. S. A. 2017; terferon-beta represses cancer stem cell properties in. *Proceedings of the National Academy of Sciences of the United States of America* (2017) doi:10.1073/pnas.1713728114.
235. Hassan, A. O. *et al.* Adenovirus vector-based multi-epitope vaccine provides partial protection against H5, H7, and H9 avian influenza viruses. *PLoS ONE* (2017) doi:10.1371/journal.pone.0186244.
236. Salaun, B., Lebecque, S., Matikainen, S., Rimoldi, D. & Romero, P. Toll-like receptor 3 expressed by melanoma cells as a target for therapy? *Clinical Cancer Research* (2007) doi:10.1158/1078-0432.CCR-07-0274.
237. Yuan, M. M. *et al.* TLR3 expression correlates with apoptosis, proliferation and angiogenesis in hepatocellular carcinoma and predicts prognosis. *BMC Cancer* (2015) doi:10.1186/s12885-015-1262-5.

238. Chin, A. I. *et al.* Toll-like receptor 3-mediated suppression of TRAMP prostate cancer shows the critical role of type I interferons in tumor immune surveillance. *Cancer Research* (2010) doi:10.1158/0008-5472.CAN-09-1162.
239. Yu, P. *et al.* Nucleic Acid-Sensing Toll-like Receptors Are Essential for the Control of Endogenous Retrovirus Viremia and ERV-Induced Tumors. *Immunity* (2012) doi:10.1016/j.immuni.2012.07.018.
240. Bugge, M. *et al.* Surface toll-like receptor 3 expression in metastatic intestinal epithelial cells induces inflammatory cytokine production and promotes invasiveness. *Journal of Biological Chemistry* (2017) doi:10.1074/jbc.M117.784090.
241. Parker, B. S., Rautela, J. & Hertzog, P. J. Antitumour actions of interferons: Implications for cancer therapy. *Nature Reviews Cancer* (2016) doi:10.1038/nrc.2016.14.
242. Porritt, R. A. & Hertzog, P. J. Dynamic control of type I IFN signalling by an integrated network of negative regulators. *Trends in Immunology* (2015) doi:10.1016/j.it.2015.02.002.
243. Pradere, J. P., Dapito, D. H. & Schwabe, R. F. The Yin and Yang of Toll-like receptors in cancer. *Oncogene* (2014) doi:10.1038/onc.2013.302.
244. Zhao, S., Zhang, Y., Zhang, Q., Wang, F. & Zhang, D. Toll-like receptors and prostate cancer. *Frontiers in Immunology* (2014) doi:10.3389/fimmu.2014.00352.
245. Sheyhidin, I. *et al.* Overexpression of TLR3, TLR4, TLR7 and TLR9 in esophageal squamous cell carcinoma. *World Journal of Gastroenterology* (2011) doi:10.3748/wjg.v17.i32.3745.
246. González-Reyes, S. *et al.* Study of TLR3, TLR4 and TLR9 in breast carcinomas and their association with metastasis. *BMC Cancer* (2010) doi:10.1186/1471-2407-10-665.
247. Liu, M., Guo, S. & Stiles, J. K. The emerging role of CXCL10 in cancer. *Oncology Letters* (2011) doi:10.3892/ol.2011.300.
248. Marchesi, F., Locatelli, M., Erreni, M., Allavena, P. & Mantovani, A. Role of CX3CR1/CX3CL1 axis in primary and secondary involvement of the nervous system by cancer. *Journal of neuroimmunology* **224**, 39–44 (2010).
249. Ma, X. *et al.* CXCR3 expression is associated with poor survival in breast cancer and promotes metastasis in a murine model. *Molecular Cancer Therapeutics* (2009) doi:10.1158/1535-7163.MCT-08-0485.

250. Foulkes WD, Smith IE, R.-F. J. Triple negative breast cancer. *N Engl J Med* **363**, 1938–48 (2012).
251. O’Toole, S. A. *et al.* Therapeutic targets in triple negative breast cancer. *Journal of Clinical Pathology* **66**, 530–542 (2013).
252. Anders, C. & Carey, L. a La. Understanding and treating triple-negative breast cancer. *Oncology (Williston Park, NY)* **22**, 1233–1243 (2008).
253. Carey, L. A. *et al.* Race, breast cancer subtypes, and survival in the Carolina Breast Cancer Study. *JAMA : the journal of the American Medical Association* **295**, 2492–502 (2006).
254. Vona-Davis, L. & Rose, D. P. The influence of socioeconomic disparities on breast cancer tumor biology and prognosis: a review. *Journal of women’s health (2002)* **18**, 883–93 (2009).
255. Field, L. A. *et al.* Identification of differentially expressed genes in breast tumors from African American compared with Caucasian women. *Cancer* **118**, 1334–1344 (2012).
256. Martin, D. N. *et al.* Differences in the tumor microenvironment between African-American and European-American breast cancer patients. *PLoS ONE* **4**, (2009).
257. Dietze, E. C., Sistrunk, C., Miranda-Carboni, G., O’Regan, R. & Seewaldt, V. L. Triple-negative breast cancer in African-American women: Disparities versus biology. *Nature Reviews Cancer* vol. 15 248–254 (2015).
258. Yersal, O. & Barutca, S. Biological subtypes of breast cancer: Prognostic and therapeutic implications. *World journal of clinical oncology* **5**, 412–24 (2014).
259. Guarneri, V. & Conte, P. Metastatic breast cancer: therapeutic options according to molecular subtypes and prior adjuvant therapy. *The oncologist* **14**, 645–56 (2009).
260. Li, J. *et al.* Proteomic-based approach for biomarkers discovery in early detection of invasive urothelial carcinoma. *Proteomics - Clinical Applications* **2**, 78–89 (2008).
261. Mohammed, S. I. *et al.* Point-of-care test for cervical cancer in LMICs. *Oncotarget* **7**, 18787–18797 (2016).
262. Telonis, A. G. & Rigoutsos, I. Race disparities in the contribution of miRNA isoforms and tRNA-derived fragments to Triple-negative breast cancer. *Cancer Research* **78**, 1140–1154 (2018).
263. Hong, C. & Tontonoz, P. Liver X receptors in lipid metabolism: opportunities for drug discovery. *Nature Reviews Drug Discovery* **13**, 433–444 (2014).

264. Laucencikiene, J. & Ryd , M. Liver X receptors and fat cell metabolism. *International Journal of Obesity* **36**, 1494–1502 (2012).
265. Peet, D. J. *et al.* Cholesterol and bile acid metabolism are impaired in mice lacking the nuclear oxysterol receptor LXRA. *Cell* **93**, 693–704 (1998).
266. Kim, H.-J., Andersson, L. C., Bouton, D., Warner, M. & Gustafsson, J.-A. Stromal growth and epithelial cell proliferation in ventral prostates of liver X receptor knockout mice. *Proceedings of the National Academy of Sciences of the United States of America* **106**, 558–63 (2009).
267. Zhuang, L., Kim, J., Adam, R. M., Solomon, K. R. & Freeman, M. R. Cholesterol targeting alters lipid raft composition and cell survival in prostate cancer cells and xenografts. *Journal of Clinical Investigation* **115**, 959–968 (2005).
268. Pommier, A. J. C. *et al.* Liver X Receptors Protect from Development of Prostatic Intra-Epithelial Neoplasia in Mice. *PLoS Genetics* **9**, (2013).
269. Bruss, V., Lu, X., Thomssen, R. & Gerlich, W. H. Post-translational alterations in transmembrane topology of the hepatitis B virus large envelope protein. *EMBO J* **13**, 2273–2279 (1994).
270. Wu, Q. *et al.* 27-Hydroxycholesterol promotes cell-autonomous, ER-positive breast cancer growth. *Cell Reports* **5**, 637–645 (2013).
271. Despres, J. P. *et al.* Relation of high plasma triglyceride levels associated with obesity and regional adipose tissue distribution to plasma lipoprotein-lipid composition in premenopausal women. *Clin Invest Med* **12**, 374–380 (1989).
272. George, S. M. *et al.* Postdiagnosis diet quality, the combination of diet quality and recreational physical activity, and prognosis after early-stage breast cancer. *Cancer Causes and Control* **22**, 589–598 (2011).
273. Lee, E. *et al.* Characteristics of triple-negative breast cancer in patients with a BRCA1 mutation: Results from a population-based study of young women. *Journal of Clinical Oncology* **29**, 4373–4380 (2011).
274. Ogden, C. L., Flegal, K. M., Carroll, M. D. & Johnson, C. L. Prevalence and trends in overweight among US children and adolescents, 1999–2000. *JAMA* **288**, 1728–1732 (2002).
275. Brewer, T. M. *et al.* Statin use in primary inflammatory breast cancer: a cohort study. *British Journal of Cancer* **109**, 318–324 (2013).

276. Vedel-Krogh, S., Nielsen, S. F. & Nordestgaard, B. G. Statin Use Is Associated with Reduced Mortality in Patients with Interstitial Lung Disease. *PLoS One* **10**, e0140571 (2015).

PUBLICATIONS

Manuscripts

Published Articles

1. Tumor-Draining Lymph Secretome En Route to the Regional Lymph Node in Breast Cancer Metastasis. *Breast Cancer* (Dove Med Press). Mohammed SI, **Torres-Luquis O**, Zhou W, Lanman NA, Espina V, Liotta L. 2020 Mar 25;12:57-67. doi: 10.2147/BCTT.S236168. eCollection 2020. [PMID: 32273752](#).
2. Lymph-circulating tumor cells show distinct properties to blood-circulating tumor cells and are efficient metastatic precursors. *Mol Oncol*. Mohammed SI, **Torres-Luquis O**, Walls E, Lloyd F. 2019 Jun;13(6):1400-1418. doi: 10.1002/1878-0261.12494. Epub 2019 May 23. [PMID: 31026363](#).
3. LXR/RXR pathway signaling associated with triple-negative breast cancer in African American women. *Breast Cancer* (Dove Med Press). **Torres-Luquis O**, Madden K, N'dri NM, Berg R, Olopade OF, Ngwa W, Abuidris D, Mittal S, Lyn-Cook B, Mohammed SI. 2018 Dec 20;11:1-12. doi: 10.2147/BCTT.S185960. eCollection 2019. [PMID: 30588086](#).
4. Activation of TLR3 contributes to tumor cell migration and metastasis through the lymphatic system. Torres-Luquis O, Mohammed SI. **Submitted to Frontier**.
5. Lymphatic system and breast cancer metastasis. Torres-Luquis O, Mohammed SI. **Under submission**.

Book

1. Introduction to Microbiology. Fricker AD, Muralidharan K, **Torres-Luquis O**. Laboratory Manual, 15E. Department of Biological Sciences. Purdue University.

Other contributions

1. Xenopus-FV3 host-pathogen interactions and immune evasion. Robert J, Edholm ES, Jazz S, **Torres-Luquis O**, Francisco JA. *Virology*. 2017; 511. doi: 10.1016/j.virol.2017.06.005.